

**ASSESSMENT OF RISK PRIORITY NUMBER OF 2.5 MW
POLYCRYSTALLINE SILICON PHOTOVOLTAIC POWER PLANT AT
NAVRONGO, GHANA IN SUB-SAHARA AFRICA.**

KNUST

BY:

ALHASSAN SULLAIMAN
(BSc. Mechanical Engineering)

A Thesis Submitted to the Department of Mechanical Engineering, Kwame Nkrumah
University of Science and Technology, Kumasi in partial fulfilment of the
requirement for the award degree of

MASTER OF PHILOSOPHY IN MECHANICAL ENGINEERING

April 2019

KNUST



DECLARATION

I hereby declare that this submission is my own work towards the MPhil and that, to the best of my knowledge , it contains no material previously published by another person or material which has been accepted for the award of any other degree of the university, except where due acknowledgement has been made in the text.

KNUST

Alhassan Sullaiman

(PG 5964616)

Signature

Date

Prof. Gabriel Takyi

(Supervisor)

Signature

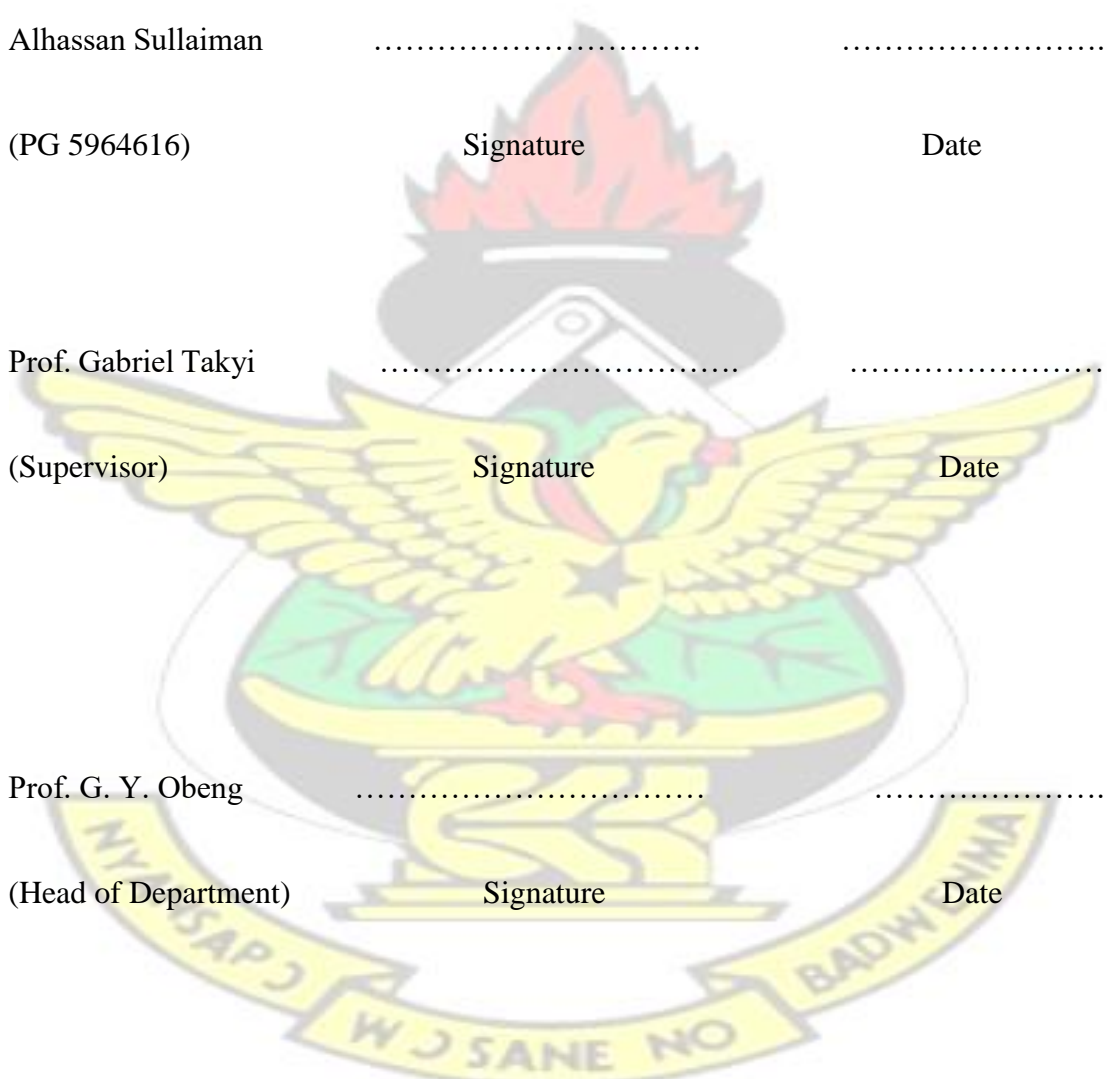
Date

Prof. G. Y. Obeng

(Head of Department)

Signature

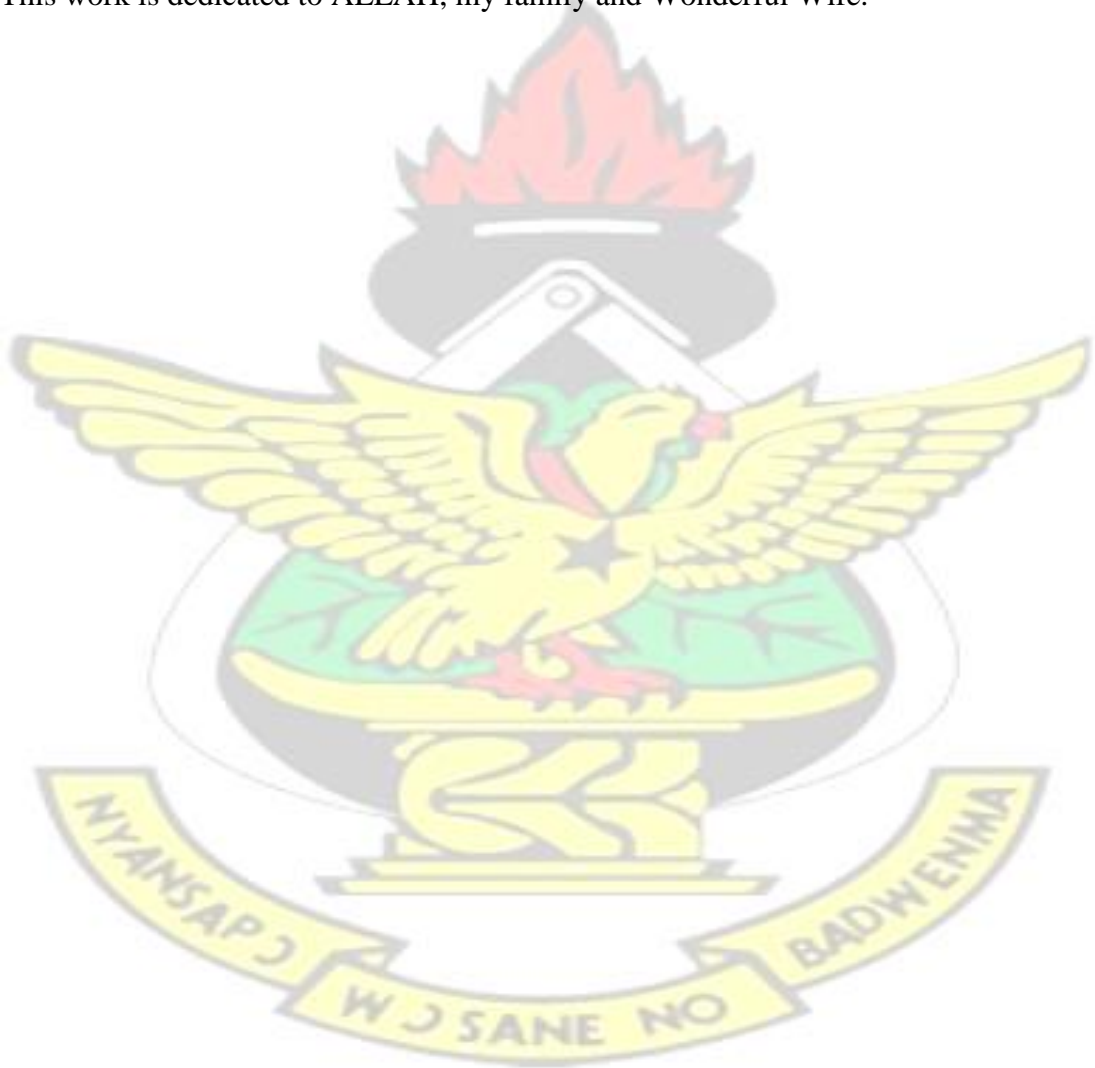
Date



DEDICATION

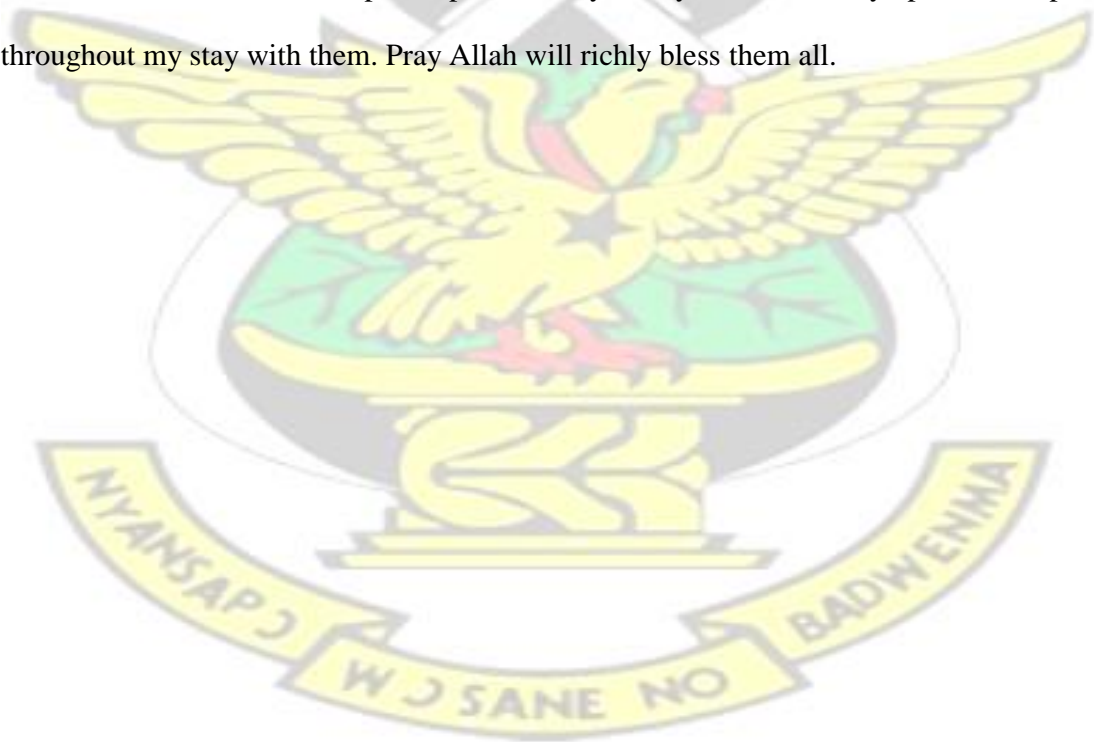
KNUST

This work is dedicated to ALLAH, my family and Wonderful Wife.



ACKNOWLEDGEMENT

I am indebted to Almighty Allah, the maker of my soul for his blessings, guidance and protection throughout my life and studies. Without Him, this work would not have been realised. I would like to thank my Supervisor, Dr. Gabriel Takyi for his insights, guidance and esteemed support throughout this study. It was a privilege to work under an eminent personality like him. In addition, I would like to thank Mr. Frank Nyarko for his support, encouragement, input and study materials he provided me. I really found them very handy and informative. I would also want to acknowledge Volta River Authority (VRA) for the permission to use their Solar Power Plant for my case study. It would have been impossible to complete my work without their help. I would also want to thank the technicians especially Mr. Fatawu, Mr. Abdul Rashid and Mr. Gibson for their assistance in the collection of data at the solar power plant facility. They have been very open and helpful throughout my stay with them. Pray Allah will richly bless them all.



ABSTRACT

Understanding failures of photovoltaic (PV) modules is one key factor in enhancing the reliability and service lifetime of PV modules; and hence reducing the cost of PV systems and financial implications on investment. This study seeks to identify the field failures associated with installed PV modules in the Ghanaian climatic condition, which minimize the performance of modules, and pose reliability issues to the solar plants as well as financial implications to manufacturers and investors in the PV sector. Physical examination of the modules using visual inspection checklist and their corresponding electrical performance parameters (I-V characteristics) measurement using multimeter and I-V tracer were performed on two models of the five (5) year old 2.5 MW PV power plant at Navrongo. A MatLab program was used to evaluate the failures and degradation modes of 144 Polycrystalline silicon (Poly-Si) framed modules under the hot dry climate of Navrongo. The program is a statistical reliability tool that uses Risk Priority Number (RPN) to determine the dominant failures by means of ranking and prioritizing the failure modes. The visual inspection revealed front glass slightly soiled, junction box lid fell off, cell interconnect discoloration and backsheet crack between cells as the peculiar failure issues either affecting the performance of the modules and/ or posing safety concern to personnel and properties on site. Mean degradation rates of 1.11%/year and 1.23%/year were respectively computed for Model A (Jinko solar) and Model B (Suntech technologies) types of modules for the power plant studied. These degradation rates values are beyond the standard warranty limit of 1.0%/year reported in literature. In addition, short circuit current (I_{sc}) and fill factor (FF) were determined as the dominant I-V parameters affecting the power degradation rates of the Model A and Model B modules respectively. The study also determined the total Global RPN value of 606 for the Model A type of modules for this plant, whereas that for Model B is 583. These RPN values fall within the reported values ranging from 500 to 755 in literature. With this information, investors can have an insight on the worth of a PV Plant and viability of their investment before making a decision. From this study, it can be concluded that, the five years old PV plant in operation is not performing very well and needs urgent attention to avoid loss based on the degradation rates of the fielded modules.

TABLE OF CONTENTS

DECLARATION	I
DEDICATION	II
ACKNOWLEDGEMENT	III
ABSTRACT	III
LIST OF FIGURES	IX
LIST OF PLATES	XII
LIST OF TABLES	XIII
ABBREVIATIONS AND ACRONYMS	XIV
CHAPTER 1: INTRODUCTION	1
1.1 Background	1
1.2 Problem Statement	2
1.3 Justification	3
1.4 Main Aim	3
1.5 Scope of Work and Thesis Organisation	4
CHAPTER 2: LITERATURE REVIEW	6
2.1 Review of related studies	6
2.2 Research gap/ Contribution	9
CHAPTER 3: THEORETICAL CONSIDERATIONS	9
3.1 Durability and Reliability definitions for PV Modules/ Plant	9
3.1.1 Reliability Issues	10
3.1.2 Durability Issues	10
3.2 Defects and Failures in PV Modules	11
3.3 Field Failures, Degradation Modes and Mechanisms in PV Modules	12
3.4 Performance Loss/Failures	13
3.5 Safety Defects/Failures	15

3.6 Metric Definitions of PV Modules and Financial Risk Calculations	17
3.7 Failure Mode, Effect and Criticality Analysis (FMECA) For PV Plant.....	18
3.7.1 Risk Priority Number.....	19
3.8 Basic Measurement Techniques for Identifying Failures in PV Modules.....	20
3.8.1 Visual Inspection	21
3.8.2 I-V Curve	21
3.9 I-V Curve Parameters	21
3.10 Data Analysis Criteria and Equations	23
CHAPTER 4: CASE STUDY PLANT AND METHODOLOGY	25
4.1 Description of Navrongo Solar Power Plant (NSPP)	25
4.2 Methodological Approach	26
4.3 Data Collection	26
4.4 Software for Analysis	28
4.5 Developed MatLab program flowcharts	32
4.5.1 RPN Program Flowchart.....	32
4.5.2 Performance RPN Flowchart	32
4.5.3 Global RPN Flowchart.....	34
4.5.4 Correlation Program Flowchart	36
4.7 Determination of the Performance and Safety RPN using Pmax Degradation Rates	38
4.8 Determination of the Performance RPN using I_{sc} , V_{oc} and FF Degradation Rates.	42
CHAPTER 5: DISCUSSIONS OF RESULTS	44
5.1 RPN program results.....	44

5.1.1 Determination of Global RPN for Model A	44
5.1.2 Defects Ranking Plot for Global RPN	49
5.1.3 Pie Chart for Reliability, Durability and Safety failures	51
5.2 Correlation program output Plots	52
5.2.1 Histogram for Pmax Rd for Model A	53
5.2.2 Determination of Dominant IV Parameter Degradation Rates	54
5.2.3 Comparison of Average Degradation Rates (%/year) of IV Parameters for Performance Defects.....	60
5.3 Analysis of Results for NSPP- Model B.....	62
5.3.1 Determination of Global RPN – Performance RPN + Safety RPN	62
5.3.2 Defects Ranking Plot for Global RPN for Model-B.....	64
5.3.3 Pie Chart for Reliability, Durability and Safety failures for Model-B	66
5.4 Correlation program output Plots for NSPP- Model B.....	67
5.4.1 Histogram for Pmax Rd for Model-B	67
5.4.2 Determination of Dominant I-V Parameter Degradation Rates.....	68
5.4.3 Comparison of Median Degradation Rates (%/year) of IV Parameters for Performance Defects.....	74
5.5 Comparison of key findings of NSPP Model A and Model B Results.....	75
5.5.1 Summary comments	77
CHAPTER 6: CONCLUSIONS AND RECOMMENDATIONS.....	78
6.1 Conclusion	78

6.2 Recommendations.....	79
REFERENCES	81
APPENDIX A: SAMPLE PICTURES OF DEFECTS.....	82
APPENDIX B: MOORTHY’S MATLAB PROGRAM-SOP.....	89
APPENDIX C: MATLAB RESULTS.....	96
APPENDIX D: RPN RAKING TABLES	107

KNUST



LIST OF FIGURES

Figure 3- 1: Hypothetical plot of Durability and Reliability Issues of PV Modules .	11
Figure 3- 2: Metric definitions for PV Modules	19
Figure 3- 3: I-V Curve Diagram of an illuminated PV module	23
Figure 4- 1: Flow Chart for Computing Performance RPN.	34
Figure 4- 2: Flow Chart for Computing Safety RPN	35
Figure 4- 3: Flow Chart for Computing Global RPN	36
Figure 4- 4: Flow Chart for Correlation Analysis	38
Figure 4- 5: Performance RPN output plot for Model A using Pmax degradation rate 40	40
Figure 4- 6: Safety RPN output plot for Model A using Pmax degradation rate.	41
Figure 4- 7: Performance RPN output plot using I-V Parameter's degradation rate. .	43
Figure 5- 1: Global RPN Plot for Model- A using occurrence, detection and severity 46	46
Figure 5- 2: Global RPN plot using Severity and Occurrence for Model- A.	47
Figure 5- 3: Defects - Ranking Plot for Model –A.	49

Figure 5- 4: Pie Chart of Reliability, Durability and Safety Issues for Model- A 50

Figure 5- 5: Histogram of Pmax degradation rate for Model- A 52

Figure 5- 6: Box Plot of I-V Parameters degradation rates for Model- A 54

Figure 5- 7: Linear Relation Plot of I-V Parameters for Model-A 55

Figure 5- 8: Combined Histogram of Isc and Pmax degradation rate for Model-A. . 56

Figure 5- 9: Combined Histogram of FF and Pmax degradation rate for Model-A .. 57

Figure 5- 10: Combined Histogram of Voc and Pmax degradation rate for Model-A
.....
58

Figure 5- 11: Comparison Plot of Median degradation rates of I-V Parameters for
Model-A
60

Figure 5- 12: Global RPN Plot for Model- B 61

Figure 5- 13: Global RPN Plot Using Severity and Occurrence for Model- B 63

Figure 5- 14: Defects - Ranking Plot for Model –B 64

Figure 5- 15: Pie Chart of Reliability, Durability and Safety Issues for Model- B ... 65

Figure 5- 16: Histogram of Pmax degradation rate for Model- B..... 67

Figure 5- 17: Box Plot of I-V Parameters degradation rates for Model- B 69

Figure 5- 18: Linear Relation Plot of I-V Parameters for Model-B 70

Figure 5- 19: Combined Histogram of Voc and Pmax degradation rate for Model- B

Figure 5- 20: Combined Histogram of FF and Pmax degradation rate for Model- B 72

Figure 5- 21: Combined Histogram of Isc and Pmax degradation rate for Model- B 73

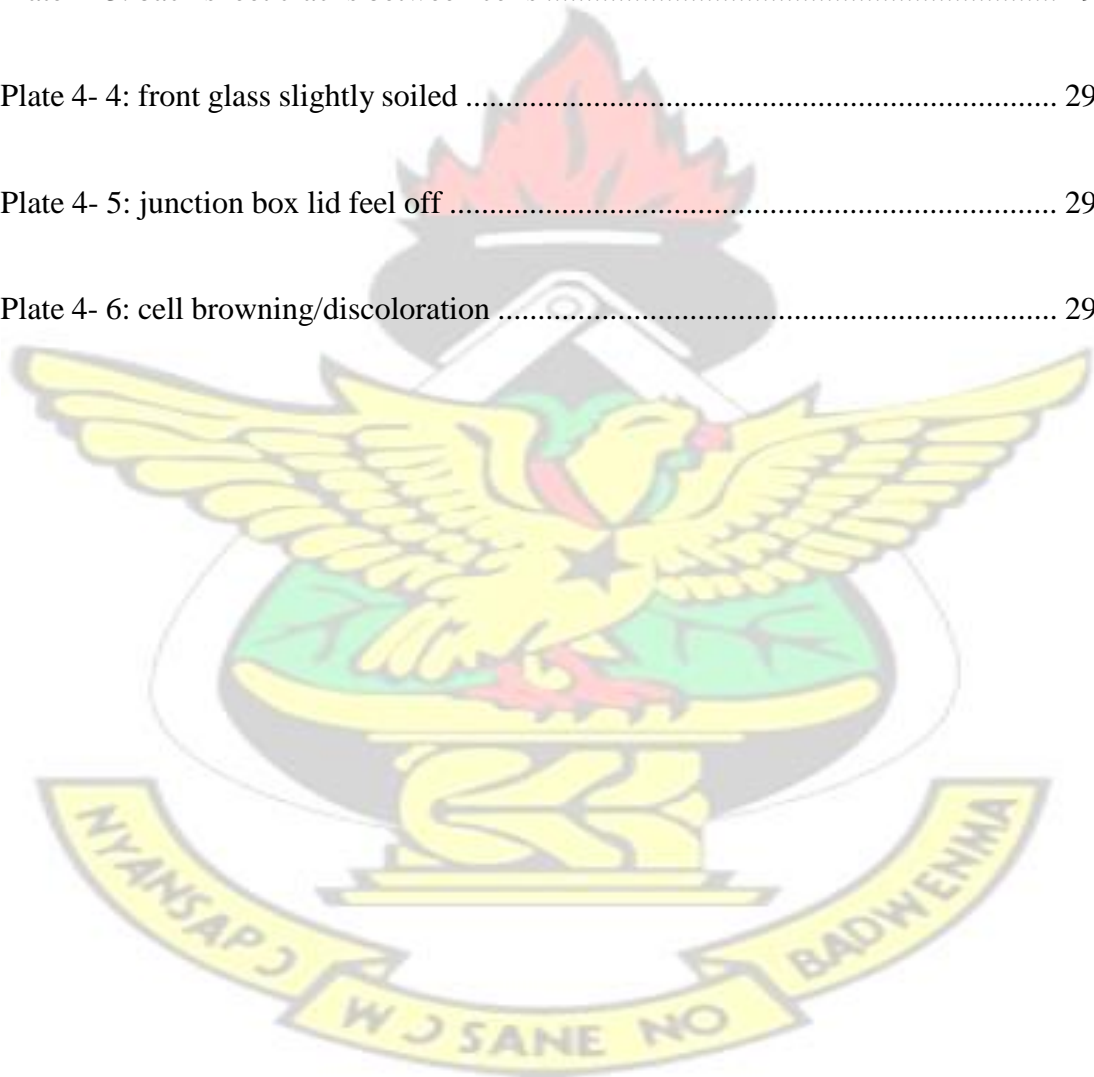
Figure 5- 22: Comparison Plot of Median degradation rates of I-V Parameters for

Model-B 74



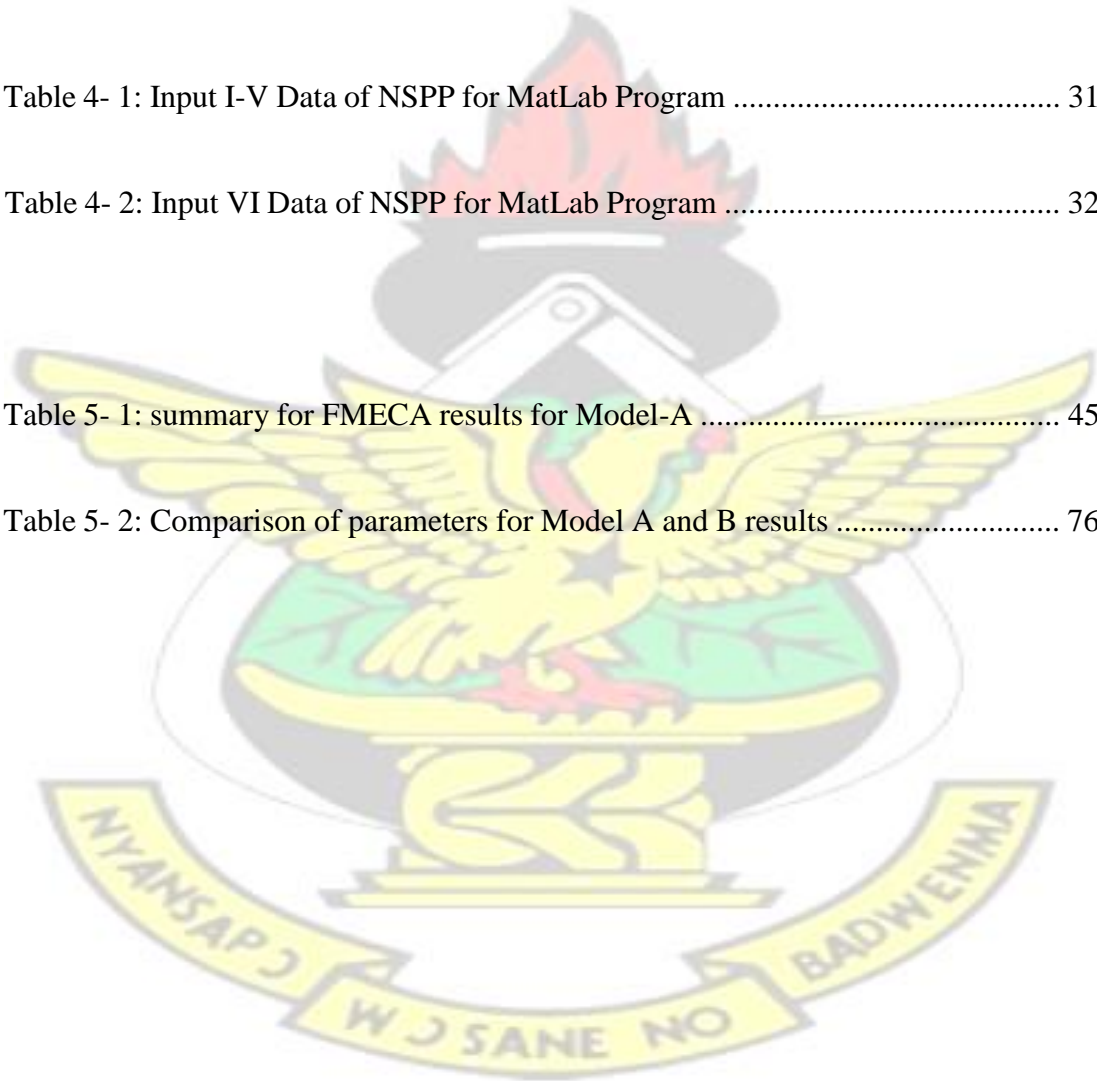
LIST OF PLATES

Plate 4- 1: Photograph of NSPP site	27
Plate 4- 2: cell cracks/ cell snail tracks	28
Plate 4- 3: back sheet cracks between cells	29
Plate 4- 4: front glass slightly soiled	29
Plate 4- 5: junction box lid feel off	29
Plate 4- 6: cell browning/discoloration	29



LIST OF TABLES

Table 3- 1: Performance failures of PV modules.	15
Table 3- 2: Safety failures of PV Modules.....	17
Table 4- 1: Input I-V Data of NSPP for MatLab Program	31
Table 4- 2: Input VI Data of NSPP for MatLab Program	32
Table 5- 1: summary for FMECA results for Model-A	45
Table 5- 2: Comparison of parameters for Model A and B results	76



ABBREVIATIONS AND ACRONYMS



ABCS	America Boards for Codes and Standards
ASU- PRL	Arizona State University- Photovoltaic Reliability Laboratory
CNF	Cumulative Number of Frequency
FF	Fill Factor
FMECA	Failure Mode, Effect and Criticality Analysis
IEC	International Electrotechnical Commission
IEEE	Institute of Electrical and Electronics Engineers
I_{max}	Maximum current
I_{sc}	Short Circuit Current
I-V	current voltage
NSPP	Navrongo Solar Power Plant
P_{max}	Maximum Power
PV	Photovoltaic
R_d	Degradation Rate
RPN	Risk Priority Number
R_s	Series Resistance
R_{sh}	Shunt Resistance
VI	Visual Inspection
V_{max}	Maximum voltage
V_{oc}	Open Circuit Voltage

CHAPTER 1: INTRODUCTION

1.1 Background

The difficulty of PV technology dissemination in the world is recently associated to the reliability of the modules and its financial effect on investment. The reliability of the modules depend on the type of PV technology and the environment in which the modules operate. Optimizing the energy output of these modules eventually alleviate the panic of the reliability of the technology to investors and users of the technology (TamizhMani and Kuitche, 2013).

Photovoltaic modules installed can encounter diverse forms of failure modes and mechanisms during their operation. These failures are responsible for the degradation of power and poses safety issues to users and operators (Shrestha et al., 2015).

The solar industry requires accelerated test programs, which are specific to various climatic conditions to depict the observed field failures (TamizhMani and Kuitche, 2013). This necessitates the need to find out all possible failures in varied climatic conditions that can affect the modules during its lifetime in operation (Moorthy, 2015). Based on the field failure data gathered, suitable accelerated test programs could be developed which will aid in improving the reliability of the modules.

To meet this goal, failure modes accountable for the module power degradation needs to be analyzed statistically to determine the overriding failure modes in the modules installed. Failure Mode Effect and Criticality Analysis (FMECA), is a statistical reliability tool that is used to determine dominant failure modes by ranking and prioritizing failures in the modules.

FMECA utilizes the Risk Priority Number (RPN) technique that gives the product of Severity, Occurrence and Detection of the failures for prioritizing the failure modes.

The greater the RPN value, the dominant and severe the failure mode (Shrestha et al., 2015).

Statistical analysis on data obtained from numerous PV power plants to find out dominant failures and I-V parameters responsible for power degradation of modules were carried out by Janakeeraman et al., (2014), Mallineni et al., (2014), Shrestha et al., (2015), Rajasekar, (2015) and Boppana, (2015) . For more accurate, fast, and consistent process of obtaining the RPN values, Moorthy, (2015) automated the entire process by developing a computer program to aid researchers in related solar PV projects.

1.2 Problem Statement

Increase in reliability failure, safety issues and performance degradation losses of PV modules in power plants will have serious financial implications due to reduction in energy generation than estimated, safety risks, increase in operating and maintenance costs, and high warrant due rates. These failures and performance degradation rates are reliant on climate conditions of the location where the power plant is placed (Mallineni et al., 2014).

Previous researchers developed statistical FMECA (RPN) technique for the PV industry to computatively determine the risks (safety or performance) associated with modules deployed on the field. All previous works by Janakeeraman et al., (2014), Shrestha et al., (2015), Rajasekar, (2015), Boppana, (2015) and Moorthy, (2015) were performed on PV Plants **outside** sub-Sahara Africa. In an attempt to fill this gap and

contribute to the ongoing field of research, a performance field assessment of solar PV power plants located in sub-Saharan Africa is required.

1.3 Justification

There is the need for continuous improvement on the work already done by performing the statistical evaluation on PV power plants installed in sub-Saharan Africa.

Knowledge of the dominant defects peculiar to the Sub-Saharan climatic conditions will assist researchers in the industry for improvement in new climate specific accelerated test programs and modules designs. Investors can estimate the worth of a PV power plant having in mind the RPN of the plant and to inform their decision in investing in a particular PV power plant.

Manufacturers can use the results to figure out the flaws in their designs and enable them rectify them for better reliable products with low warranty returns (Kurtz et al., 2013). PV plant owners can use the outcome to quickly pinpoint the modules with failures and understand the failure modes causing them. This gives them the privilege to either replace the modules by resorting to the manufacturer's warranty provided or decide for modules resilient to those failure modes concerning their environmental conditions (Kurtz et al., 2013).

1.4 Main Aim

The main aim is to assess Risk Priority Number (RPN) of 2.5 MW PV polycrystalline silicon power plant installed at Navrongo in Ghana located in sub-Saharan Africa.

The specific objectives are to:

- generate the RPN of the observed module failures on the field.
- determine the overall RPN of the power plant (that is the state of health of the plant) using Mat Lab and excel spreadsheet.
- determine the annual degradation rate of the modules in the PV power plant using collected field data.
- determine the dominant safety and performance failures involved in the PV power plant.
- rank and prioritize the defects of PV modules using statistical reliability technique.

1.5 Scope of Work and Thesis Organisation

This research introduces the failure modes and defect mechanisms responsible for power degradation and its associated safety issues in a PV power plant. The study is limited to Polycrystalline technology and defects that can be seen with the eye using Visual Inspection checklist and measurement of the I-V characteristics of the modules.

In chapter one, Introduction to the topic, problem statement and objectives for embarking on such research are spelt out.

Chapter two discusses the Literature Review on similar works and publications on the assessment of RPN, as well as ranking and prioritization of PV module defects.

Chapter three discusses Theoretical considerations (definitions, statistical theories, algorithms) related to the study.

Chapter four concentrates on the methodology used for the data collection and process used in the development of the adopted MATLAB computer program.

Chapter five is dedicated to the detail analysis of statistical results of the program and its effects on the performance parameters of the modules.

Conclusion and recommendations for further studies are done in chapter six.



CHAPTER 2: LITERATURE REVIEW

This chapter will focus on reviewing works relevant to this research project. Not much research has been conducted on the Risk priority Number technique on the performance and reliability assessment of fielded photovoltaic modules and the failure modes and mechanisms responsible for the power degradation of modules on site. In view of this, few available literatures were reviewed for this study.

2.1 Review of related studies

A statistical analysis on the cell parameters responsible for power degradation of fielded PV modules in a hot-dry climate was reported by Janakeeraman et.al (2014). Statistical analysis of the I-V data collected on 1900 modules from 8 different PV power plants in Arizona to identify the I-V parameters which are responsible for degradation of power and correlated it with defects/failures on a power plant level using MINITAB statistical software. The statistical analysis of the results presented in this paper was obtained using the null hypothesis technique. This analysis indicates that the major degradation modes for the modules having glass/polymer construction are encapsulant discoloration (causing I_{sc} drop) and solder bond degradation (causing FF drop due to series resistance increase). The study also reported a power degradation rate ranging between 0.6%/year and 2.5% per year for the hot-dry climatic condition of Tempe, Arizona. However, the RPN values for the defects and entire PV plant and could not be reported.

In another literature on **statistical methods to determine dominant degradation modes of fielded PV modules** presented by Umachandran et.al (2015). The study correlated the visual defect data on 647 PV modules obtained from 5 different PV power plants in

Arizona (hot-dry climate) and New York (cold-dry climate) with I-V parameters to identify particular defect/failure which is responsible for affecting the dominant I-V parameter causing Pmax degradation. Analysis of the data using **MINITAB** software indicates that power is affected the most in hot-dry climate due to solder bond issues leading to high series resistance increase, while encapsulant delamination defect is being predominant in cold-dry climate leading to higher Isc drop and noticeable Voc loss due to triggering of bypass diodes. The report also presented the mean power degradation rates ranging between 0.49%/year and 1.13%/year for both hot-dry and cold-dry climatic condition. The RPN values however, were not determined in this study.

Boppana (2015) carried out a study on the **Outdoor Soiling Loss Characterization and Statistical Risk Analysis of Photovoltaic Power Plants**. The second part of the work performs statistical risk analysis for a power plant through FMECA (Failure Mode, Effect, and Criticality Analysis) based on non-destructive field techniques and count data of the failure modes. Risk Priority Number is used for the grading guideline for criticality analysis. The analysis was done on a 19-year-old power plant in a cold-dry climate to identify the most dominant failure and degradation modes peculiar to the cold-dry climate. Visual inspection and I-V data were collected on 360 framed polycrystalline silicon PV modules for this study and analysed using MINITAB and EXCEL. Results from the study indicates 0.6%/year mean power degradation rate for framed modules in the cold-dry climate and a global RPN of 760 for the plant. Interconnect discoloration was determined as the dominant degradation mode for framed modules for the cold-dry climate which was attributed to the extent of moisture ingress. However, the study limited the defects collection to physical visual inspection of the modules and defects that cannot be seen with the eye were not considered in the analysis.

In addition, a study conducted on the **Indoor Soiling Method and Outdoor Statistical Risk Analysis of Photovoltaic Power Plants** by Rajasekar (2015) seeks to determine the most dominant failure modes of field aged PV modules using experimental data obtained in the field and statistical analysis, FMECA (Failure Mode, Effect, and Criticality Analysis). The failure and degradation modes of about 744 poly-Si glass/polymer frameless modules fielded for 18 years under the cold-dry climate of New York was evaluated using MINITAB and EXCEL spreadsheet. The results from the study shows that the average power degradation from the data gathered is 0.73% per year for the frameless modules with a global RPN value of 704 for the PV plant. Encapsulant delamination was the dominant failure/degradation mode for frameless modules from the study. Also, the study considered only visual inspection of the modules in gathering the defects on the PV modules.

Furthermore, **Automation of Risk Priority Number Calculation of Photovoltaic Modules and Evaluation of Module Level Power Electronics** was presented by Moorthy (2015). The first part of the study involves programming of the statistical risk analysis of photovoltaic (PV) power plants. The primary focus of the project was to automatically generate Risk Priority Number (RPN) for each defect/failure based on **two Excel spreadsheets and a developed MatLab** program for the statistical analysis. The automation developed and presented in this project generates about 20 different reliability risk plots in about 3-4 minutes without the need of several manual labour hours traditionally spent for these analyses. The study validates the results from the developed MatLab program to the manual procedure usually used for similar analysis can be used as an alternative for related studies. The study simulated data on 46 polycrystalline PV modules in a cold-dry climate using the developed program. The

results shows that the mean power degradation rate was determined to be 0.522%/year as compared to 0.51%/year from the manual process. The global RPN value for the PV plant was also determined as 764 similar to the manual process. Only visual inspection was also used in collecting data on the defects on the modules.

2.2 Research gap/ Contribution

In all studies and cases thus considered thus far, it is evident that the data collection were gathered in places which includes Arizona, Tempe, Phoenix, and New York of the United States of America. However, performance of PV modules and their degradation modes are technology and climate specific. This necessitates the need to analyze PV modules in other environment to enhance the understanding on the dominant failure modes and their impact on the performance of the PV modules in those environment. In view of this, this study concentrates on the sub-Sahara Africa (specifically Ghana) to analyze the performance and dominant failure modes of PV modules in the Ghanaian climatic condition.

CHAPTER 3: THEORETICAL CONSIDERATIONS

This chapter discusses theoretical considerations related to the study which includes terminologies and definitions, statistical techniques used for the analysis of the defects and measurement techniques generally employed in collecting the field data.

3.1 Durability and Reliability definitions for PV Modules/ Plant

The main parameters accountable for module lifetime on the field are the reliability and durability issues. Thus the concern that a technology will underachieve or become outmoded early is one of the main obstacles to the dissemination of PV project (TamizhMani and Kuitche, 2013). However, knowledge on the difference between

these two parameters is of utmost importance to this research as it helps in categorizing the various types of failures encountered on the field.

3.1.1 Reliability Issues

PV modules are said to be reliable when there is a greater chance of the modules executing their proposed purposes adequately for 25 years under the prevailing field conditions. When the modules are replaced or unmounted from site before the warranty time is due, resulting from any kind of failure, including the power dropping beyond warranty limit, then those failures may be classified as hard or reliability failures (TamizhMani and Kuitche, 2013). Reliability failed modules are ascribed to the manufacturing and/ or design issues and referred to as catastrophic failures. Modules that are degrading beyond 1% per year of warrant limit, without the safety failures qualify for warranty claims proportional to the rate of degradation (M Köntges et al., 2014).

3.1.2 Durability Issues

Soft or degradative losses are those attributed to modules degrading at a rate lower than the warranty limit (Mallineni et al., 2014). Thus, all modules that degrade less than 1%/year, excluding the safety failures, are referred to as durability-failed modules. The durability issues are attributed to the material issues (Marc Köntges et al., 2014).

However, towards the end of the module's lifespan, several degradative mechanisms may advance and lead to wear-out failures due to augmented degradative losses (TamizhMani and Kuitche, 2013) as depicted in the hypothetical representation of the

reliability failures and durability losses of PV modules over the duration of operation in figure 3-1.

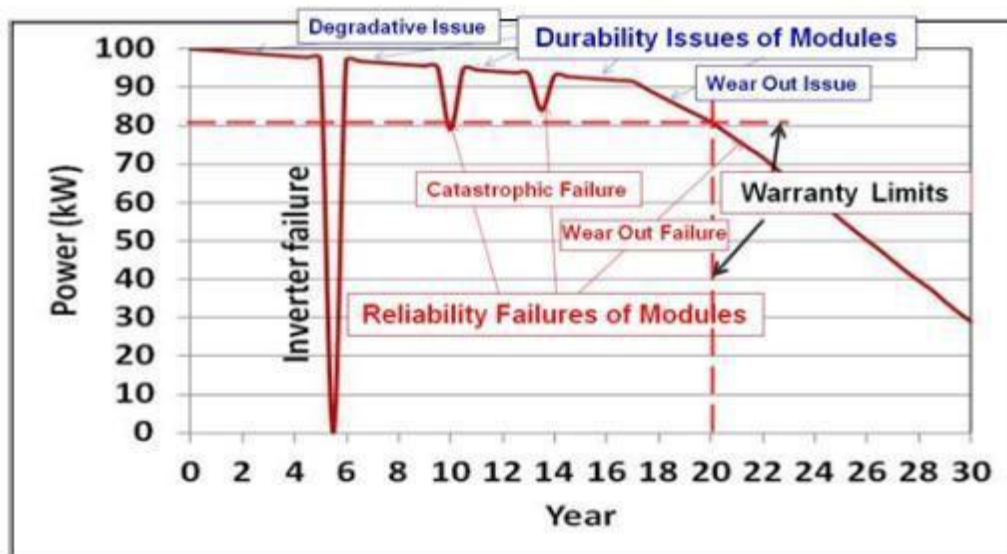


Figure 3- 1: Hypothetical plot of Durability and Reliability Issues of PV Modules

Source: (TamizhMani and Kuitche, 2013).

3.2 Defects and Failures in PV Modules

Anything that is not expected to be in a PV module is considered a defect. A defect may suggest a PV module failure or not. In addition, a defect signifies a module part that is physically different from a perfect one and might not eventually lead to a power loss. A defect is a much broader term than a failure (Marc Köntges et al., 2014).

However, when the defect leads to a power loss in the module, then it is referred as module failure. Module failures are irreversible by normal process and/ or poses a safety concern that needs to be addressed. A mere cosmetic issue that does not result in the stated consequences is not regarded a PV module failure. A PV module failure is necessary for the warranty when it occurs under conditions the module normally operates (Marc Köntges et al., 2014) and (Packard et al., 2012b).

Further discussions and illustrations can be assessed from the literature by

TamizhMani and Kuitche, (2013), Marc Köntges et al., (2014) and Packard et al., (2012b).

3.3 Field Failures, Degradation Modes and Mechanisms in PV Modules.

The type of PV technology and environment in which the modules function determine the kind of field failures, degradation modes and mechanisms of the fielded panels and their influence on power degradation (TamizhMani and Kuitche, 2013). The failure or degradation modes in PV modules show symptoms, whereas failure or degradation mechanisms represent the course for arriving at these symptoms.

A failure mechanism is responsible for one or more failure modes. A failure mechanism could be triggered by one or more failure causes and a failure mode could trigger one or more failure effects. The investigation method of field failure for PV modules can be designated as shown in the following sequence.

Failure mechanism (cause)  Failure mode (effect).

PV modules working life is typically dictated by the degradation rates rather than failure rates, although the failure modes and rates could significantly influence the degradation rates of the PV modules (TamizhMani and Kuitche, 2013), (Boppana, 2015) and (Kurtz et al., 2013).

Some typical field failure and degradation modes of crystalline-silicon PV modules in the field are discussed in (Packard et al., 2012a), (Shrestha et al., 2015), (Marc Köntges et al., 2014) and can be accessed for more explanations. Eighty six (86) possible failures that can affect PV module performance and cause safety challenges were discovered (Moorthy, 2015).

3.4 Performance Loss/Failures

A power loss arises when the measured module power is lower than the power on the nameplate of the module. The factors causing this loss are attributed to the performance failures of the modules (M Köntges et al., 2014).

Reports from National Renewable Energy Laboratory (NREL) and power plant experience from Arizona State University-Photovoltaic Reliability Laboratory (ASUPRL) identified sixty one (61) of the eighty six (86) failures identified in literature as performance issues affecting the PV module output power. Out of the 61 defects, twenty two (22) defects affected cell, five (5) defects affected encapsulant, seven (7) defects affected glass (front and rear), four (4) defects affected edge seal, five (5) defects affected frame, eight (8) defects affected junction box, three (3) defects affected backsheet, three (3) specific to thin film PV modules and one (1) defect each affected bypass diode and wires. In addition, two (2) more module mismatch and solder bond failure were identified to be responsible for performance loss summing the total list of performance defects to 61 as indicated in Table 3-1.

Table 3- 1: Performance failures of PV modules.

Glass	Frame	Junction box	Cell
Front glass lightly soiled Front glass heavily soiled Front glass crazing Front glass chip Front glass milky discoloration Rear glass crazing Rear glass chipped	Frame bent Frame discoloration Frame adhesive degraded Frame adhesive oozed out Frame adhesive missing in areas	Junction box lid loose Junction box warped Junction box weathered Junction box adhesive loose Junction box adhesive fell off Junction box wire attachments loose Junction box wire attachments fell off Junction box wire attachments arced	Cell discoloration Cell burn Mark Cell crack Cell moisture penetration Cell worm mark Cell foreign particle embedded Cell Interconnect discoloration Gridline discoloration Gridline blossoming Busbar discoloration Busbar corrosion Busbar burn marks Busbar misaligned Cell Interconnect ribbon discoloration
Edge Seal	Encapsulant	Backsheet	
Edge seal delamination Edge seal moisture penetration Edge seal discoloration Edge seal squeezed / pinched out	Encapsulant delamination over the cell Encapsulant delamination under the cell Encapsulant delamination over the junction box Encapsulant delamination near interconnect or fingers Encapsulant discoloration (yellowing/browning)	Backsheet wavy Backsheet discoloration Backsheet bubble	Cell Interconnect ribbon corrosion Cell Interconnect ribbon burn mark Cell Interconnect ribbon break String Interconnect discoloration String Interconnect corrosion String Interconnect burn mark String Interconnect break Hotspot less than 20°C
Wires	Thin Film	Bypass diode	Others
Wires corroded	Thin Film Module Discoloration Thin Film Module Delamination - Absorber coating Thin Film Module Delamination - AR coating	Bypass diode short circuit	Module mismatch Solder bond Fatigue / Failure

(Moorthy, 2015)

3.5 Safety Defects/Failures

A safety failure is the failure, which may pose risk to someone who is working with or simply passing by the PV modules M Köntges et al., (2014).

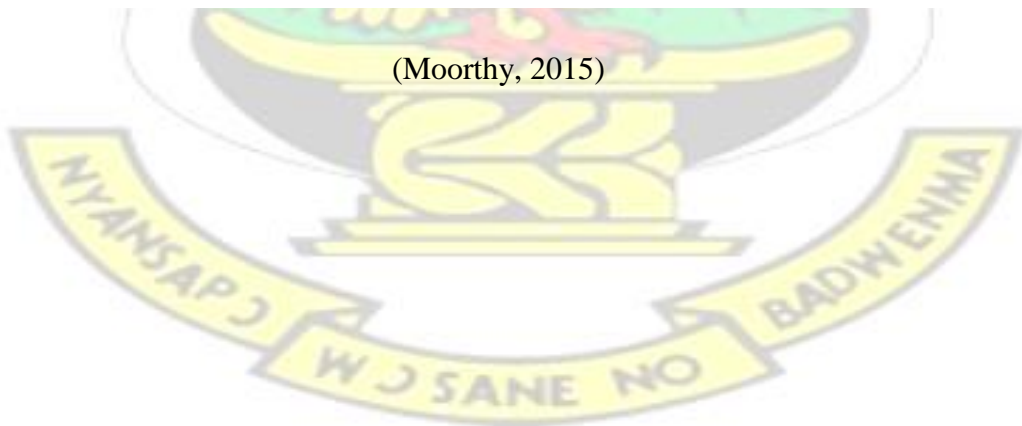
Likewise, to the performance failures reported by NREL and ASU-PRL, out of the 86 defects identified, 25 of them were accredited to failures, which can endanger the safety of the personnel operating the PV modules. Out of the 25 failures, five (5) affected the frame. Five (5) affected the junction box, four (4) affected the glass (rear and front), three (3) affected the wires and connectors, two (2) failures affect the cell, five (5) affecting the backsheet and one (1) failure affecting the bypass diode. Table 3-2 summarizes the safety failure distinguished based on the components affected.



Table 3- 2: Safety failures of PV Modules.

Glass	Frame	Bypass diode	Junction box
Front glass crack	Frame grounding severe corrosion	Bypass diode open circuit	Junction box crack
Front glass shattered	Frame grounding minor corrosion		Junction box burn
Rear glass crack	Frame major corrosion		Junction box loose
Rear glass shattered	Frame joint separation		Junction box lid fell off
	Frame cracking		Junction box lid crack
Wires	Backsheet	Cell	
Wires insulation cracked / disintegrated	Backsheet peeling	String interconnect arc tracks	
Wires burnt	Backsheet delamination	Hotspot over 20°C	
Wires animal bites / marks	Backsheet burn mark		
	Backsheet crack / cut under cell		
	Backsheet crack / cut between cells		

(Moorthy, 2015)



3.6 Metric Definitions of PV Modules and Financial Risk Calculations

Increase in modules becoming prematurely obsolete, degrading in power whilst in operation and causing safety issues have severe financial implications on investment.. These aforementioned issues greatly depend on the environmental conditions in which the power plant is installed (Mallineni et al., 2014).

A wide-range of collected works and analysis carried out by NREL on almost 2000 publications illustrate that the module degradation rate can be as high as 4%/yr. (Boppana, 2015), but the median and mean degradation rates are respectively computed as 0.5% year and 0.8%/year (Kurtz et al., 2013). These degradation rates are from various climate conditions, different type of PV technology and number of years on the field.

However, a universal metric definition within the PV industry for classification and evaluation of the safety, reliability and durability issues/losses is inconsistent and not established. 'Definition of metrics 'is a standard of measurement by which the quality of a product can be evaluated. The definition of metrics for safety failures, reliability failures and degradation losses require to be established explicitly for a consistent wide financial model development and acceptance within the PV industry.

(Mallineni et al., 2014) provided a metric definition for reliability failures, degradation loss and safety failures for the PV modules to assess the performance of PV power plant in terms of financial risks encountered with failures as shown in figure 3-2.

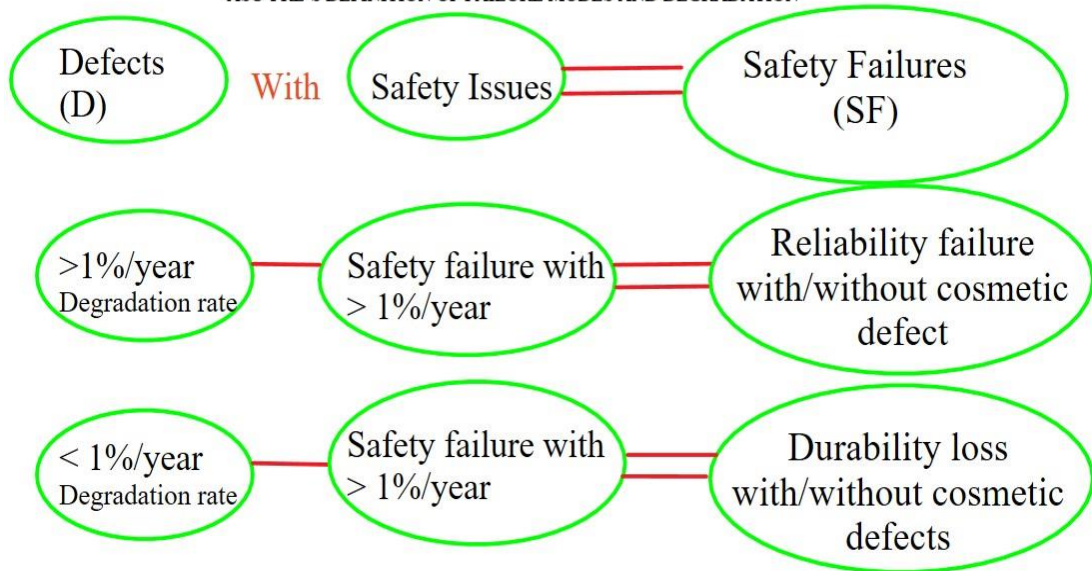


Figure 3- 2: Metric definitions for PV Modules

(Mallineni et al., 2014)

For instance, the conventional 20/20 warranty (20% degradation over 20 years) as per the standard demonstrated in figure 3-2 demonstrates that all modules, which are degrading at a rate greater than 1%/year, excluding any safety-failed modules, are considered as reliability failed modules and they qualify for warranty return. In the same view, all the modules degrading at a rate lower than 1%/yr. with the exclusion of safety failed modules are classified as durability issues and do not meet the warranty claim TamizhMani and Kuitche, (2013), Mallineni et al., (2014) and Shrestha et al., (2015).

These metric definitions can be used on the collected field data to objectively perform the financial risk assessment of the PV Power plant.

3.7 Failure Mode, Effect and Criticality Analysis (FMECA) For PV Plant

Failure Mode, Effect and Criticality Analysis (FMECA) is one of the most popular qualitative risk assessment technique for identifying, assessing and eliminating

potential failure mode in processes, designs, components and systems in a wide range of industry (Liu et al., 2013).

According to IEC 60812 2006-01 standard, FMECA can be used to find failure modes that can possibly affect a system performance which yields positive results. FMECA is an organized method, which scrutinizes a system or element of all possible failure modes, their causes and effect on performance as well as on other elements in a system (Shrestha et al, 2014). Carrying out FMECA gives a better understanding of the behavior of a component as it determines the effect of each failure mode and its causes. The technique prioritizes the failures according to their criticality, occurrences and detectability and thus depicting eventual flaws in the system, thus aid in improving the reliability of the component or system Janakeeraman et al., (2014), Lazzaroni et al., (2012) and Umachandran et al., (2015).

3.7.1 Risk Priority Number

The risk priority number (RPN), a FMECA technique quantifies the criticality of the failure mode as stipulated in IEC 60812 2006-01 Standard (Shrestha et al., 2015).

The determination of RPN is computed as:

$$RPN= S*O*D \dots\dots\dots (3.1)$$

Where

- ❖ S denotes severity, which approximates how extreme the impact of the failure will have on the system or the user. It is the degree of criticality of the failure mode.

- ❖ **O** means occurrence, which denotes the likelihood of a failure mode to manifest for a stipulated period. It may be defined as a grading number rather than the actual probability of occurrence.
- ❖ **D** means detection, is an approximate of the ability to detect and mitigate the failure before the system or user is affected. The higher the detection value, the difficulty the detection for the failure mode. This implies that the low possibility of detection will result to higher RPN value.

The failure modes are then prioritized in accordance with their RPN and much focus is given to high RPN values. The RPN combined with the degree of severity enables the critical failure mode to be known, so that resources could be focused to relieve the effects. If there are failure modes with comparable RPN, those with higher severity values are addressed first (Shrestha et al, 2015).

Mani GovindaSamy TamizhMani developed the following criteria for the scoring of the various parameters for the evaluation of the RPN value as shown in appendix D.

Shrestha et al., (2015) provided a method for manually employing FMECA for PV power plants to identify the dominant failure modes affecting a particular PV power plant and identified the dominant failure mode in various PV power plants.

3.8 Basic Measurement Techniques for Identifying Failures in PV Modules.

There are various setups, tests and best practices used to identify failure modes in the laboratory or on the field, which gives better representation of the failures and allows for analysis for those failure modes. Some of these methods include visual inspection (VI), I-V curve, Ultra-Violet (UV) fluorescence, and electroluminescence, thermography and signal transmission method. The basic measurement methods which

are easy to carry out that is VI and I-V curve would be considered in this thesis. Detailed description and sample failures for all the various methods are discussed by (M Köntges et al., 2014).

3.8.1 Visual Inspection

Visual Inspection is one of the effective and fastest ways to identify failures in PV modules. The visual inspection in accordance to IEC PV standard (IEC61215, IEC61646) is done before and after the modules have been subjected to environmental, mechanical and electrical stresses in the laboratory. The documentation of visually observed failures allow the analysis of failures applicable for statistical evaluation from numerous countries and experts (Phinikarides et al., 2014). During visual inspection, only defects detectable with the bare eye are noted (Köntges et al., 2014).

3.8.2 I-V Curve

The measurement of the open circuit voltage, short circuit current and other parameters help to define the characteristics of a PV module. Determination of module I-V curve under natural sunlight condition usually requires a portable I-V tracer, and pyranometer as reference spectrum for rating global radiation. IEC 60891 standard elaborates more on the I-V measurements method (M Köntges et al., 2014).

3.9 I-V Curve Parameters

Typical key parameters responsible for the performance of PV modules can be extracted from the I-V curve. An ideal I-V curve of an irradiated PV module has the profile presented in figure 3-3.

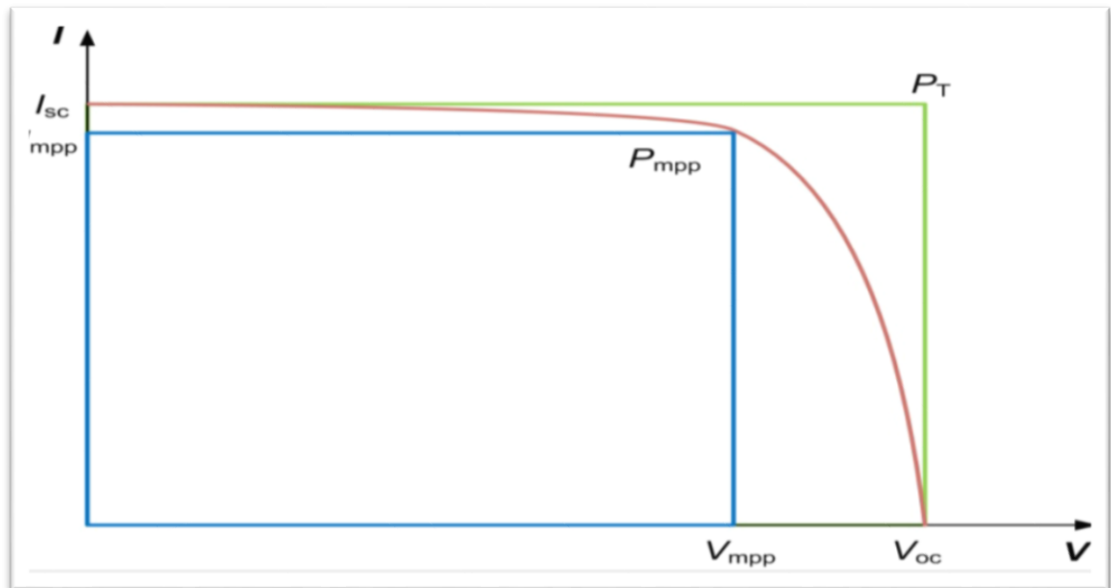


Figure 3- 3: I-V Curve Diagram of an illuminated PV module
(Phinikarides et al., 2014)

When the voltage across the module is zero, the measured current is known as the short circuit current (I_{sc}). The open circuit voltage (V_{oc}) is the highest voltage recorded from a PV module and occurs at zero current.

The maximum power (P_{max}) is a point on the I-V curve of a PV module under illumination, where the product of maximum power point current (I_{mpp}) and its voltage (V_{mpp}) is maximum. The fill factor (FF) is a measure of the quality of the solar PV.

The FF can be interpreted graphically as the ratio of the rectangular areas depicted in Figure 3-3. That is,

$$FF = \frac{\text{area of blue rectangle}(V_{mpp} \times I_{mpp})}{\text{area of green rectangle}(V_{oc} \times I_{sc})} \dots\dots\dots (3.2)$$

3.10 Data Analysis Criteria and Equations

Various FMECA criteria were used in computing the RPN values for the observed defects. The detection table and occurrence table proposed by (Shrestha et al., 2015) were used as indicated in Appendix D.

However, the severity table was adjusted based on the studies undertaken by ASUPRL, which reveals that PV modules have degraded beyond 2.0% / year as opposed to that proposed by (Shrestha et al., 2015). This modification is to cater for the changes in rank 8, 9, and 10 for computing the RPN of defects as shown in Appendix D.

In addition, the following equations were used in determining the degradation rates of the performance parameters;

The drop and degradation rate of any performance parameter are given as equations 1 and 2 respectively;

$$\text{Drop}_{\text{Parameter}} = \frac{\text{Rated} - \text{Measured}}{\text{Rated}} \times 100 \quad (3.3)$$

$$\text{Degradation Rate}_{\text{parameter}} = \frac{\text{Drop}_{\text{parameter}}}{\text{Age of PV plant}} \quad (3.4)$$

The cumulative number of frequency, which is used in ranking the occurrence of observed defects, is also determined from equation 3.4;

$$\text{CNF} = \frac{\text{Number of system \% defects}}{\text{time}} \times \text{system operating time} \quad (3.5)$$

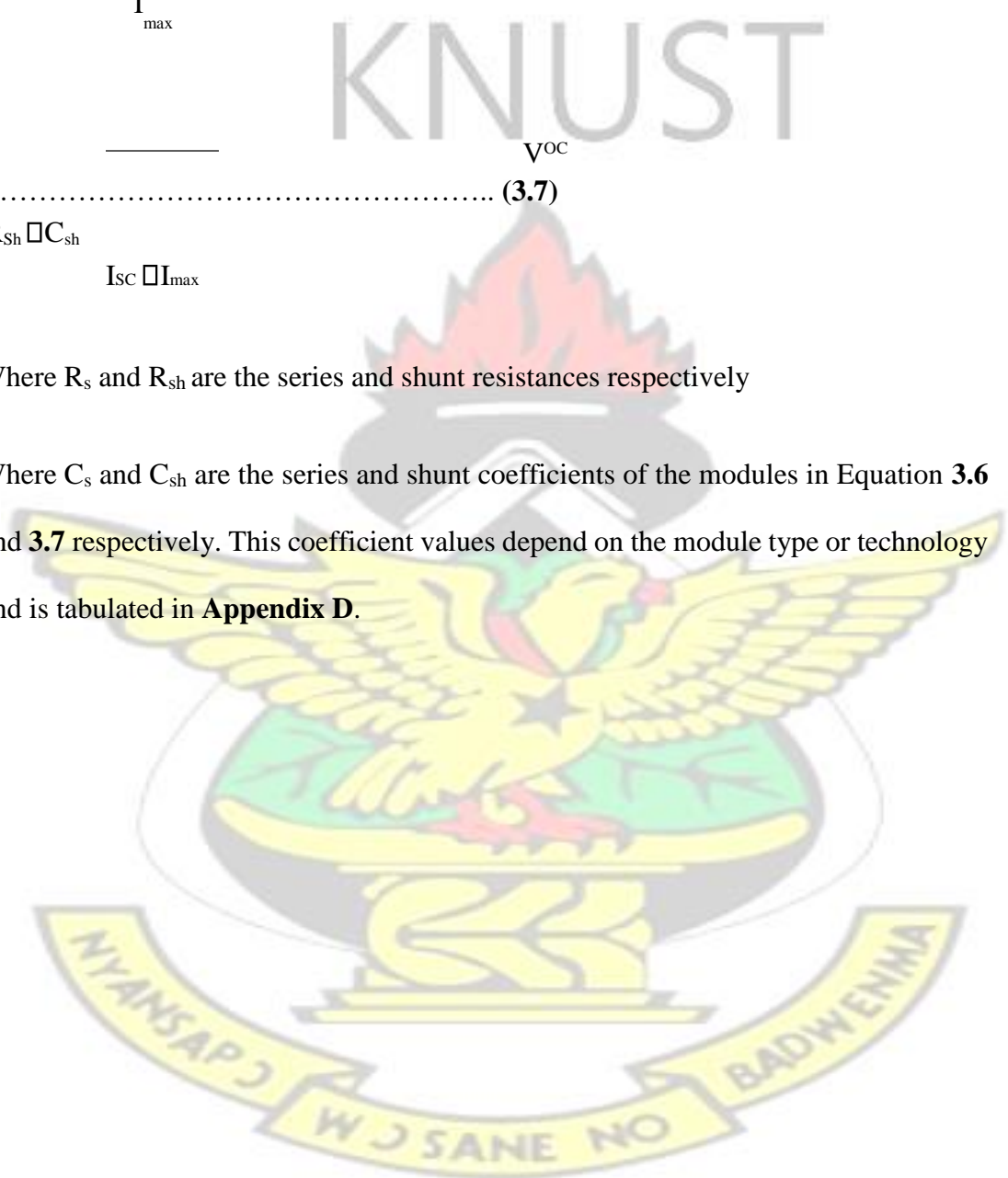
The series and shunt resistance of the modules are computed from the relations respectively as proposed by Dobos et al, (2012).

$$R_s = C_s \frac{V_{OC} - V_{max}}{I_{max}} \quad \dots \dots \dots (3.6)$$

$$R_{sh} = C_{sh} \frac{V_{OC}}{I_{SC} - I_{max}} \quad \dots \dots \dots (3.7)$$

Where R_s and R_{sh} are the series and shunt resistances respectively

Where C_s and C_{sh} are the series and shunt coefficients of the modules in Equation 3.6 and 3.7 respectively. This coefficient values depend on the module type or technology and is tabulated in **Appendix D**.



CHAPTER 4: CASE STUDY PLANT AND METHODOLOGY

This section begins with a description of the solar plant under study, the data collection technique, and discusses the software used for the analysis of the work.

4.1 Description of Navrongo Solar Power Plant (NSPP).

The NSPP is a five (5) year old, first and oldest utility-scale solar plant in Ghana with an installed capacity of 2.5 MW. It is located in the Upper East region of Ghana with latitude 10° N to 11° N and longitude -1.5° E to -3° E sited in a hot dry climatic condition. The site comprises 115 arrays with each array having approximately 72 flat panels. All panels are of the polycrystalline silicon (Poly-Si) technology and from two different manufactures namely; Jinko Solar and Suntech Technologies. For the purpose of this study, the Jinko Solar modules are referred to as 'Model-A' and Suntech Technologies modules are known as 'Model-B'. Both have the same rated power output of $295 W_p$ /module specification and module dimensions. The modules are fixed frame ground mounted with 1-axis 12° tilt towards South as shown in **plate 4-1**.





Plate 4- 1: Photograph of NSPP site

4.2 Methodological Approach

The research study was accomplished by the following methodological approach;

1. Site visit and data collection
2. Review of software for analysis
3. Simulation of collected data using reviewed MatLab program
4. Generation of plots from MatLab program
5. Analysis of results and interpretation.

4.3 Data Collection

Two sets of data were taken from the plant for the analysis, the I-V data, which entails data on the performance parameters for the PV modules, and Visual Inspection (VI) data for the physical observable defects on the modules. After systematic observation

of all the arrays on the field, a randomly selected best, median and worst array were randomly chosen for the recording of the data.

In all, 148 modules data were recorded, 74 modules from each manufacturer for both I-V data and VI data. Tools such as the radiometer, multimeter, I-V tracer and pyrometer were used in collecting the data. The developed visual inspection (VI) checklist developed by ASU-PRL is used for recording the field data.

All the I-V data collected were carried out at the peak hours of radiation with an average irradiance of 895 W/m^2 and average ambient temperature of 43°C and average relative humidity of 48%. Images of some of the failures captured at the plant are presented below with the remaining defects captured in Appendix A.

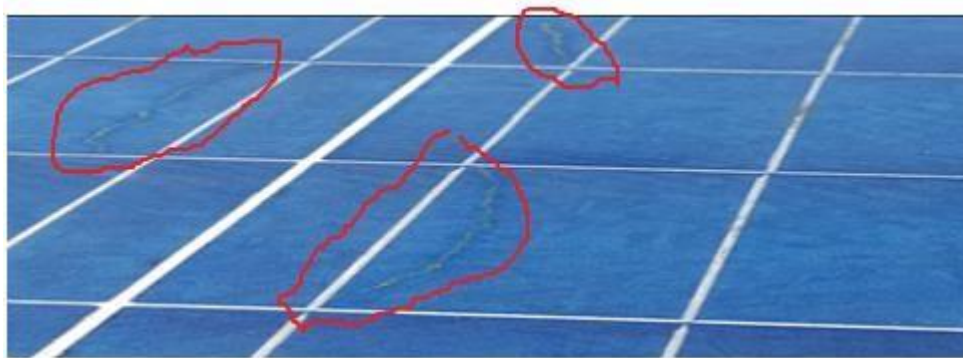


Plate 4- 2: cell cracks/ cell snail tracks



Plate 4- 3: back sheet cracks between cells



Plate 4- 4: front glass slightly soiled



Plate 4- 5: junction box lid feel off



Plate 4- 6: cell browning/discoloration

4.4 Software for Analysis

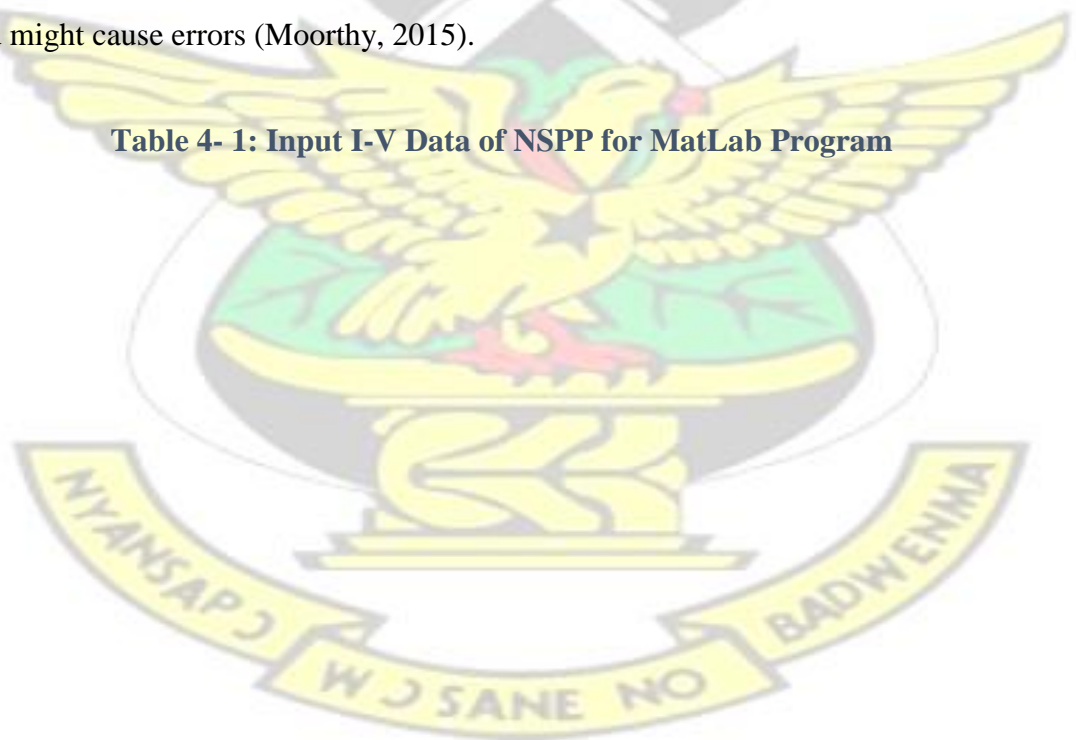
A MatLab Program developed by Moorthy for similar studies was adopted, reviewed and modified for this work. The software is made up of two main programs with various subroutines within them; the RPN program and the correlation program. The RPN program computes and presents the various RPN values for each observable field defect and automatically determines the reliability issues affecting the plant using FMECA procedure. The correlation program was designed to compute various

statistical plots and determine the correlations between P_{max} degradation rate and other I-V parameters to indicate which I-V characteristic is responsible or affect P_{max} based on the field defects. In all, approximately twenty different reliability plots were generated within five minutes for the analysis as would be discussed in the next chapter.

The input needed for the program to run is the observed defects/failures measured on the field and the I-V characteristic measurement of the modules. Thus the IV data and VI data are used as the input data for this work.

Both IV and VI data are excel spreadsheet with names 'IV data.xlsx' and 'VI data.xlsx' respectively and should follow the same format as shown in **Table 4-1** and **Table 4-2**. No alterations whatsoever should be done as it will affect the results from the program and might cause errors (Moorthy, 2015).

Table 4- 1: Input I-V Data of NSPP for MatLab Program



Module	Rated Isc	Rated Voc	Rated Imax	Rated Vmax	Rated FF	Rated Pmax	Measured Isc	Measured Voc	Measured Imax	Measured Vmax	Measured FF	Measured Pmax	Age
ST-1	8.57	45.10	8.27	35.70	76.39	295.00	8.14	41.80	7.84	31.20	71.89	244.61	5
ST-2	8.57	45.10	8.27	35.70	76.39	295.00	7.64	41.53	7.34	31.19	72.15	228.93	5
ST-3	8.57	45.10	8.27	35.70	76.39	295.00	7.98	41.41	7.64	31.20	72.13	238.37	5
ST-4	8.57	45.10	8.27	35.70	76.39	295.00	8.12	42.24	7.65	32.98	73.56	252.80	5
ST-5	8.57	45.10	8.27	35.70	76.39	295.00	7.90	41.94	7.50	31.88	72.16	239.10	5
ST-6	8.57	45.10	8.27	35.70	76.39	295.00	7.74	41.21	7.48	30.47	71.45	227.92	5
ST-7	8.57	45.10	8.27	35.70	76.39	295.00	7.65	41.69	7.25	31.95	72.63	231.64	5
ST-8	8.57	45.10	8.27	35.70	76.39	295.00	7.69	41.26	7.11	31.86	71.39	226.52	5
ST-9	8.57	45.10	8.27	35.70	76.39	295.00	7.76	41.19	7.48	31.07	72.71	232.40	5
ST-10	8.57	45.10	8.27	35.70	76.39	295.00	7.64	41.31	7.00	31.56	70.00	220.92	5
ST-11	8.57	45.10	8.27	35.70	76.39	295.00	7.54	40.79	7.11	31.21	72.15	221.90	5
ST-12	8.57	45.10	8.27	35.70	76.39	295.00	7.66	41.92	7.38	30.89	70.99	227.97	5
ST-13	8.57	45.10	8.27	35.70	76.39	295.00	8.10	41.91	7.89	30.61	71.14	241.51	5
ST-14	8.57	45.10	8.27	35.70	76.39	295.00	7.87	40.75	7.32	30.94	70.62	226.48	5
ST-15	8.57	45.10	8.27	35.70	76.39	295.00	7.81	40.74	7.31	31.66	72.74	231.43	5

Table 4- 2: Input VI Data of NSPP for MatLab Program

Module	Front glass lightly soiled	Front glass heavily soiled	Front glass crack	Front glass crazing	Front glass shattered	Front glass chip	Front glass milky discoloration	Rear glass crazing	Rear glass crack	Rear glass shattered
ST-1	1	0	0	0	0	0	0	0	0	0
ST-2	1	0	0	0	0	0	0	0	0	0
ST-3	1	0	0	0	0	0	0	0	0	0
ST-4	1	0	0	0	0	0	0	0	0	0
ST-5	1	0	0	0	0	0	0	0	0	0
ST-6	1	0	0	0	0	0	0	0	0	0
ST-7	1	0	0	0	0	0	0	0	0	0
ST-8	1	0	0	0	0	0	0	0	0	0
ST-9	1	0	0	0	0	0	0	0	0	0
ST-10	1	0	0	0	0	0	0	0	0	0
ST-11	1	0	0	0	0	0	0	0	0	0
ST-12	1	0	0	0	0	0	0	0	0	0
ST-13	1	0	0	0	0	0	0	0	0	0
ST-14	1	0	0	0	0	0	0	0	0	0
ST-15	1	0	0	0	0	0	0	0	0	0

Also, the number of columns for the VI database is 86 defects/failures with the exception of the 'module' column. To specify the existence of a defect/failure for the VI database, a '1' is entered, otherwise a '0' to denote an absence as indicated in **Table 4-2**.

4.5 Developed MatLab program flowcharts.

The MatLab Program used for the analysis of the collected data is in two main parts; that is the RPN program and Correlation program. The Steps for the development of the entire MatLab program can be accessed in (Moorthy, 2015). Brief information and flow charts for each sub program is provided in this work.

4.5.1 RPN Program Flowchart

The RPN program is made up of sub programs for determining the Safety RPN, Performance RPN, Global RPN and a Pie Chart. Based on the objectives of this work, various statistical analysis of the Program output information could be made. The flowchart for determining the various RPN values as summarized in Section 4.5.2 to 4.5.4.

4.5.2 Performance RPN Flowchart

The steps to follow in calculating the Performance RPN using MATLAB is outlined in **figure 4-1**.

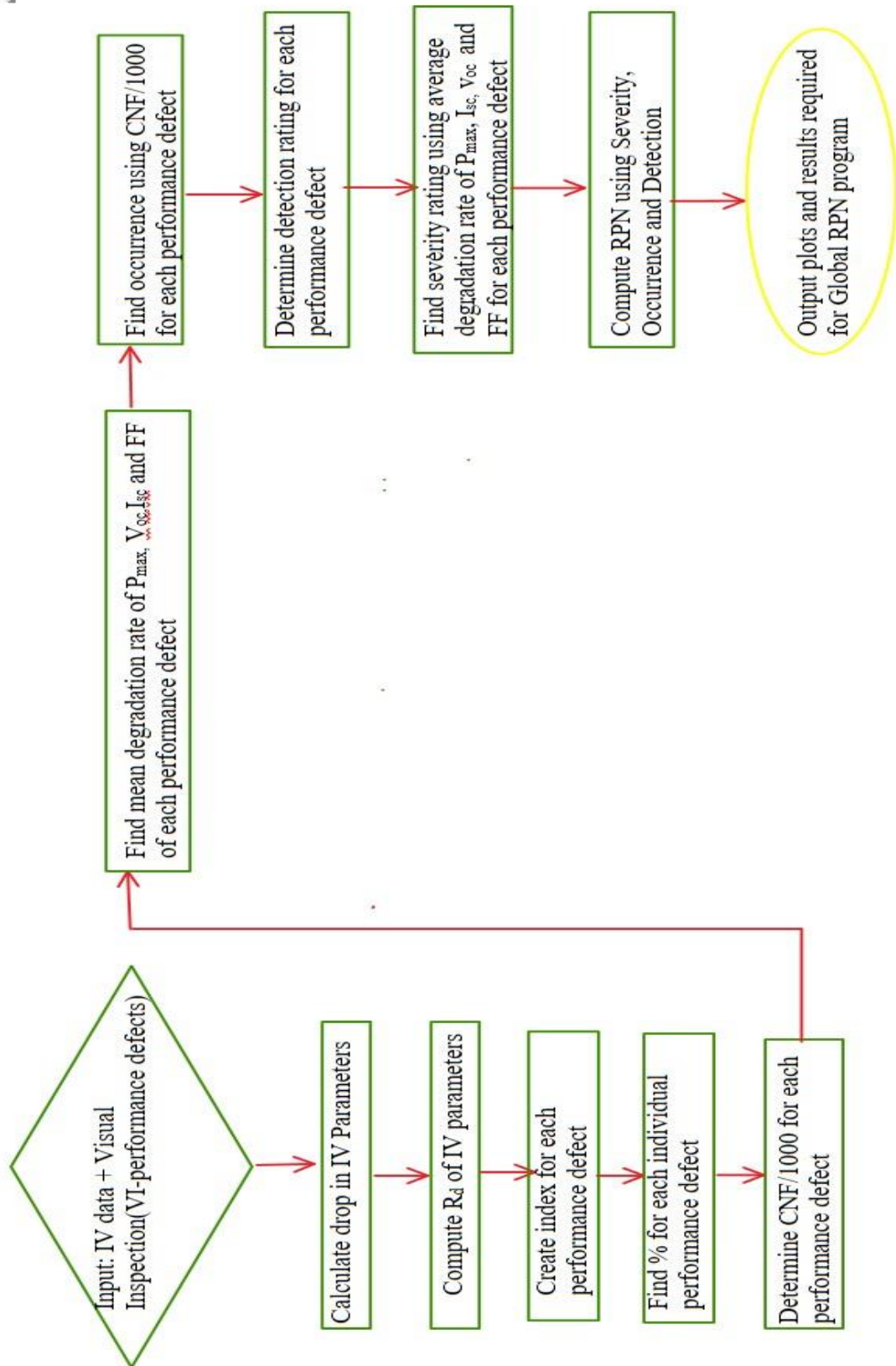


Figure 4- 1: Flow Chart for Computing Performance RPN.

4.5.3 Safety RPN flowchart

Similar to the Performance RPN procedure, the following steps are involved in computing the Safety RPN values using the MATLAB program as outlined in **figure 4-2**.

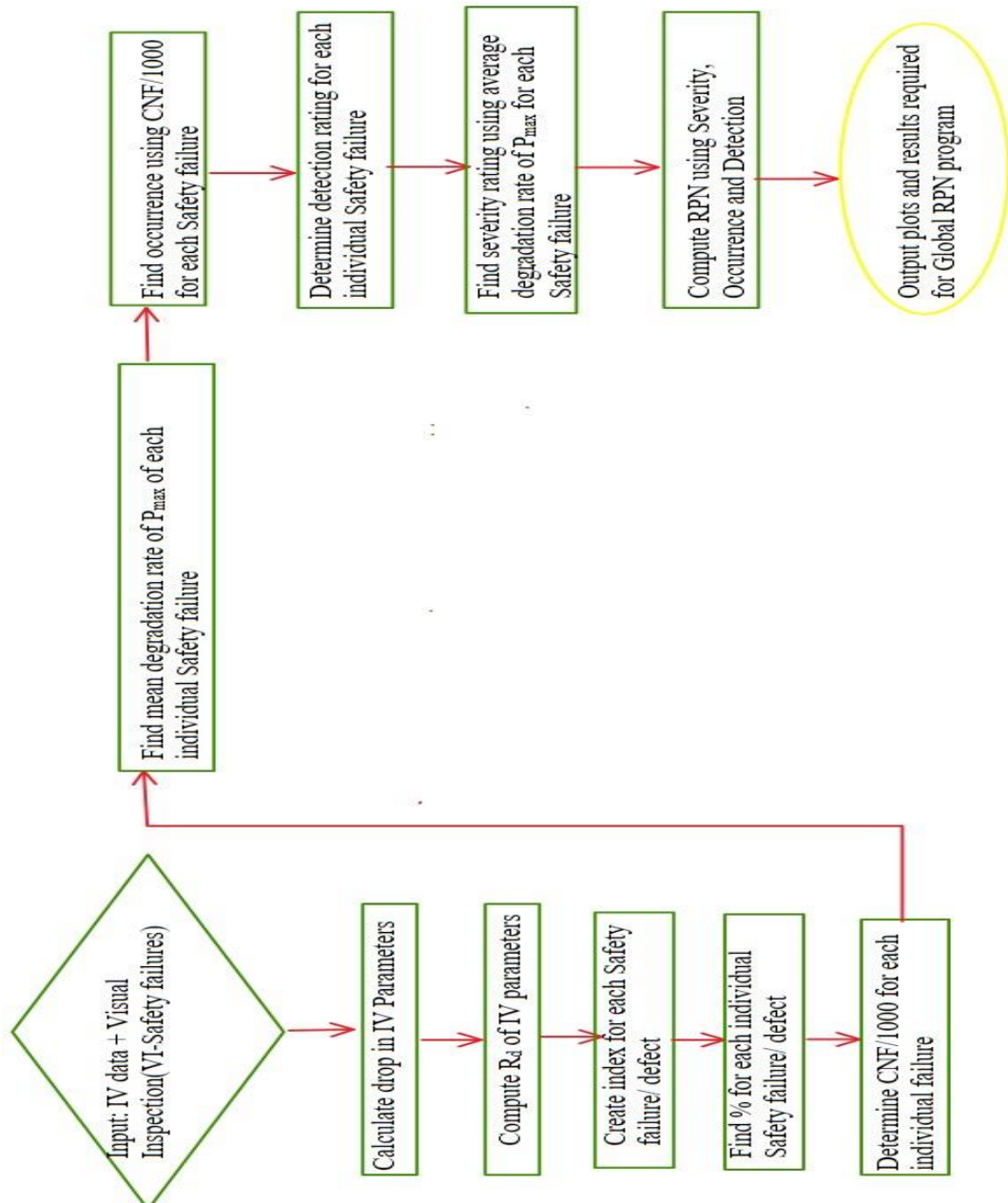


Figure 4- 2: Flow Chart for Computing Safety RPN

(Moorthy, 2015)

(Moorthy, 2015)

4.5.3 Global RPN Flowchart

Based on the safety and performance RPN program, the Global RPN process is determined as outlined in **figure 4-3**.

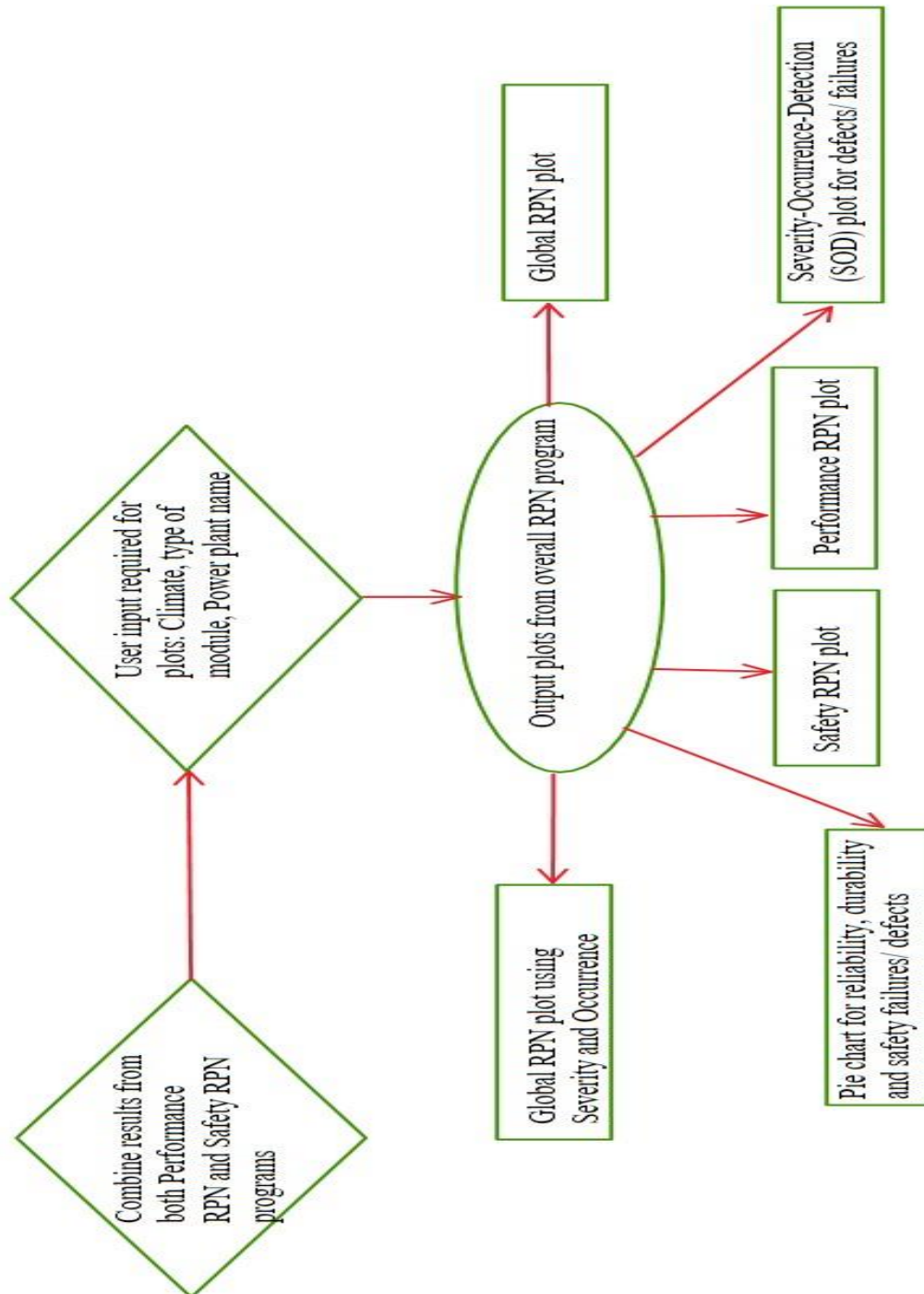


Figure 4- 3: Flow Chart for Computing Global RPN

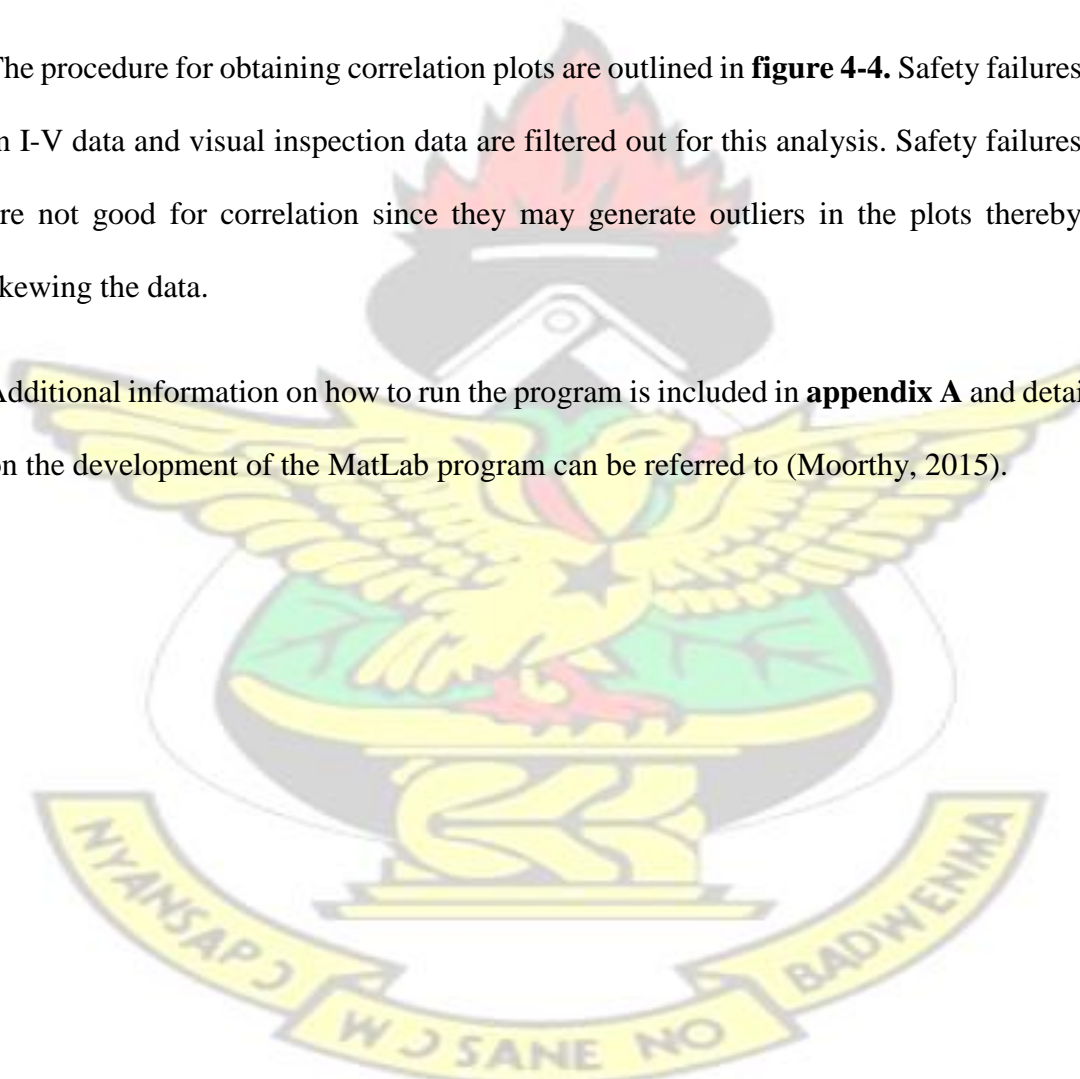
The Global RPN program integrates results of both safety and performance RPN for computing Global RPN for the overall plant. At the end of the program, various plots are generated for analysis. Such plots include safety RPN, Performance RPN, Global RPN charts and pie chart for comparing reliability, durability and safety failures.

KNUST

4.5.4 Correlation Program Flowchart

The procedure for obtaining correlation plots are outlined in **figure 4-4**. Safety failures in I-V data and visual inspection data are filtered out for this analysis. Safety failures are not good for correlation since they may generate outliers in the plots thereby skewing the data.

Additional information on how to run the program is included in **appendix A** and details on the development of the MatLab program can be referred to (Moorthy, 2015).



(Moorthy, 2015)

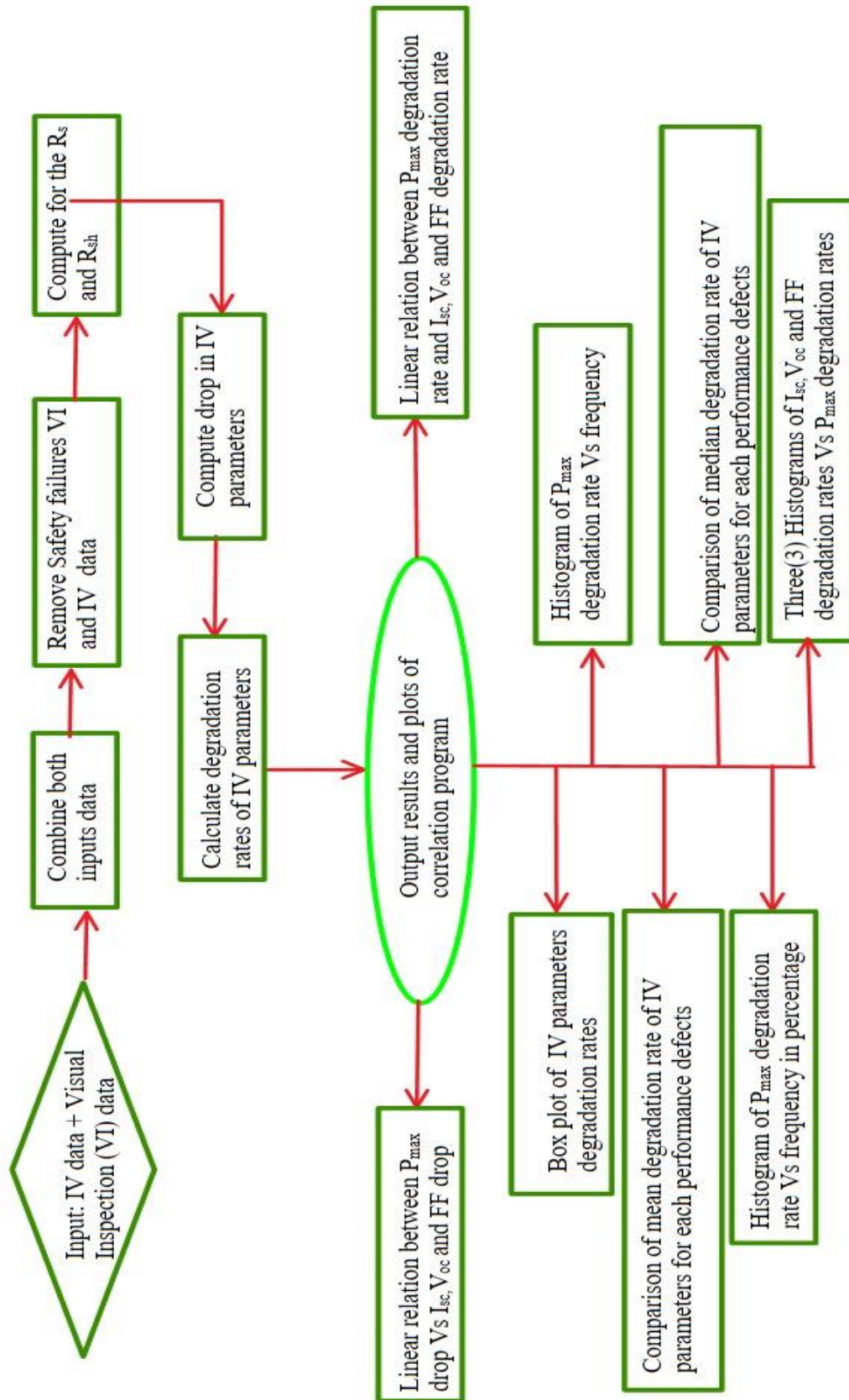
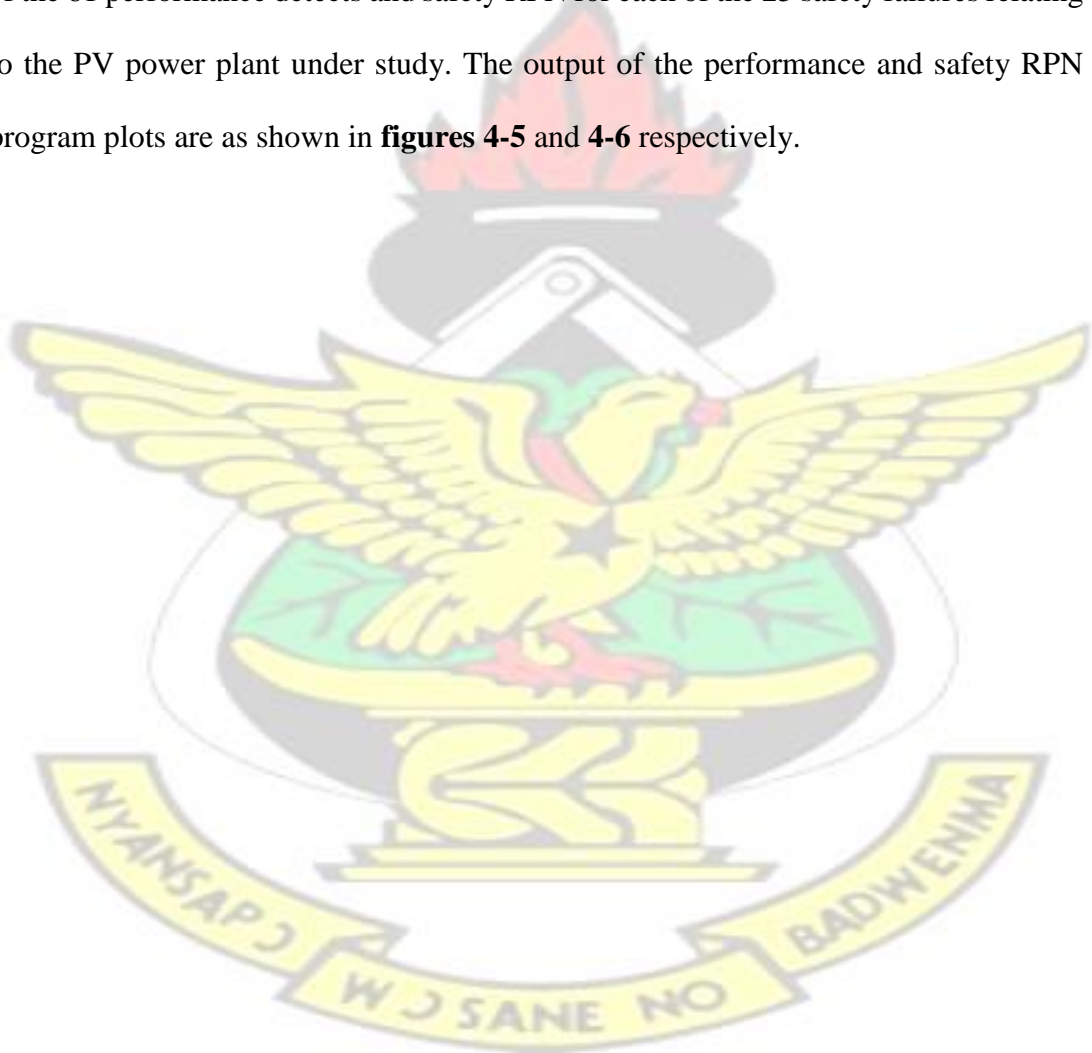


Figure 4- 4: Flow Chart for Correlation Analysis

4.7 Determination of the Performance and Safety RPN using P_{max} Degradation Rates.

The Safety and Performance RPN values can automatically be computed using FMECA-RPN method given by Shrestha et al for the observed data set from any PV power plant resorting to the severity calculated using P_{max} degradation rate. Based on the output results, a bar plot is generated to recognize the performance RPN for each of the 61 performance detects and safety RPN for each of the 25 safety failures relating to the PV power plant under study. The output of the performance and safety RPN program plots are as shown in **figures 4-5** and **4-6** respectively.



(Moorthy, 2015)

KNUST

Performance RPN - NSPP-Model A

Modules - 74 (Poly-Si); Hot Dry climate; Field Age - 5; Total Performance RPN - 1026

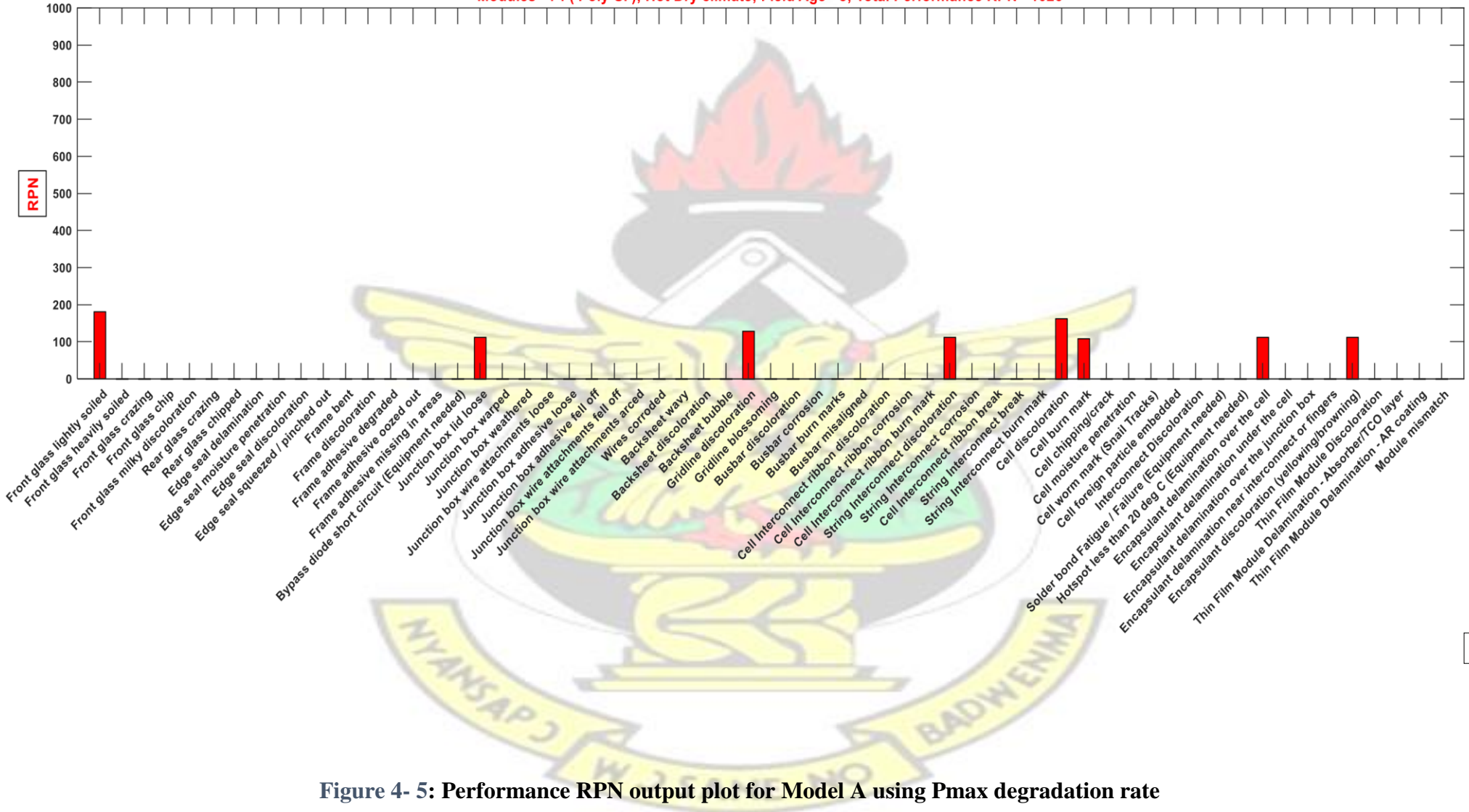
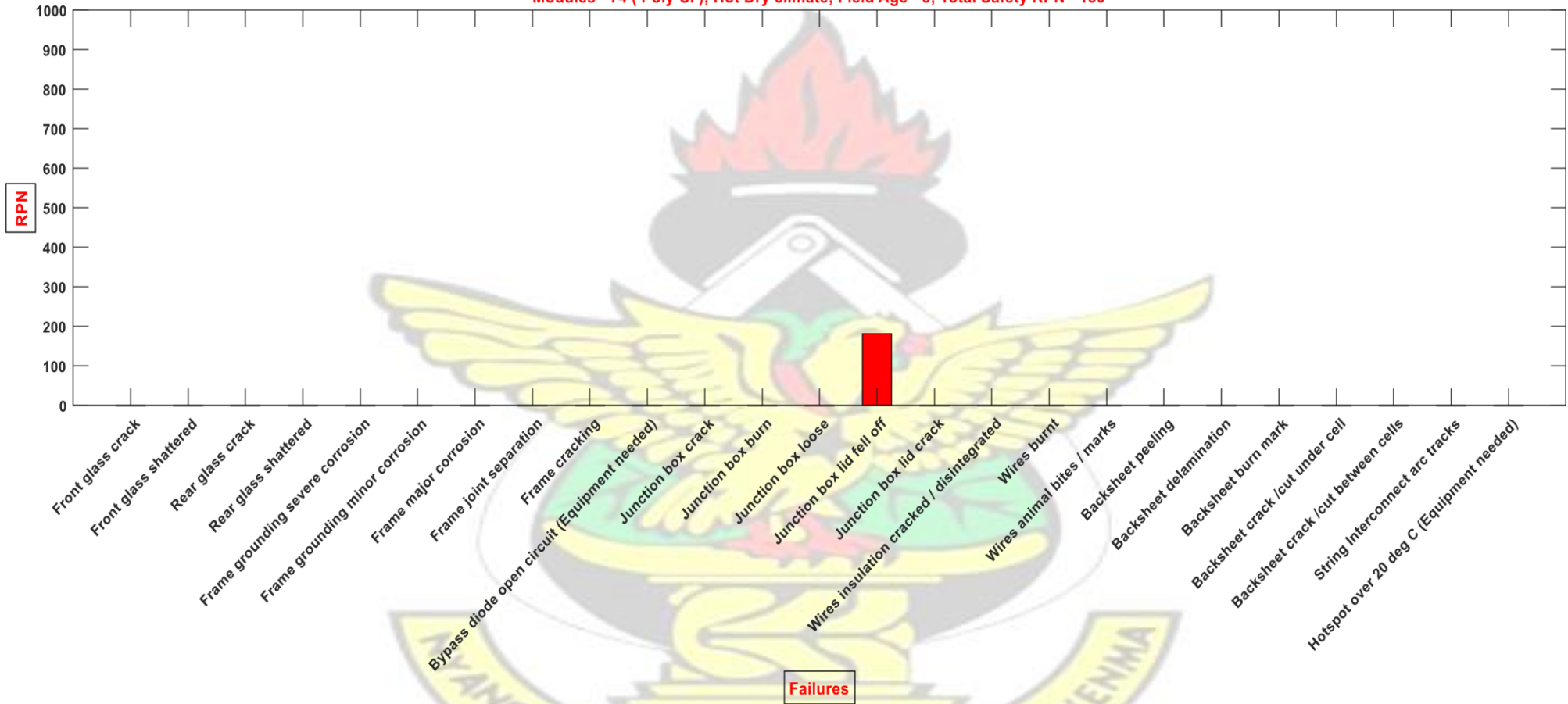


Figure 4- 5: Performance RPN output plot for Model A using Pmax degradation rate

KNUST

Safety RPN - NSPP-Model A
Modules - 74 (Poly-Si); Hot Dry climate; Field Age - 5; Total Safety RPN - 180



Failures

Figure 4- 6: Safety RPN output plot for Model A using Pmax degradation rate.

KNUST



From figures 4-5 and 4-6, it can be seen that only defects present in the PV plant are indicated with bars and the defects with the longest bars have maximum RPN values indicating dominant failures. Also, total performance RPN is given in the plot, which can be used for rating PV power plants in relation to performance and safety issues of the modules.

4.8 Determination of the Performance RPN using I_{sc} , V_{oc} and FF Degradation Rates.

The performance RPN can also be determined using the degradation rates (%/yr.) of IV parameters such as I_{sc} , V_{oc} and FF separately from the P_{max} scenario above. Based on the output, a bar plot is generated to specify the performance RPN for the defects that are present in the PV plant under study. The output of this analysis is presented in figure 4-7.

From figure 4-7, the IV parameter that is influencing the P_{max} degradation based on the RPN value for different defects can be identified. It can also be used as a measureable information along with correlation results to identify the IV parameter responsible for the P_{max} degradation rate for a specific defect.

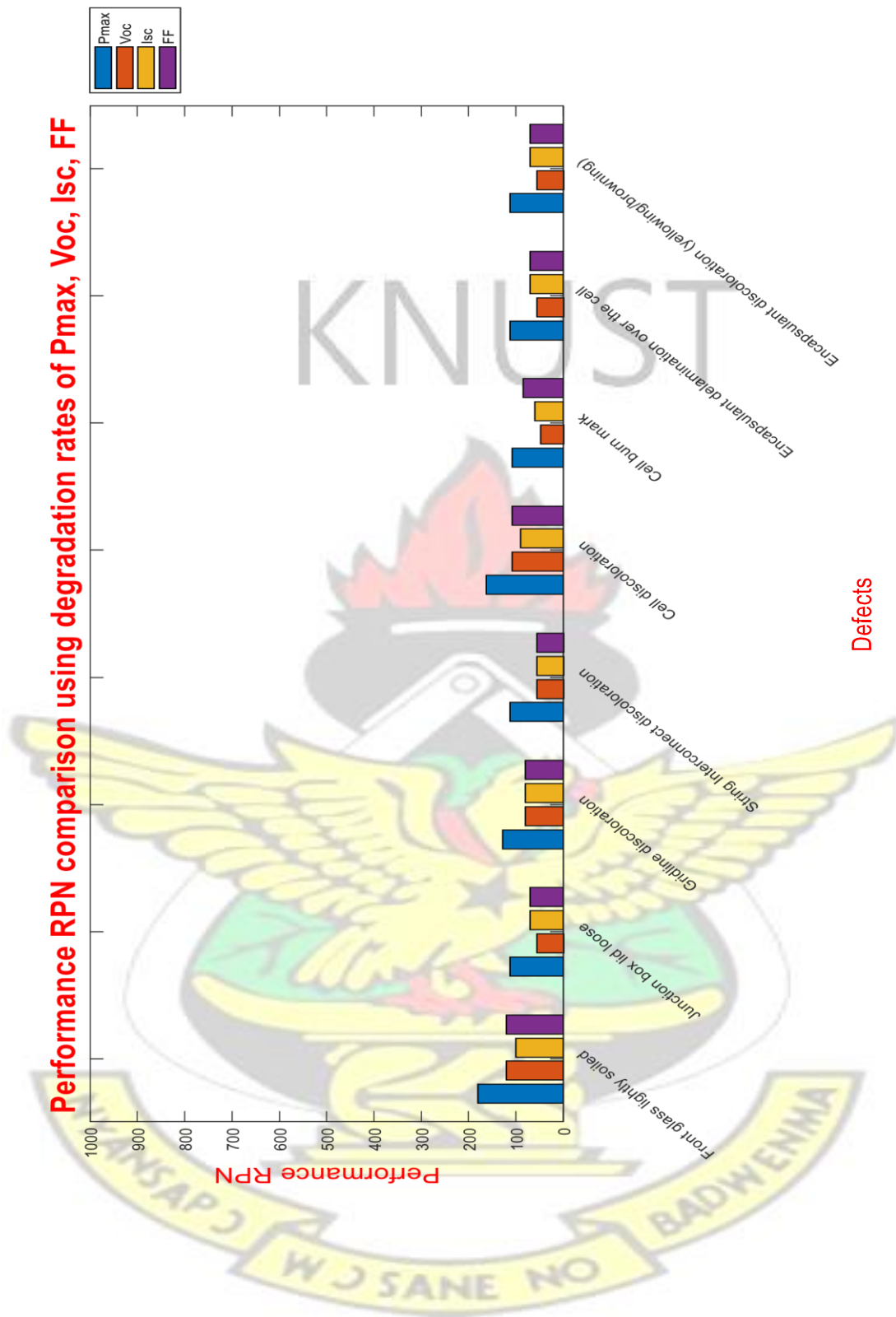


Figure 4- 7: Performance RPN output plot using I-V Parameter's degradation rate.

CHAPTER 5: DISCUSSIONS OF RESULTS

This chapter discusses the output of the developed MatLab Program; that is the RPN program and correlation program and their corresponding interpretations.

5.1 RPN program results

As explained in the previous chapter, the Global RPN program was coded to carry out the FMECA-RPN computations for this study. The results of the program are discussed as follows.

5.1.1 Determination of Global RPN for Model A

The Global RPN adds the Safety and Performance RPN together. **Table 5-1** summarizes the results for the FMECA analysis. Also, the global RPN plot gives the defects present in the PV plant as performance defects and Safety failures combine as one bar plot as shown in **figure 5-1**. Failure mode in a particular PV plant that needs immediate attention to avoid performance loss, property loss and threat or loss of personnel is obtained. It also aids in identifying issues with the design, material selection and manufacturing issues by PV module manufacturers in future productions.

KNUST

Table 5- 1: summary for FMECA results for Model-A

Defects/failure modes	Total count	Percentage	Average_Degradation	CNF/1000	Severity	Occurence	Detection	RPN	RPN_S
Encapsulant delamination over the cell	2	2.702702703	1.761077966	5.405405405	8	7	2	112	56
Encapsulant discoloration (yellowing/browning)	2	2.702702703	1.761077966	5.405405405	8	7	2	112	56
Gridline discoloration	4	5.405405405	1.918338983	10.81081081	8	8	2	128	64
Junction box lid loose	2	2.702702703	1.761077966	5.405405405	8	7	2	112	56
String Interconnect discoloration	3	4.054054054	1.592745763	8.108108108	8	7	2	112	56
Cell burn mark	1	1.351351351	2.266074576	2.702702703	9	6	2	108	54
Cell discoloration	13	17.56756757	2.323067014	35.13513514	9	9	2	162	81
Front glass lightly soiled	34	45.94594595	2.41378325	91.89189189	9	10	2	180	90
Junction box lid fell off	12	16.21621622	2.40510226	32.43243243	10	9	2	180	90



KNUST



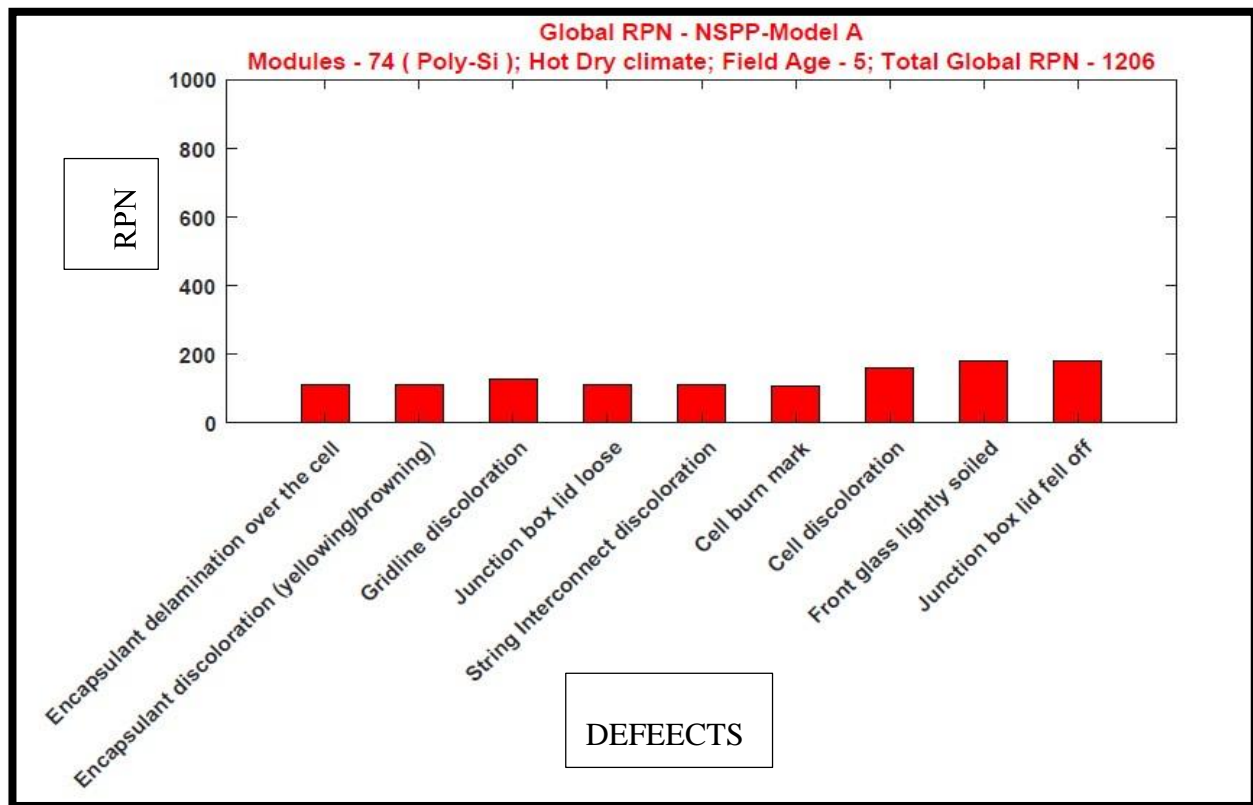


Figure 5- 1: Global RPN Plot for Model- A using occurrence, detection and severity

Discussions

The defects that are present on the 74 observed modules of model A is presented in figure 5-

1. It was realized that;

- i. The RPN values are nearly constant for the first 6 defects and increases in the remaining 3 defects observed on the field, namely cell discoloration, front glass slightly soiled and junction box lid fell off.
- ii. Junction box lid fell off was obtained as the safety issue, wherein, the rest of the failures in the figure are considered to add to the increase in degradation rate (performance issues).

- iii. In all, nine defects were determined of which ‘front glass slightly soiled’ and ‘junction box lid fell off’; both having RPN value of 180 each were the dominant defects for the modules considered.
- iv. The global RPN for this model A was determined automatically with the software as 1206 as shown in **figure 5-1**. This value represents the addition of all the RPN of failures observed on the field for the Model. This information can lead to grading of the PV plant and the financial risk computations of the modules for decision making for future products.

Moreover, considering all the failures can easily be detected by physical observation, the Global RPN was again computed using the occurrence and severity neglecting detection as indicated in figure 5-2. The following observations were made from the plot;

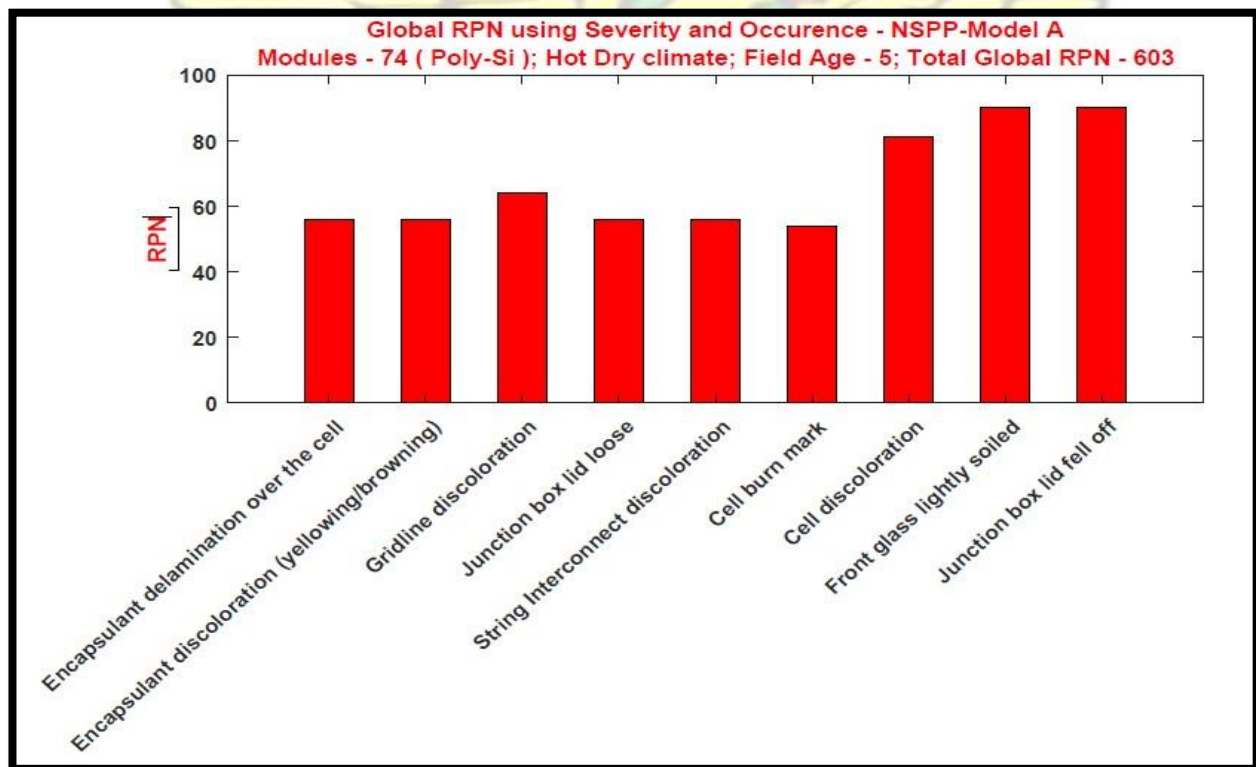


Figure 5- 2: Global RPN plot using Severity and Occurrence for Model- A.

Discussion

- i. It can be deduced from **figure 5-2** that the RPN values of the defects were halved shown in **Table 5-1**.
- ii. This could be due to the visual inspection that was used in the collection of the data and was assigned a detection value of two (see **Appendix D for Detection ranking**). For instance, the RPN value of front glass slightly soiled is 90. This provides a better view on the RPN value instead of 180 as depicted in figure 5-1.

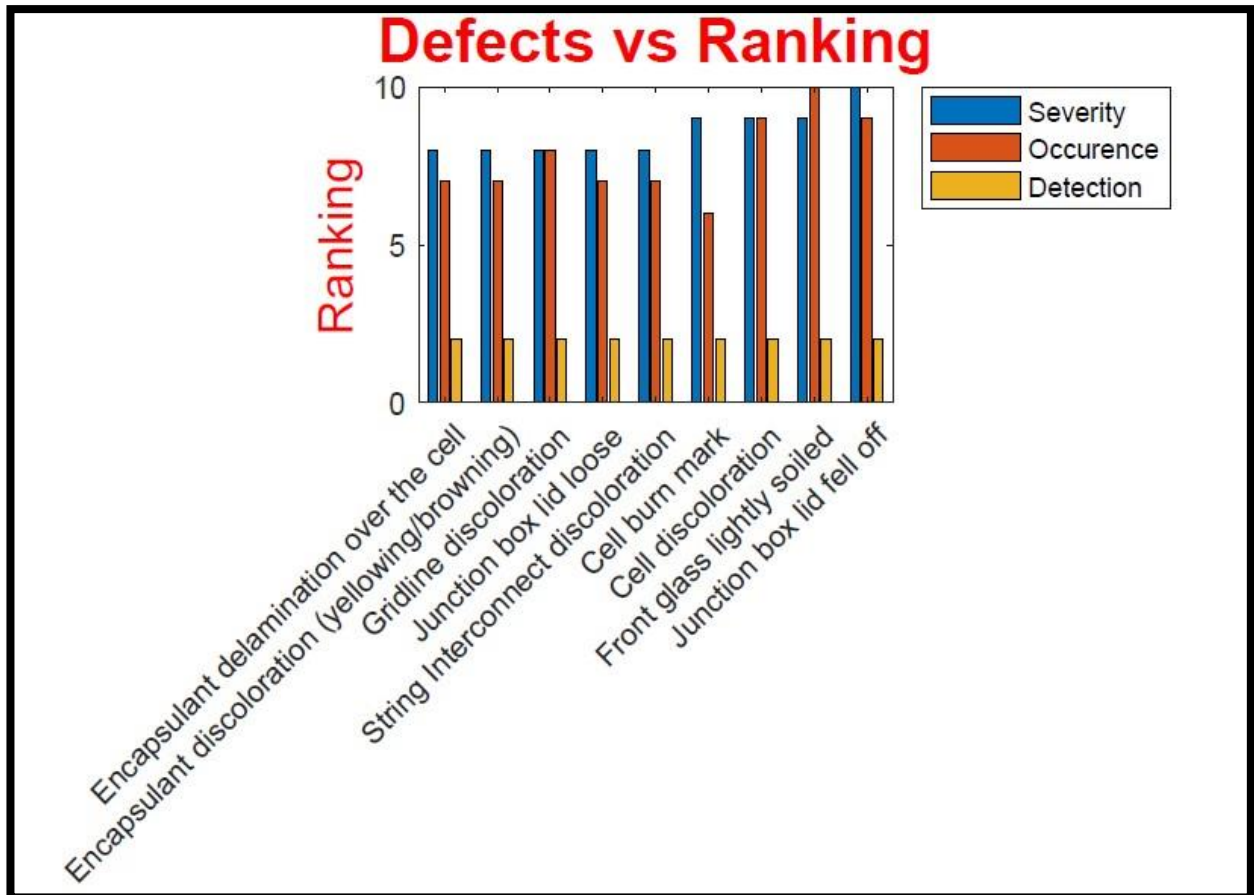
5.1.2 Defects Ranking Plot for Global RPN

The defects - ranking plot gives visual representation of the failures present in the PV plant as plotted in figure 4-3 for Model A. The x-axis contains the failures and the yaxis contains their ranking with respect to occurrence, severity and detection. This plot helps to identify failures that occur more frequently and more severe in the plant.

Figure 5- 3: Defects - Ranking Plot for Model –A.

Discussions

From figure 5-3, it can be observed that;



- i. All the failures present have detection rank of two as explained earlier.
- ii. Front glass slightly soiled can be seen to occur more frequently among the modules since it has the highest occurrence value. This can be associated with the fact that the site is located in an environment with relatively dusty particles in the atmosphere.
- iii. Again, the effect of ‘junction box lid fell off’ on the modules performance is more severe compared to the other defects with the highest severity ranking.

5.1.3 Pie Chart for Reliability, Durability and Safety failures.

The proportion occupied by Durability loss, Reliability failures and safety failures is represented graphically using the pie chart shown in figure 5-4. This helps to quantify the percentage of modules that need urgent replacement to avert property loss and personnel threat or loss in the PV plant. Also, percentage of modules which are still functioning well with power degradation rates less than 1%/ year (Durability loss) are established whilst those which can qualify for warranty for losing power at a rate of more than 1%/ year (Reliability failures) are known.

Figure 5- 4: Pie Chart of Reliability, Durability and Safety Issues for Model- A



Discussion

When extrapolating the measured module degradation and including the safety failures, It can be deduced that, for Model-A;

- i. Thirty-two percent (32%) of the modules meet the manufacturer's warranty of 1%/year and are safe. That is, their degradation rate is lower than the standard limit and can still operate on the field.
- ii. Sixteen percent (16%) of modules being safety failures; hence can pose safety issues to users on the field.
- iii. Fifty-one percent (51%) of modules have degradation rates higher than the manufacturer's usual warranty of 1%/ year as indicated in figure 5-4 and needs to be replaced to maximize the performance of the plant.

5.2 Correlation program output Plots

The correlation program is coded to assist in computing different statistical plots and determine the correlation between P_{\max} degradation rate and the remaining I-V parameters to specify which I-V parameter is responsible for P_{\max} degradation based on the field defects.

It is to be noted that, after careful observation of the data and reference from literature; it was filtered using 2.0%/year degradation rate as upper limit. This presupposes that, modules with safety failures and degradation rates greater than 2.0%/year were excluded from the analysis. This is to avoid skewing of the data because of outliers. Out of the 74 modules data collected, 42 modules were considered for the model-A correlation analysis. The output plots of the program is as follows.

5.2.1 Histogram for Pmax Rd for Model A

Histogram is plotted for P_{\max} degradation rate (%/year) to aid identify the distribution of Pmax degradation rates of the PV modules and the frequency of modules for a specific degradation rate as shown in **figure 5-5**.

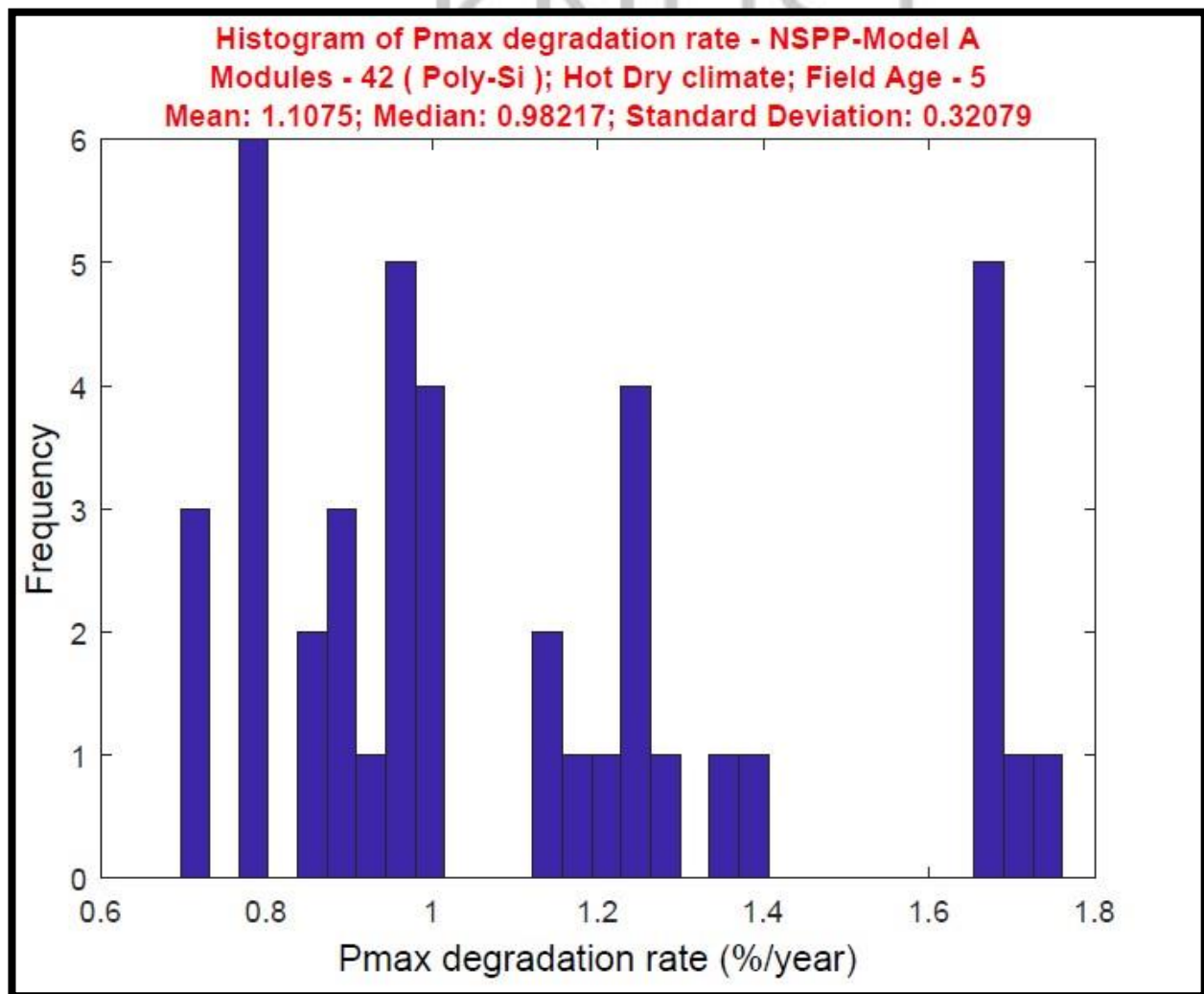


Figure 5- 5: Histogram of Pmax degradation rate for Model- A

Discussions

The histogram shown in Figure 5-5 provides the average and median degradation rate of power for Model-A. The following inferences could be deduced from the plot;

- i. The histogram fits a near-normal distribution. The average degradation rate of power for Model A is 1.11%/year.
- ii. Out of the 42 modules considered, 24 modules (approximately 57%) meet the maximum degradation rate of 1.0%/year typically given by module producers.
- iii. The median and average degradations are very close to each other (that is, 1.11%/year vs. 0.98%/year), indicating a tight quality management system during production.

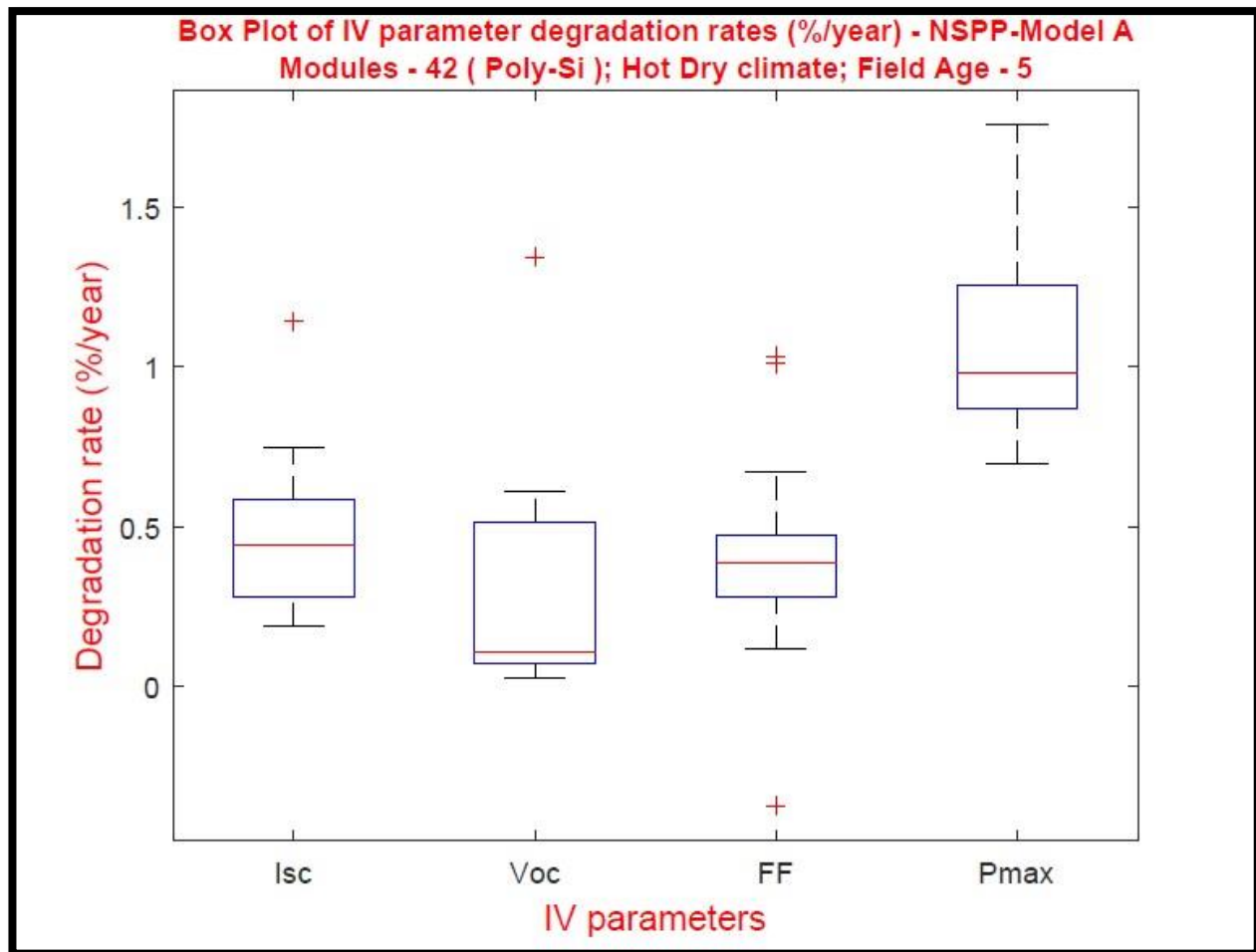
5.2.2 Determination of Dominant IV Parameter Degradation Rates

Grouped by the I-V parameters, box plot of the degradation rates (%/year) was plotted as shown in figure 5-6. This helps to find the correlation of P_{max} degradation rate with the other I-V parameters (V_{oc} , I_{sc} and FF) degradation rates of the modules. Also dominant I-V parameter responsible for the P_{max} degradation is determined in a specific PV plant.

5.2.2.1: Box Plot of I-V parameters degradation rates for Model- A

The box plot for the various I-V parameters degradations rates for model-A is shown in figure 5-6.

Figure 5- 6: Box Plot of I-V Parameters degradation rates for Model- A



Discussions

It was observed that four different box plots were generated; each for the different I-V parameters of the modules. From figure 5-6; it can be deduced that;

- i. Apparently, Isc degradation rate (%/year) and FF degradation rate have effect on Pmax degradation (%/year). This is so because the median degradation rates values of Isc and FF are close to that of Pmax from the box plot.
- ii. The order of IV parameters influencing Pmax degradation rates (%/year) is given as $Isc > FF \gg Voc$.

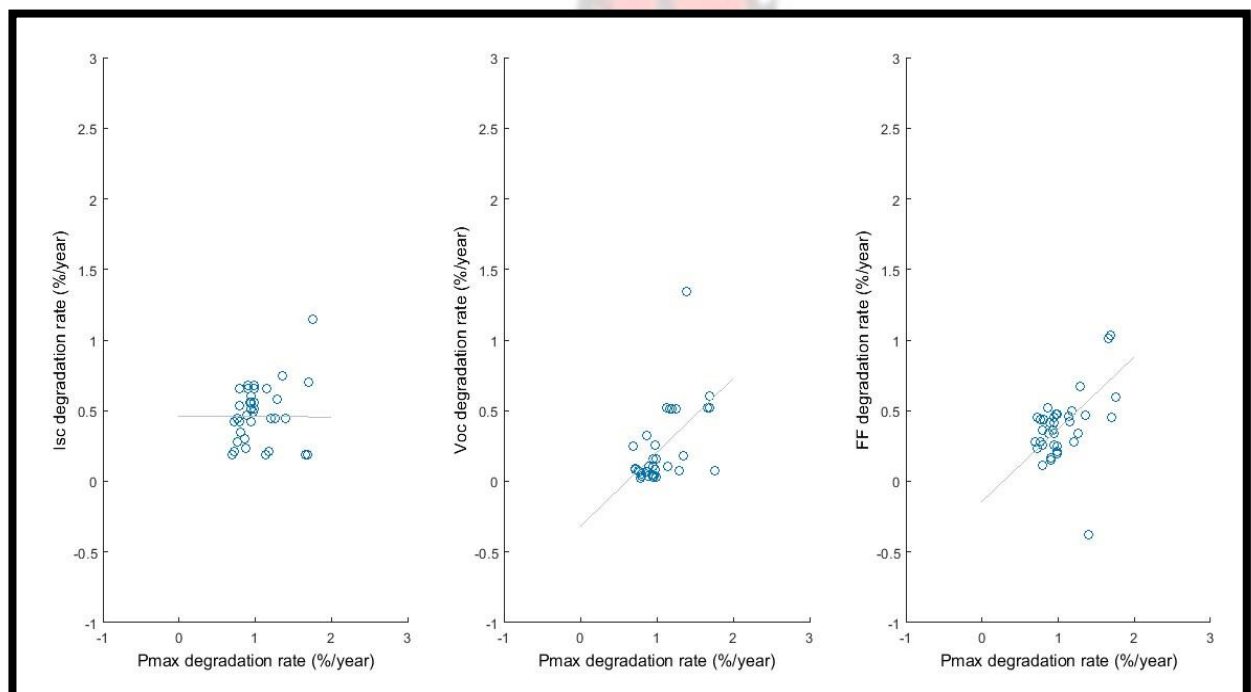
The linear relation between Pmax degradation rates and that of Isc, Voc and FF is plotted as indicated in figure 5-7. This will help us understand the linear relationship

between Pmax degradation rate and other major IV parameters. **5.2.2.2: Linear**

Relation plot of I-V parameters for model-A

Figure 5-7 shows the linear relation plot of I-V parameters for model A. This plot further aids in determining the particular I-V parameter degradation that affects that of the maximum power degradation rate in the modules.

Figure 5- 7: Linear Relation Plot of I-V Parameters for Model-A



Discussions

It can be seen from figure 5-7 that;

- iii. There is a linear relationship between the FF degradation rate and Pmax degradation rate and that of Voc degradation rate and P_{max} .
- iv. However, the linear relation between I_{sc} degradation rate and that of P_{max} is relatively insignificant as compared to V_{oc} and FF.

- v. It was deduced that, Isc has relatively similar degradation rates to Pmax degradation rates and what causes this trend is to be determined with other statistical techniques.

Moreover, plotting histogram of Isc/Voc/FF degradation rates and that of Pmax on the same plot helps in finding the influence of Isc/Voc/FF degradation rates on Pmax degradation rates in a form of overlap of the histograms or otherwise as shown in figure 5-8, figure 5-9 and figure 5-10.

5.2.2.3: Combined Histogram of Isc and Pmax degradation rate for Model-A

Figure 5-8 shows the combined histogram of Isc and Pmax degradation rate for Model-A.

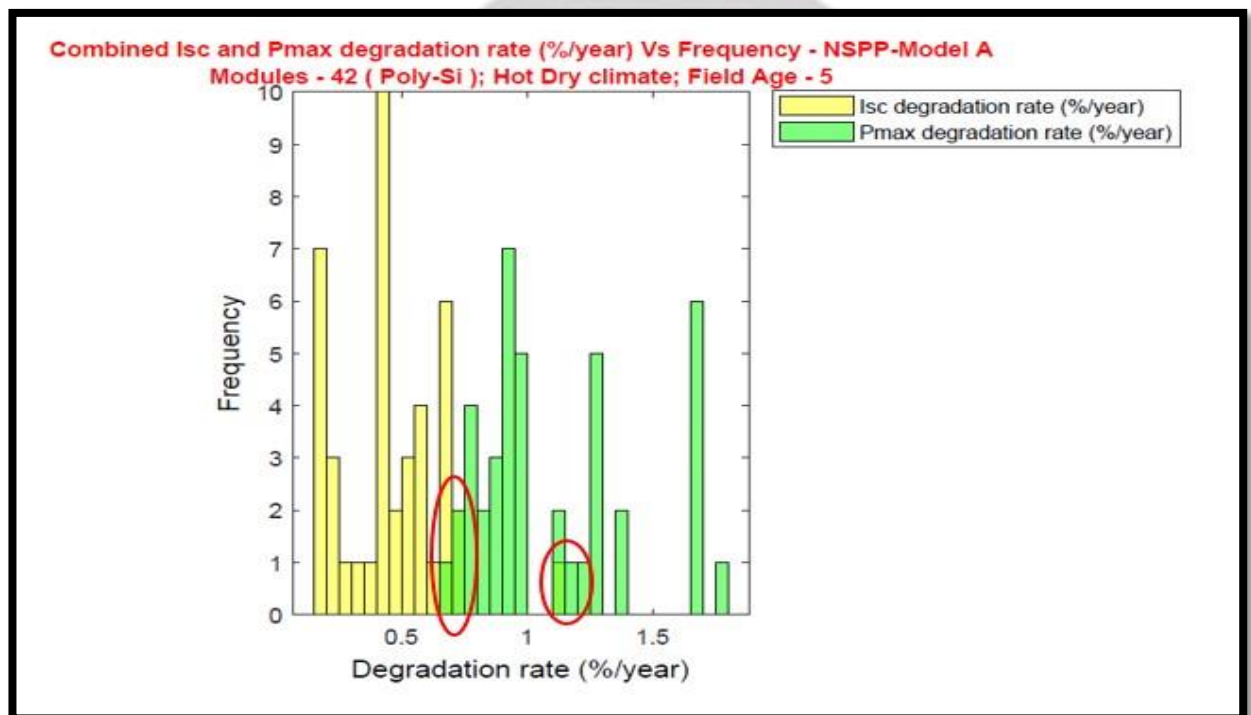


Figure 5- 8: Combined Histogram of Isc and Pmax degradation rate for ModelA.

5.2.2.4: Combined Histogram of FF and Pmax degradation rate for Model-A

Figure 5-9 shows the combined histogram of FF and Pmax degradation rate for Model-A.

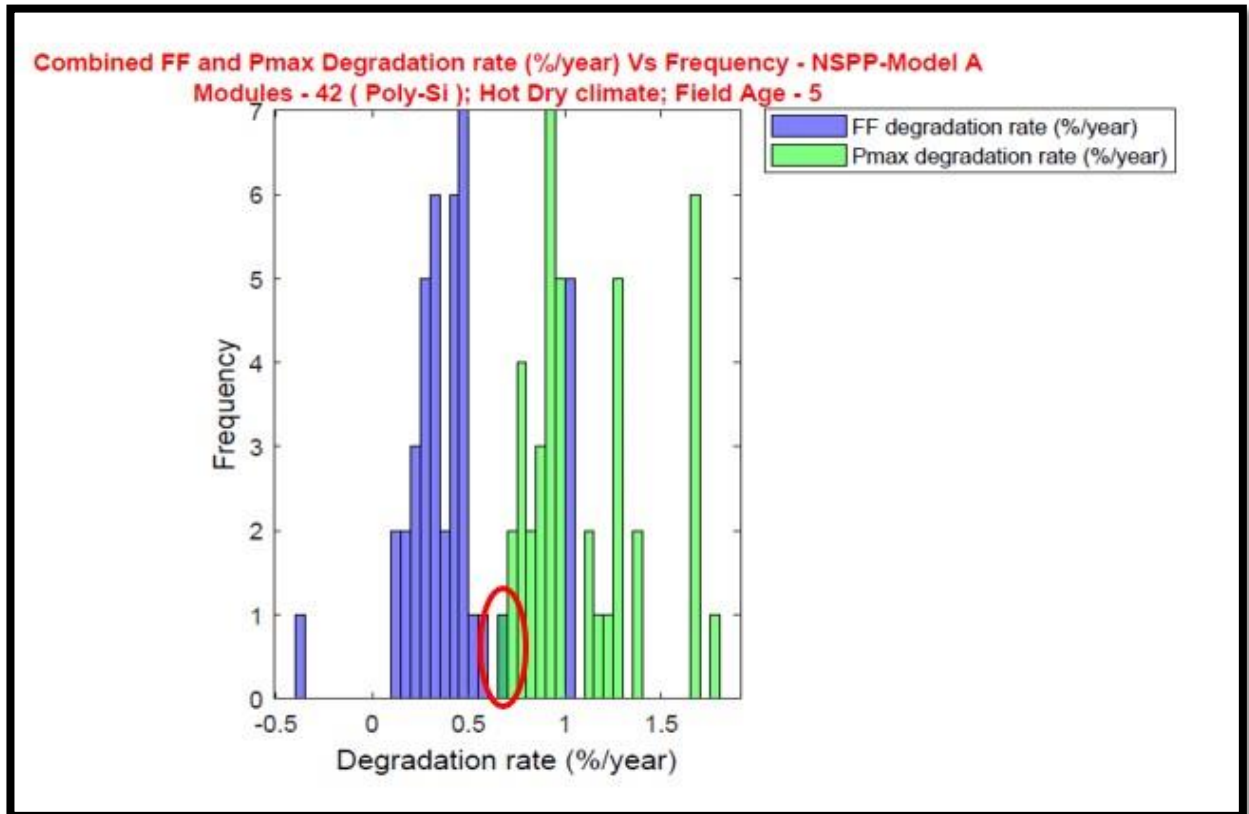
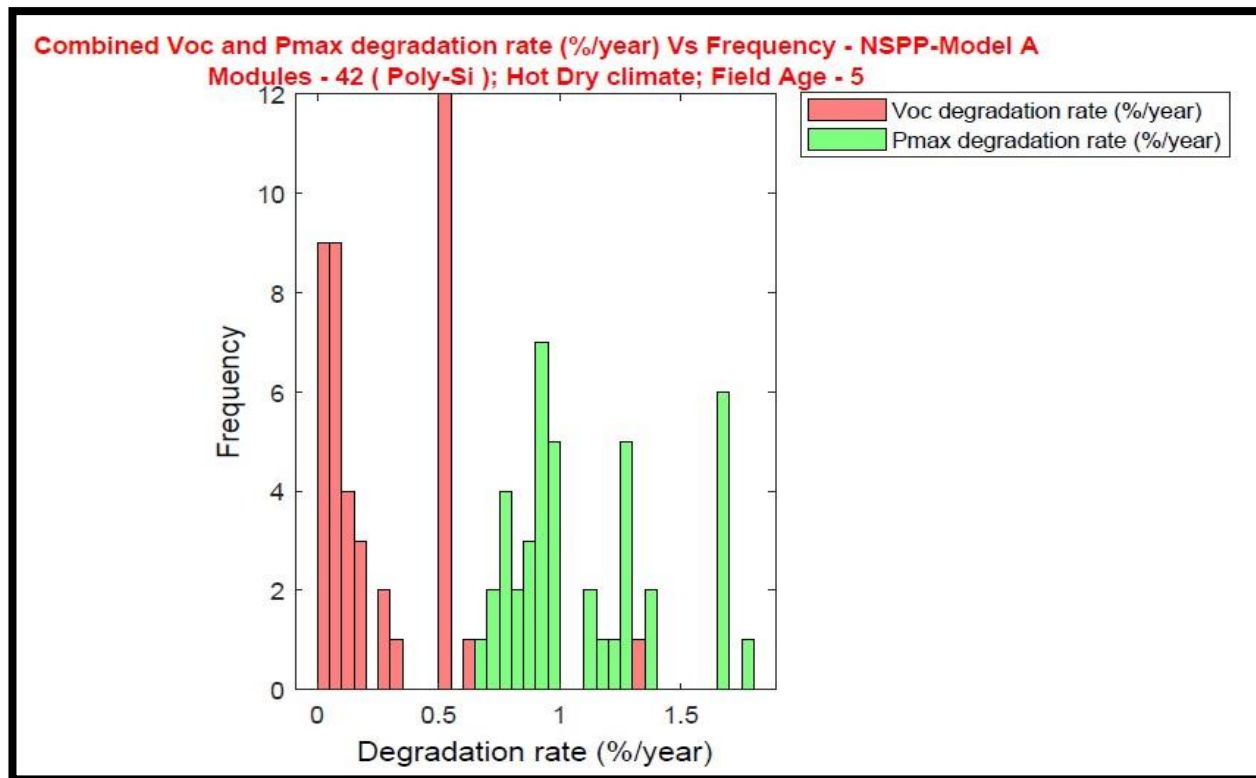


Figure 5- 9: Combined Histogram of FF and Pmax degradation rate for Model-A

5.2.2.5: Combined Histogram of Voc and Pmax degradation rate for Model-A

Figure 5-10 shows the combined histogram of Voc and Pmax degradation rate for Model- A.

Figure 5- 10: Combined Histogram of Voc and Pmax degradation rate for Model-A



Discussion

- i. It is evident from **figure 5-8** that, there is an overlap between I_{sc} and P_{max} degradation rates around 0.6%/year to 0.7%/year and around 1.2%/year to 1.25%/year, which suggests that degradation of I_{sc} is affecting P_{max} .
- ii. Again, it can be noticed that there is an overlap between FF degradation rates and P_{max} degradation rates in **figure 5-9** around 0.6%/year, which also denotes even FF degradation has an influence on P_{max} degradation but not in the same scale as I_{sc} degradation, which can be identified from the frequency or count of modules, affected.
- iii. In contrast, there is no overlap between V_{oc} and P_{max} degradation rates as shown in **figure 5-10**. This suggests that degradation of V_{oc} is not affecting degradation of P_{max} .

5.2.3 Comparison of Average Degradation Rates (%/year) of IV Parameters for Performance Defects

To identify the effect of degradation rates of various IV parameters on Pmax degradation rates based on failures, the median degradation rate (%/year) of IV parameters for different failures was plotted in figure 5-11. This plot is helpful in knowing the IV parameter that dominantly affect Pmax degradation rate for a particular defect based on average degradation rate and the order of parameters influencing Pmax degradation.



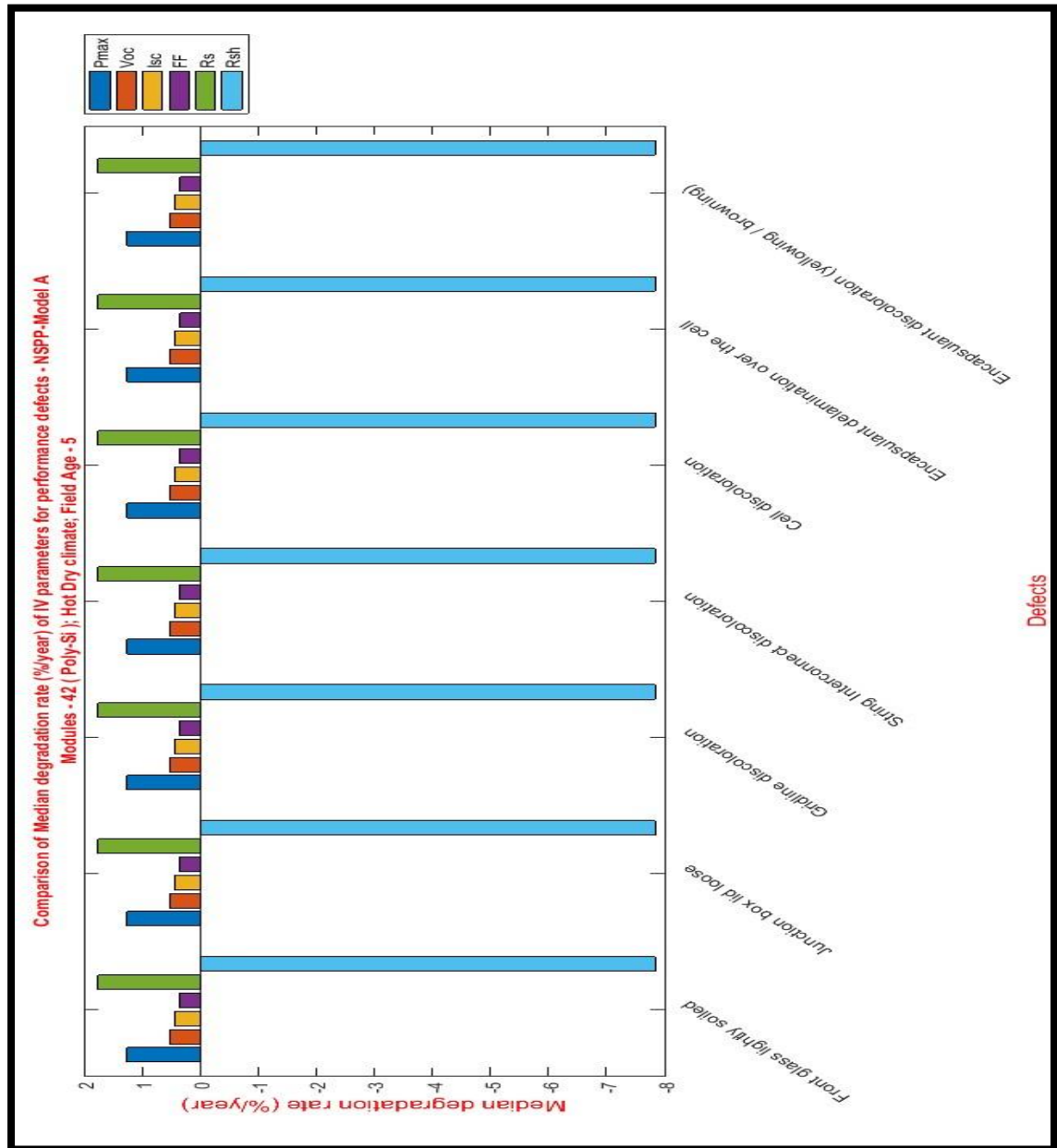


Figure 5- 11: Comparison Plot of Median degradation rates of I-V Parameters for Model-A Discussions

i. It is evident in figure 5-11, that for Gridline discoloration and string interconnect discoloration, the order of parameters affecting Pmax degradation will be as follows; $R_s > V_{oc} = I_{sc} > FF \gg R_{sh}$. ii. In addition, R_s has higher values for all the defects, which suggests that it affects degradation of Pmax using the defects.

iii. Similar conclusions can be drawn for the same plot using the mean degradation rates as included in Appendix C with other correlation plots.

5.3 Analysis of Results for NSPP- Model B

The sections to follow discuss the results for the second set of data collected from the same site. The summary for the FMECA Analysis results can be accessed in APPENDIX C for reference.

5.3.1 Determination of Global RPN – Performance RPN + Safety RPN

The Global RPN plot for Model-B is shown in figure 5-12.

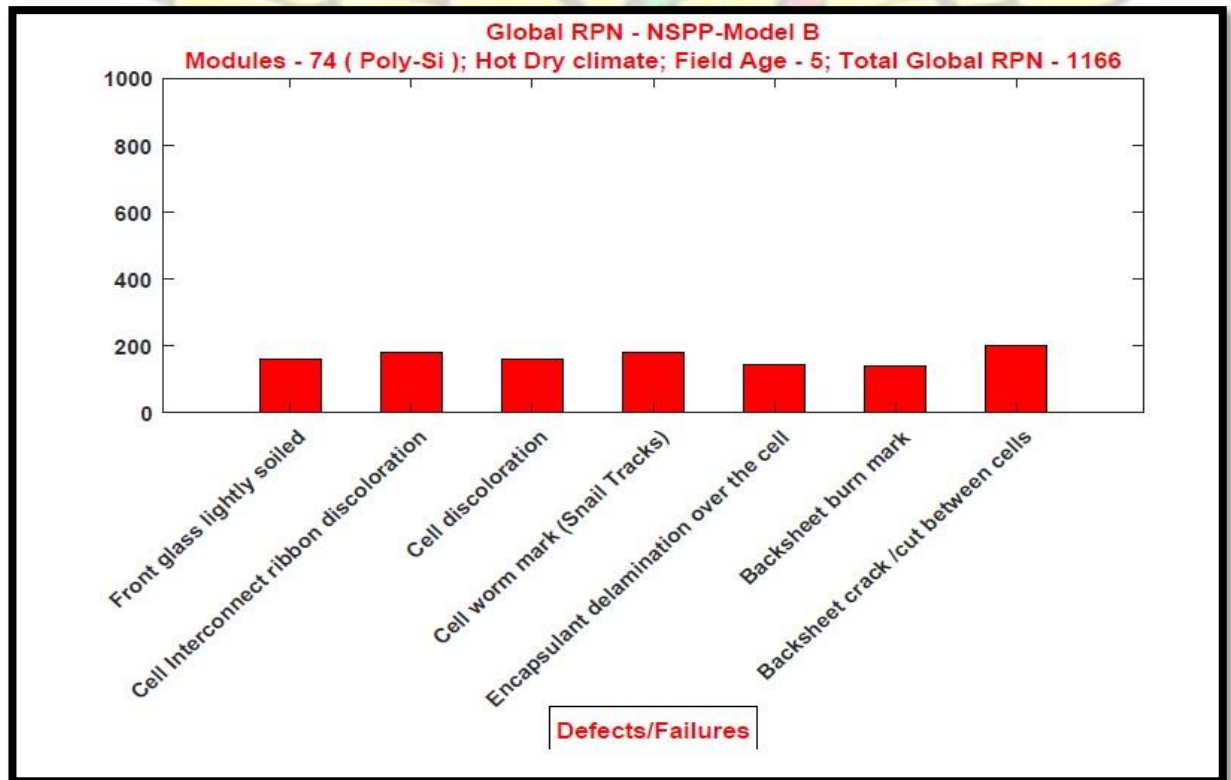


Figure 5- 12: Global RPN Plot for Model- B

Discussions

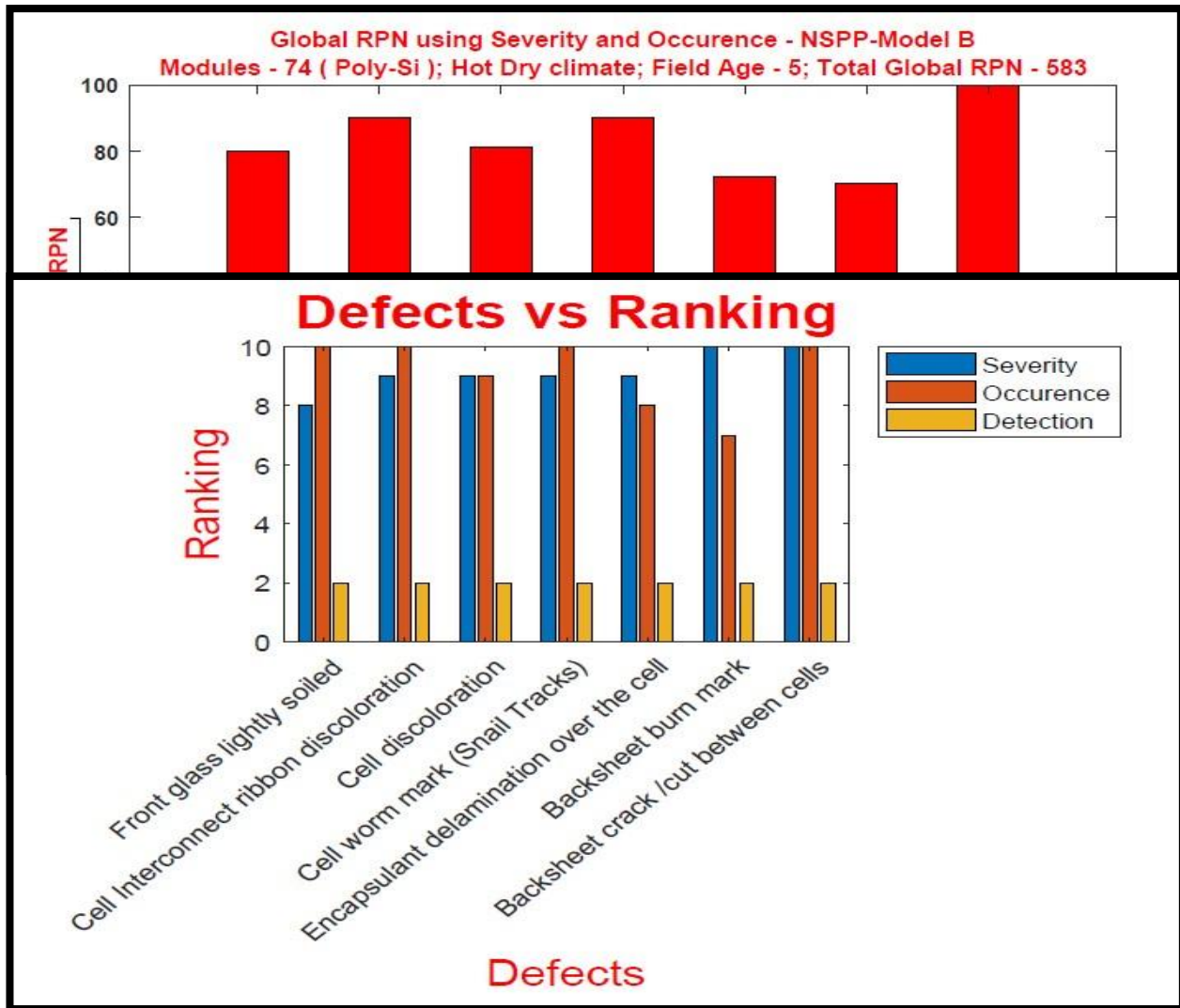
The defects that are present in 74 modules of model B is shown in figure 5-12 above.

- i. 'Backsheet burn marks' and 'Backsheet crack/cut between cells' were obtained to be the safety issues, wherein, the rest of failures are regarded to add to the increase in degradation rate (performance issues).
- ii. In all, seven defects were determined of which 'Backsheet crack/cut between cells' was determined to be the prominent safety issues for the modules considered with RPN value of 200.
- iii. Also, 'cell interconnect discoloration' and 'cell worm marks' both having RPN value of 180 each were the dominant performance failures for the modules considered.
- iv. The sum of all RPN values of defects present for this model B was calculated to be 1166.

Besides, considering all the failures can easily be detected by physical observation, the Global RPN was again computed using the occurrence and severity neglecting detection as indicated in **figure 5-13**.

Figure 5- 13: Global RPN Plot Using Severity and Occurrence for Model- B Discussions

- i. It can be deduced from **figure 5-13** that the RPN values of the defects were halved.



- ii. This could be due to the visual inspection that was used in the collection of the data and was assigned a detection value of two (see Appendix D for Detection ranking). For instance, the RPN value of backsheet crack/ cut between cells is 100. This provides a better view on the RPN value instead of 200 as depicted in figure 5-12.

5.3.2 Defects Ranking Plot for Global RPN for Model-B

The ranking values for the various RPN parameters for Model-B for the observed defects are presented in figure 5-14.

Figure 5- 14: Defects - Ranking Plot for Model –B

Discussions

It can be inferred from figure 5-14 that,

- i. All the defects present have detection ranking of two as explained earlier. The ranking values for the occurrence and severity parameters can be visualize in the plot.
- ii. ‘Front glass slightly soiled’, ‘cell interconnect discoloration’, ‘cell worm marks’ and ‘Backsheet crack between cells’ can be observed to occur more frequently among the modules since they have the highest occurrence value.
- iii. For ‘cracks between cells’, it can be associated to the fact that the site is located in an environment with high temperature; and the possibility of moisture ingress into the modules is the cause of discoloration of the cell interconnect ribbon.
- iv. Also, the influence of ‘Backsheet burn marks’ and ‘Backsheet crack/cut between cells’ on the modules performance is more severe compared to the other defects.

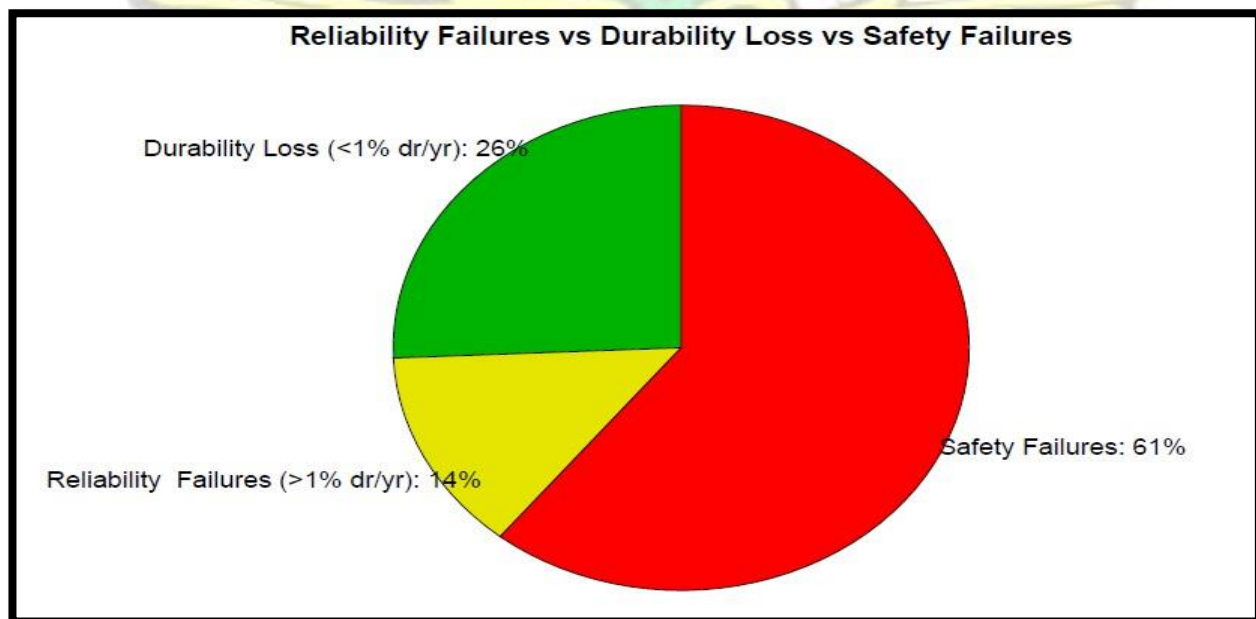
5.3.3 Pie Chart for Reliability, Durability and Safety failures for Model-B.

Figure 5-15 shows a pie chart indicating the percentage of modules that are posing safety concern to users, those with durability and reliability issues.

Figure 5- 15: Pie Chart of Reliability, Durability and Safety Issues for Model- B Discussions

When extrapolating the measured module degradation and including the safety failures, it can be deduced that,

- i. Twenty-six percent (26%) of the modules meet the manufacturer's warranty and are safe to give adequate power output.
- ii. Sixty-one percent (61%) of modules posing safety issues to users and need urgent maintenance attention to avert the threat.



- iii. Fourteen percent (14%) of modules are beyond the manufacturer's usual warranty of 1%/ year degradation rate as indicated in figure 5-15 and needs to be replaced for optimum performance from the modules.

5.4 Correlation program output Plots for NSPP- Model B

It is to be noted that modules with safety failures and degradation rates greater than 2.0%/year were excluded from the correlation analysis due to the filtering of the data. This is to avoid skewing of the data because of outliers. Out of the 74 modules data collected, fifty four (54) modules were considered for model B correlation analysis based on the upper limit fixed.

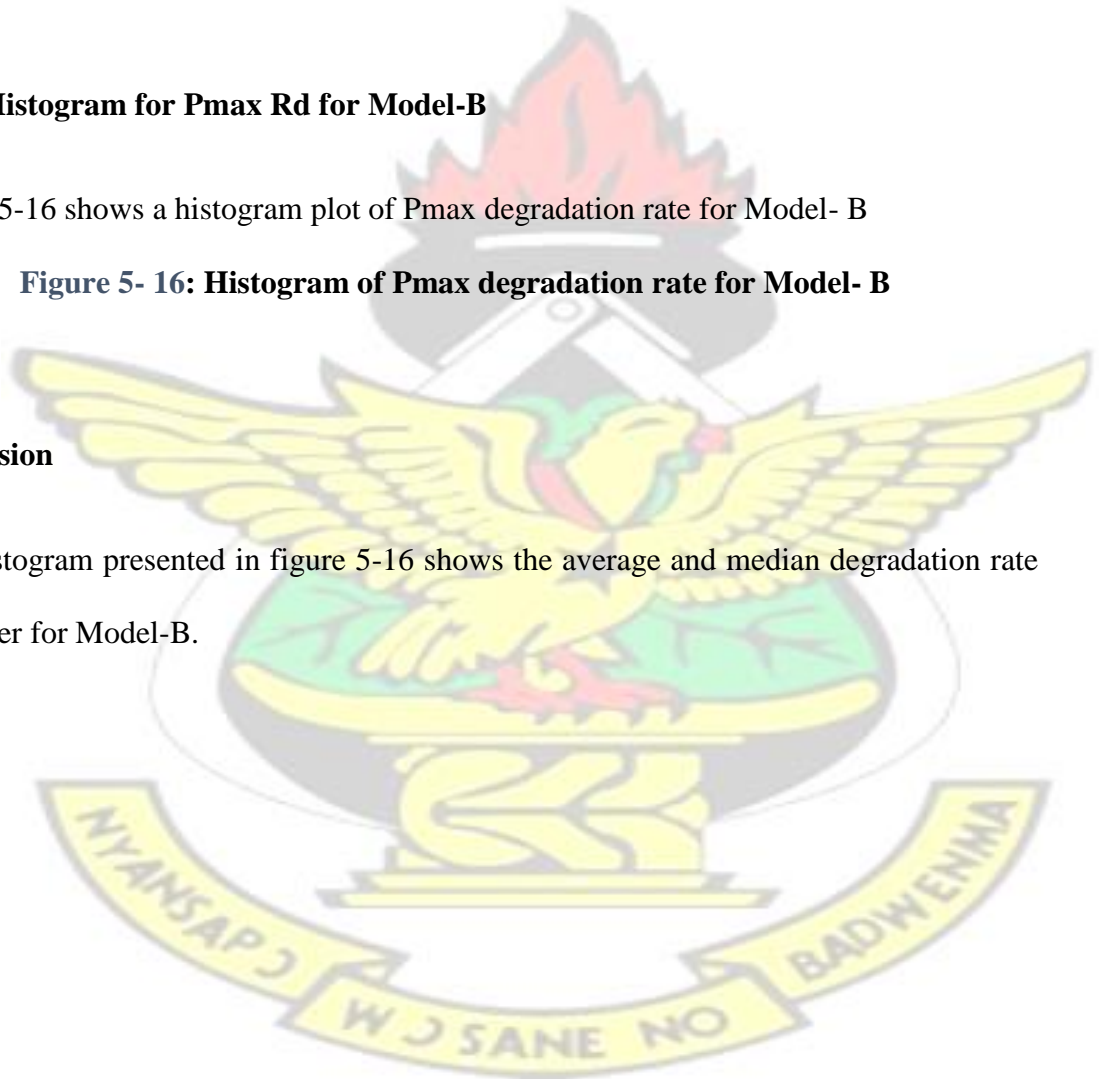
5.4.1 Histogram for Pmax Rd for Model-B

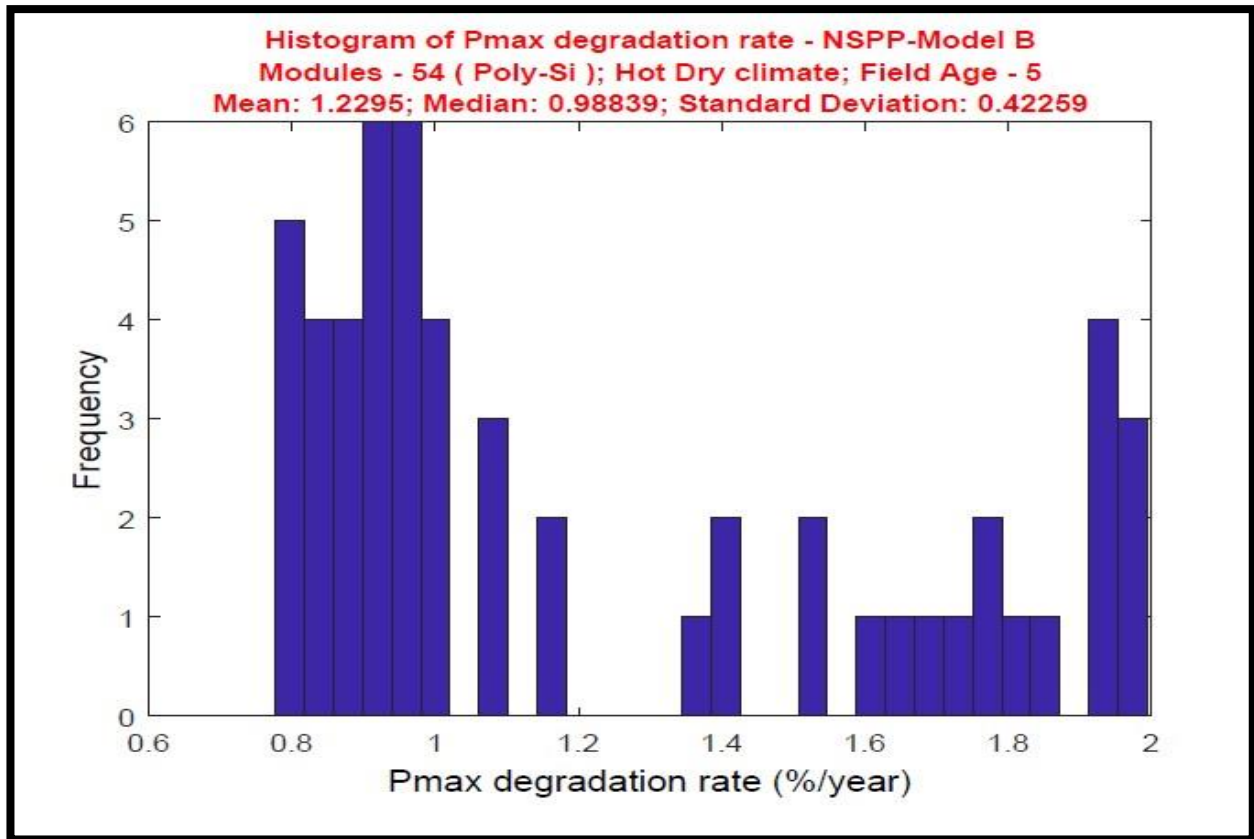
Figure 5-16 shows a histogram plot of Pmax degradation rate for Model- B

Figure 5- 16: Histogram of Pmax degradation rate for Model- B

Discussion

The histogram presented in figure 5-16 shows the average and median degradation rate of power for Model-B.





- i. The average power degradation rate for Model B is calculated as 1.23%/year.
- ii. Out of the 54 modules considered, 29 modules (approximately 54%) meet the maximum degradation rate of 1.0%/year typically provided by the module manufactures.
- iii. The median and average degradations rates are quite close (that is, 1.23%/year vs. 0.99%/year), indicating a tight quality management system during production.

5.4.2 Determination of Dominant I-V Parameter Degradation Rates

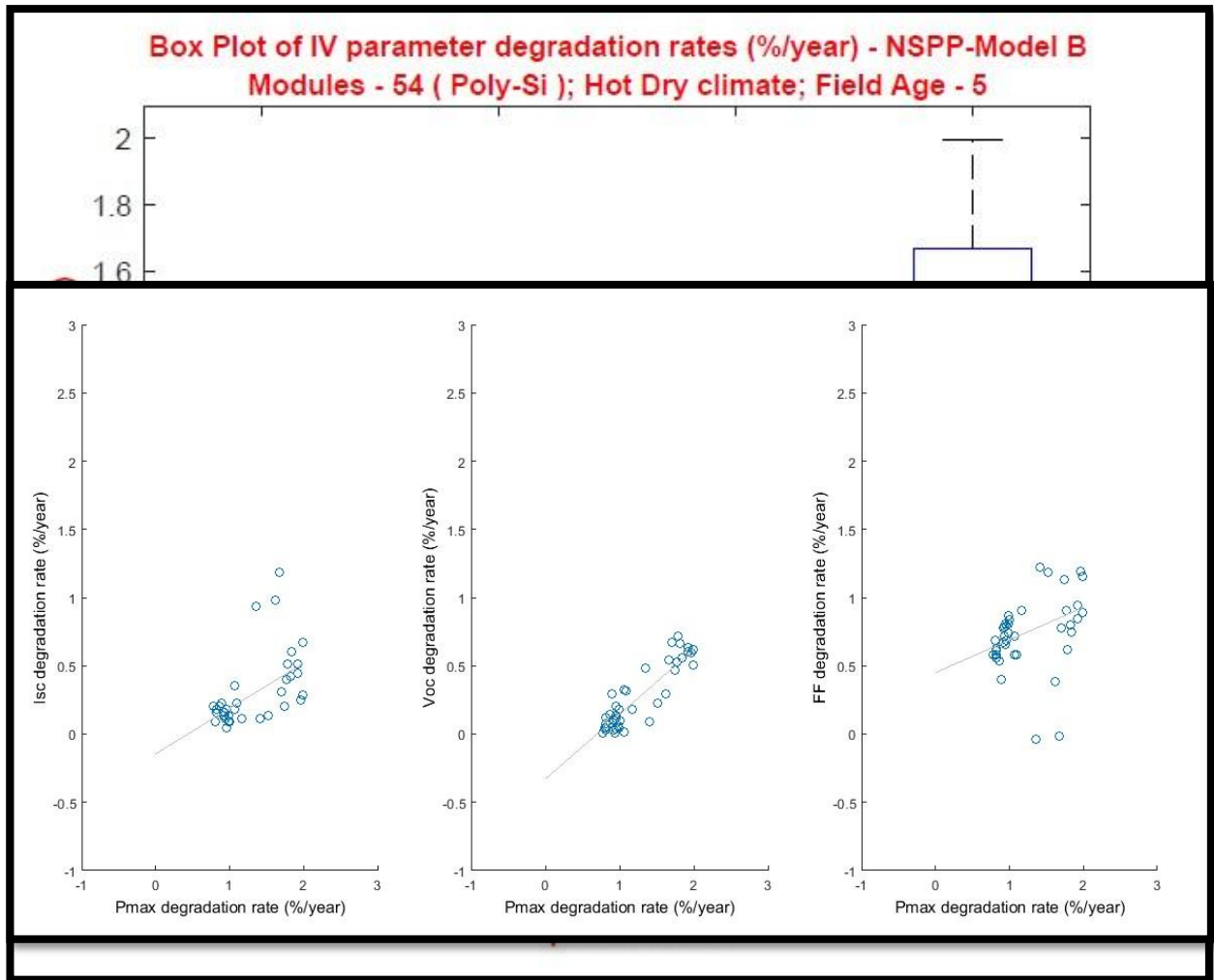
Grouped by the I-V parameters, box plot of the degradation rates (%/year) was plotted as shown in figure 5-17. This helps to find the correlation of P_{max} degradation rate with the other I-V parameters (V_{oc} , I_{sc} and FF) degradation rates of the modules. Also dominant I-V parameter responsible for the P_{max} degradation is determined in a specific PV plant.

5.4.2.1: Box Plot of I-V parameters degradation rates for Model- B

The box plot for the various I-V parameters degradations rates for model-B is shown in figure 5-17.

Figure 5- 17: Box Plot of I-V Parameters degradation rates for Model- B





Discussions

- i. It is apparent from figure 5-17 that, FF degradation rate is affecting Pmax degradation rate (%/year).
- ii. The order of IV parameters affecting Pmax degradation rate (%/year) is as follows: $FF > I_{sc} > V_{oc}$.

5.4.2.2: Linear Relation plot of I-V parameters for model-B

The linear relation between Pmax degradation rates and that of Isc, Voc and FF is plotted as indicated in figure 5-18.

Figure 5- 18: Linear Relation Plot of I-V Parameters for Model-B

Discussions

- i. It can be seen from figure 5-18 that; there is a linear relationship between all the IV parameters. That is, the degradation rates of I_{sc} , V_{oc} and FF affects P_{max} degradation rate.
- ii. However, it cannot be established from Figure 5-18, the I-V parameter which has the greatest influence on P_{max} degradation rate.

Plotting a combined Histogram between the degradation rates of P_{max} and that of V_{oc} , FF and I_{sc} on the same plot in the form of an overlap or otherwise are shown in figures 5-19, 5-20 and 5-21 respectively.



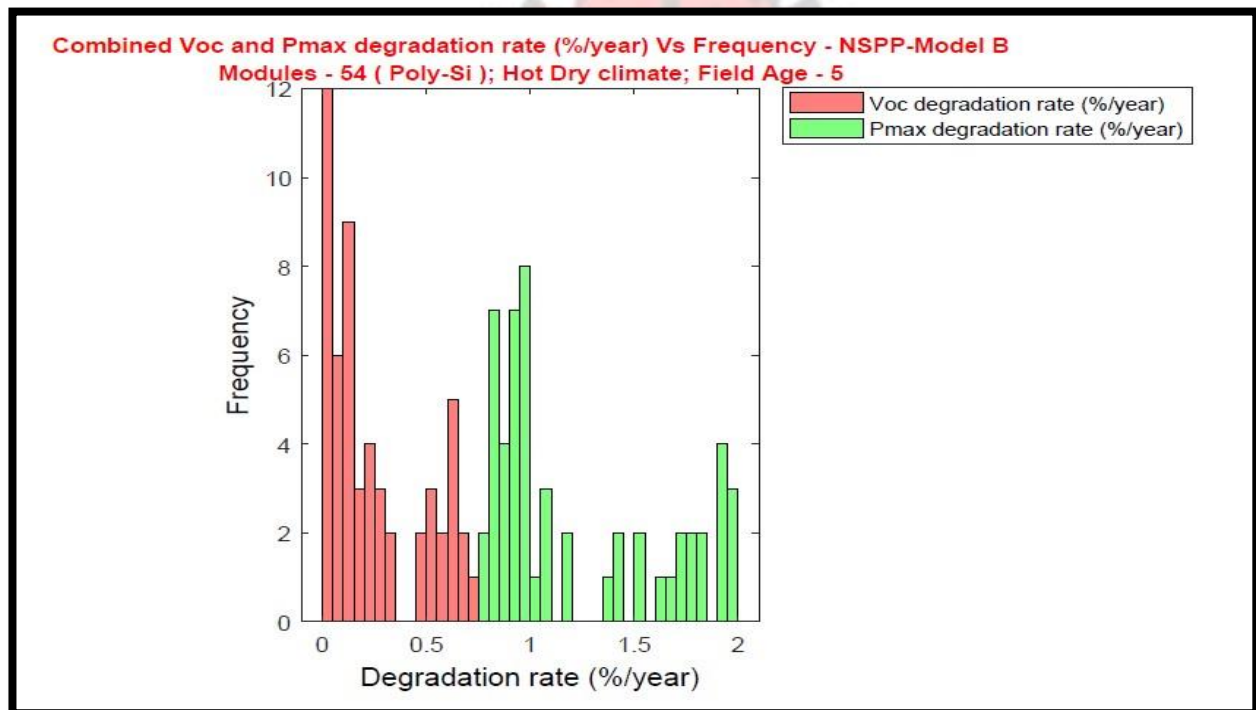
5.4.2.3: Combined Histogram of Voc and Pmax degradation rate for Model-B

Figure 5-8 shows the combined histogram of Voc and Pmax degradation rate for Model- B.

Figure 5- 19: Combined Histogram of Voc and Pmax degradation rate for Model- B

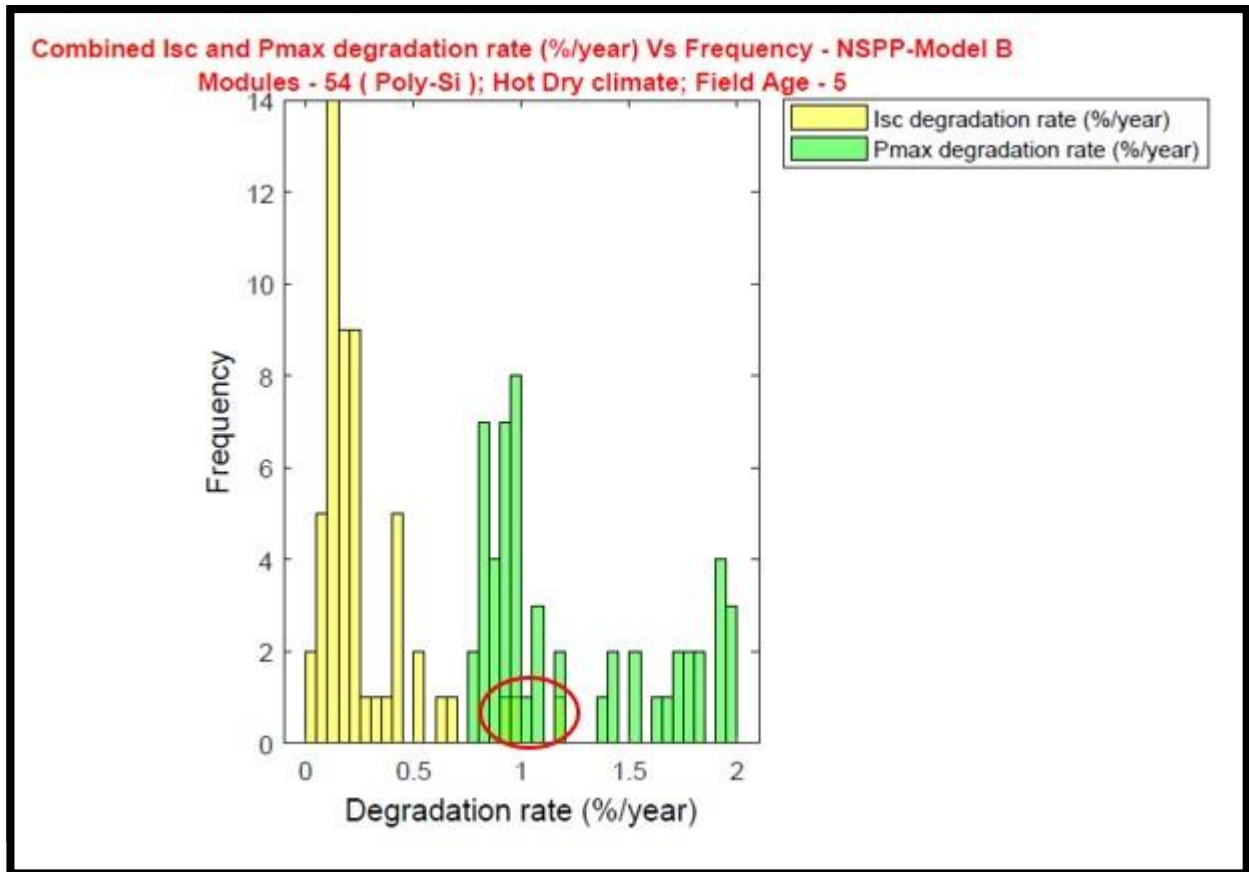
5.4.2.4: Combined Histogram of FF and Pmax degradation rate for Model-B

Figure 5-20 shows the combined histogram of FF and Pmax degradation rate for



Model- B.

Figure 5- 20: Combined Histogram of FF and Pmax degradation rate for Model- B



5.4.2.5: Combined Histogram of Isc and Pmax degradation rate for Model-B

Figure 5-21 shows the combined histogram of Isc and Pmax degradation rate for Model- B.

Figure 5- 21: Combined Histogram of Isc and Pmax degradation rate for Model- B Discussions

- i. It is evident from **figure 5-20** that, there is an overlap between FF and Pmax degradation rates around 0.8%/year to 1.2%/year, which suggests that degradation of Isc is affecting Pmax.
- ii. Also, it can be noticed that there is an overlap between Isc degradation rates and Pmax degradation rates in **figure 5-21** around 0.8%/year, which also denotes even Isc degradation has an influence on Pmax degradation but not in the same scale as Isc degradation that can be identified from the frequency or count of modules affected.

- iii. In contrast, there is no overlap between Voc and Pmax degradation rates as shown in **figure 5-19**. This suggests that degradation of Voc is not affecting degradation of Pmax.

5.4.3 Comparison of Median Degradation Rates (%/year) of IV Parameters for Performance Defects.

The comparison of degradation rates of I-V parameters for the performance defects are shown in figure 5-22.

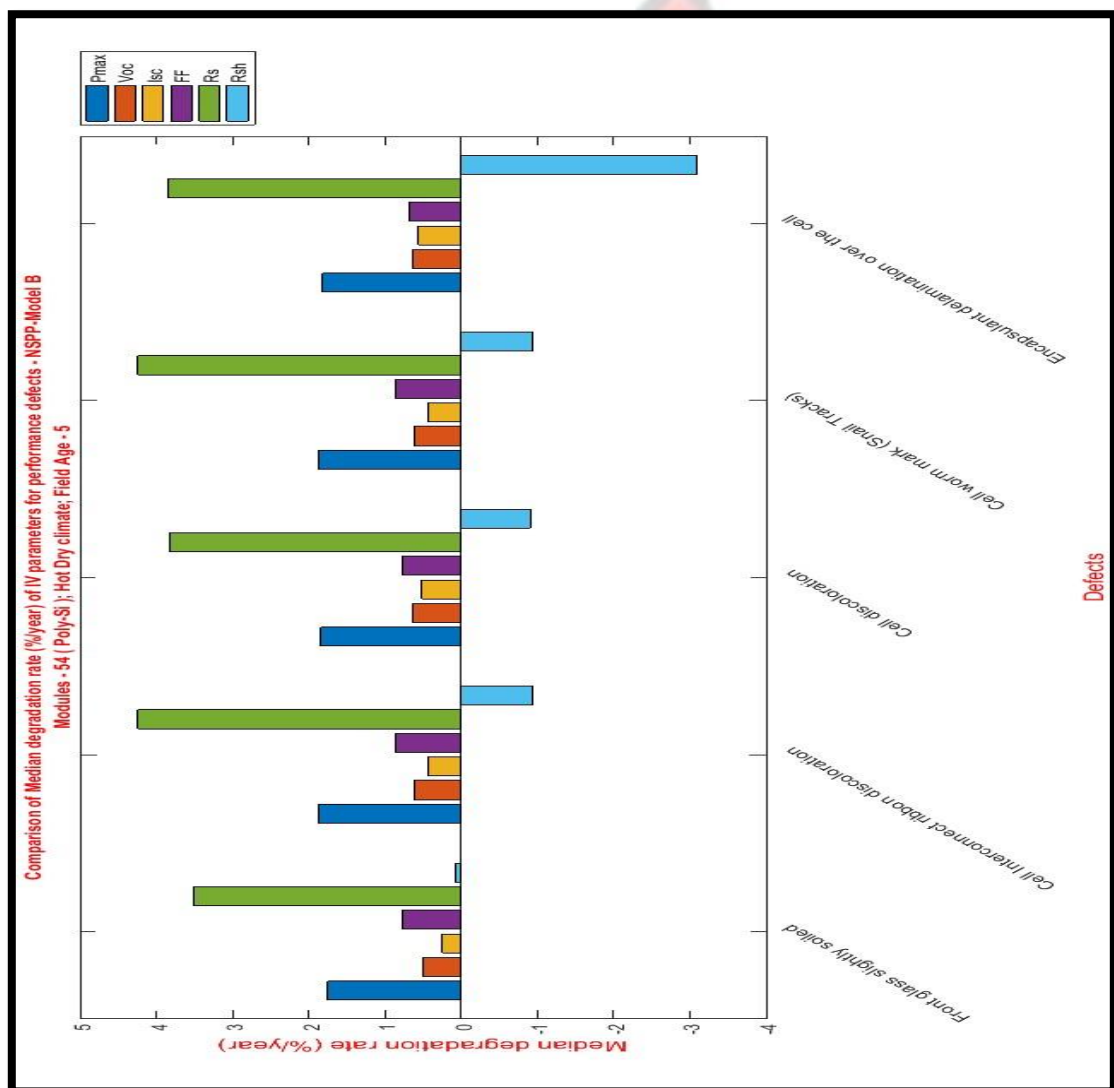


Figure 5- 22: Comparison Plot of Median degradation rates of I-V Parameters for Model-B

- i. It can be deduced from figure 5-22 that, median FF degradation rate has the highest values for all the defects excluding the R_s and R_{sh} values. This shows that FF degradation rate influences the degradation of P_{max} for the defects shown.
- ii. In addition, the order of IV parameters for each defect can be determined from the plot. For instance, cell discoloration, has the order of parameters affecting P_{max} degradation as follows; $R_s \gg FF > V_{oc} > I_{sc} > R_{sh}$.
- iii. Similar conclusions can be drawn for the same plot using the mean degradation rates as included in Appendix C with other correlation plots.

5.5 Comparison of key findings of NSPP Model A and Model B Results

This study presented the results of two set of modules from different manufactures with the same maximum power rating. Comparing the results of the models can aid appreciation of the failure modes and mechanisms for this climatic zone and presents some basis for future studies. **Table 5-1** compares some key parameters findings for the two set of Modules at the NSPP.

Table 5- 2: Comparison of parameters for Model A and B results

Variable/parameter	NSPP-Model A	NSPP-Model B
Module construction	Framed	Framed
Tilt angle (°)	12	12
System state	functional	functional
Dominant failure mode (degradation)	Front glass slightly soiled	Cell interconnect discoloration and cell worm marks
Dominant safety failure	Junction box lid fell off	Backsheet crack/cut between cells
IV parameter affecting Pmax degradation rate	$I_{sc} > FF > V_{oc}$	$FF > I_{sc} > V_{oc}$
Durability issues(% of modules)	32	26
Reliability issues (% of modules)	51	14
Safety issues (% of modules)	16	61

Mean Pmax degradation rate (%/year)	1.11	1.23
RPN Value	603	583

5.5.1 Summary comments

It can be deduced from Table 5-1 that, for the same technology (Poly-Si), type of module construction (framed modules) and fixed tilt angle operating in the same climate condition. The two models of PV modules exhibit different dominant failure modes (That is, ‘front glass slightly soiled’ for Model-A and ‘cell interconnect discoloration and cell worm marks’ for Model-B).

Moreover, using the statistical RPN and degradation rate criteria to evaluate the performance of the two models, it can be deduced that; Model-A modules performs better than Model-B modules in the same Northern Ghanaian climate (Hot-dry climate). This is because, the mean annual degradation rate computed for model-A (1.11%/yr) is lower than that of model-B (1.23%/yr) and has a higher percentage of the modules (32%) degrading below the warranty limit of 1.0%/yr compared to modelB (26%) even though model –A has a greater RPN value than model-B.

CHAPTER 6: CONCLUSIONS AND RECOMMENDATIONS

This chapter concludes the research study and proposes recommendations for future work related to the study.

6.1 Conclusion

From the study, the following key findings are made:

6.1.1 Excluding the detection rating, the total RPN for Model A is 603 and that for Model B is 583 for this site.

6.1.2 'Junction box lid fell off' was determined as the peculiar safety issue For Model A whereas, 'Backsheet crack/ cut between cells' and 'Backsheet Burn marks' were revealed as the peculiar safety issues for Model B .

6.1.3 For Model A, 'Front glass slightly soiled' was determined as the dominant performance defect and for Model B; ' cell interconnect discoloration' and ' cell worm marks' are the dominant performance failures.

6.1.4 Out of all the modules considered, 32% met the usual manufacturer's warranty of degradation of less than 1%/year for Model A and 26%/year for Model B (that is the durability issues for the site.). For safety issues, 16% was determined for Model A and 61% for Model B.

6.1.5 The average annual degradation rates were computed as 1.11%/year and 1.23%/year for Model A and Model B respectively. This suggests that both models of PV modules are degrading faster than the standard value of 1.0%/year reported in literature at an early time of its total operation lifetime.

6.1.6 The order of IV parameters influencing degradation of Maximum power of the modules for Model A and Model B respectively are $I_{sc} > FF > V_{oc}$ and $FF > I_{sc} > V_{oc}$.

In conclusion, this result means that after five years of operation, the modules from both manufacturers have not done well and need urgent attention to improve the performance of the solar power plant based on the degradation rate determined. However, model-A modules are performing better than model-B modules in the hotdry Northern Ghanaian climate.

6.2 Recommendations

The following recommendations are proposed for future studies;

- 6.2.1 Data from other plants in Ghana and sub-Saharan region should be studied to widen the scope of understanding of peculiar issues regarding the climatic condition.
- 6.2.2 Other techniques other than visual inspection should be carried out to discover more defects on PV plant.
- 6.2.3 Studies to compare IV parameters of PV modules measured with soil and after cleaning soil to appreciate the energy loss due to soiling.
- 6.2.4 Financial risk analysis and implications on investment can be carried out to appreciate the significance of the power losses.
- 6.2.5 Studies on rate of degradation of IV parameters for each defect to understand the effect of defects on performance of PV modules.

6.2.6 Older PV power plants should be studied to give better representation and effect of defects and failures on PV module performance.

KNUST



REFERENCES

- Boppana, S., (2015). Outdoor Soiling Loss Characterization and Statistical Risk Analysis of Photovoltaic Power Plants-Thesis. Arizona State University.
- Janakeeraman, S.V., Singh, J., Kuitche, J., Mallineni, J.K., TamizhMani, G., (2014). A statistical analysis on the cell parameters responsible for power degradation of fielded PV modules in a hot-dry climate, in: Photovoltaic Specialist Conference (PVSC), 2014 IEEE 40th. IEEE, pp. 3234–3238.
- Koentges, M., Kurtz, S., Packard, C., Jahn, U., Berger, K.A., Kato, K., Friesen, T., Liu, H., Van Iseghem, M., (2014). Review of failures of photovoltaic modules. IEA PVPS Task 13.
- Köntges, M, Kurtz, S., Packard, C., Jahn, U., Berger, K., Kato, K., Friesen, T., Liu, H., Van Iseghem, M., (2014). Review of failures of photovoltaic modules. IEA PVPS Task 13.
- Köntges, Marc, Kurtz, S., Packard, C., Jahn, U., Berger, K.A., Kato, K., (2014). Performance and reliability of photovoltaic systems: subtask 3.2: Review of failures of photovoltaic modules: IEA PVPS task 13: external final report IEAPVPS. International Energy Agency, Photovoltaic Power Systems Programme, Sankt Ursen.
- Kuitche, J., TamizhMani, G., (2013). Accelerated Lifetime Testing of Photovoltaic Modules Solar America Board for Codes and Standards. Rep. Sol. Am. Board Codes Stand.
- Kurtz, S., Newmiller, J., Kimber, A., Flottemesch, R., Riley, E., Dierauf, T., McKee, J., Krishnani, P., (2013). Analysis of photovoltaic system energy performance evaluation method. National Renewable Energy Laboratory (NREL), Golden, CO.
- Lazzaroni, M., Cristaldi, L., Peretto, L., Rinaldi, P., Catelani, M., 2012. Reliability Engineering: Basic Concepts and Applications in ICT. Springer.
- Liu, H.-C., Liu, L., Liu, N., (2013). Risk evaluation approaches in failure mode and effects analysis: A literature review. Expert Syst. Appl. 40, 828–838. <https://doi.org/10.1016/j.eswa.2012.08.010>
- Mallineni, J., Knisely, B., Yedidi, K., Tatapudi, S., Kuitche, J., TamizhMani, G., (2014). Evaluation of 12-year-old PV power plant in hot-dry desert climate: Potential use of field failure metrics for financial risk calculation, in: Photovoltaic Specialist Conference (PVSC), 2014 IEEE 40th. IEEE, pp. 3366–3371.
- Moorthy, M.K., (2015). Automation of Risk Priority Number Calculation of Photovoltaic Modules and Evaluation of Module Level Power Electronics.

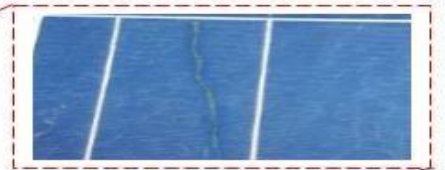
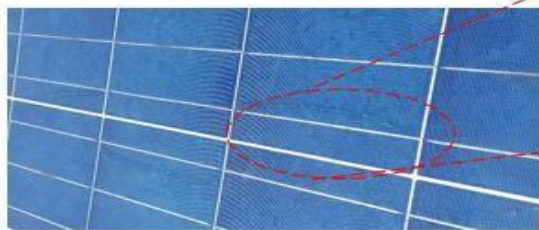
Arizona State University.

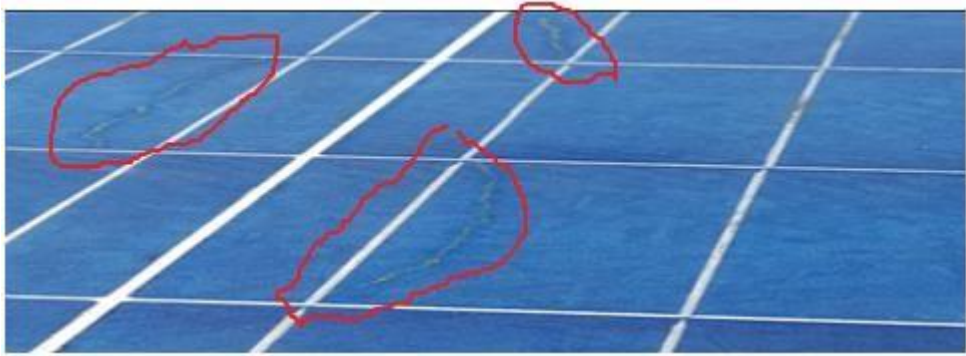
- Packard, C.E., Wohlgemuth, J.H., Kurtz, S.R., (2012a). Development of a visual inspection data collection tool for evaluation of fielded PV module condition. National Renewable Energy Laboratory (NREL), Golden, CO.
- Packard, C.E., Wohlgemuth, J.H., Kurtz, S.R., Jahn, U., Berger, K., Friesen, T., Koentges, M., (2014). Fielded PV Module Condition, in: Workshop Presented at: 27th EU PVSEC Parallel Event Workshop from IEA PVPS Task.
- Packard, C.E., Wohlgemuth, J.H., Kurtz, S.R., Jahn, U., Berger, K., Friesen, T., Koentges, M., (2012b). Fielded PV Module Condition, in: Workshop Presented at: 27th EU PVSEC Parallel Event Workshop from IEA PVPS Task.
- Phinikarides, A., Kindyni, N., Makrides, G., Georghiou, G.E., (2014). Review of photovoltaic degradation rate methodologies. *Renew. Sustain. Energy Rev.* 40, 143–152. <https://doi.org/10.1016/j.rser.2014.07.155>
- Rajasekar, V., (2015). Indoor Soiling Method and Outdoor Statistical Risk Analysis of Photovoltaic Power Plants. Arizona State University.
- Shrestha, S.M., Mallineni, J.K., Yedidi, K.R., Knisely, B., Tatapudi, S., Kuitche, J., TamizhMani, G., (2015). Determination of Dominant Failure Modes Using FMECA on the Field Deployed c-Si Modules Under Hot-Dry Desert Climate. *IEEE J. Photovolt.* 5, 174–182. <https://doi.org/10.1109/JPHOTOV.2014.2366872>
- TamizhMani, G., Kuitche, J., (2013). Accelerated lifetime testing of photovoltaic modules. *Ariz. State Univ.*
- Umachandran, N., Kuitche, J., TamizhMani, G., (2015). Statistical methods to determine dominant degradation modes of fielded PV modules, in: Photovoltaic Specialist Conference (PVSC), 2015 IEEE 42nd. IEEE, pp. 1–6.

APPENDIX A: SAMPLE PICTURES OF DEFECTS

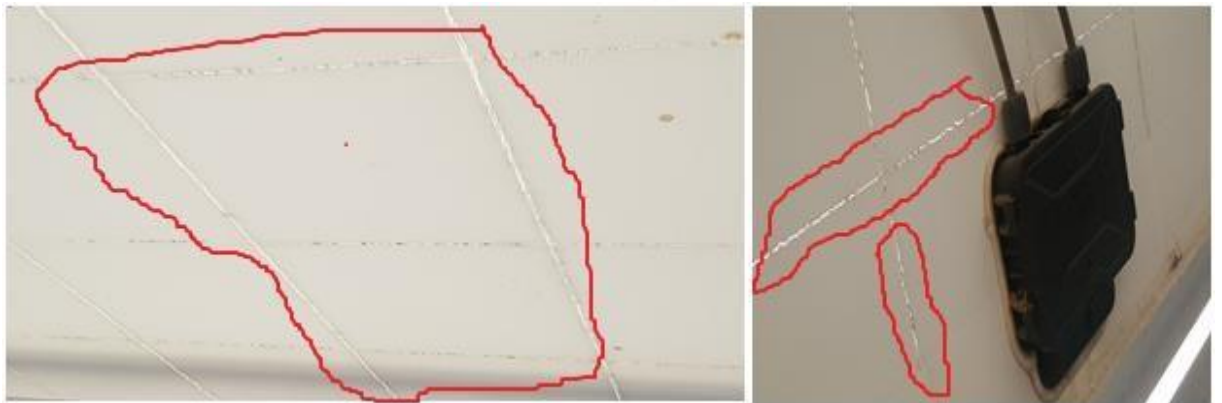
IMAGES OF OBSERVED FIELD FAILURES AT NAVRONGO SOLAR POWER PLANT (NSPP).

KNUST





Cell crack/ cell snail tracks



Back sheet cracks between cells



Front glass slightly soiled.



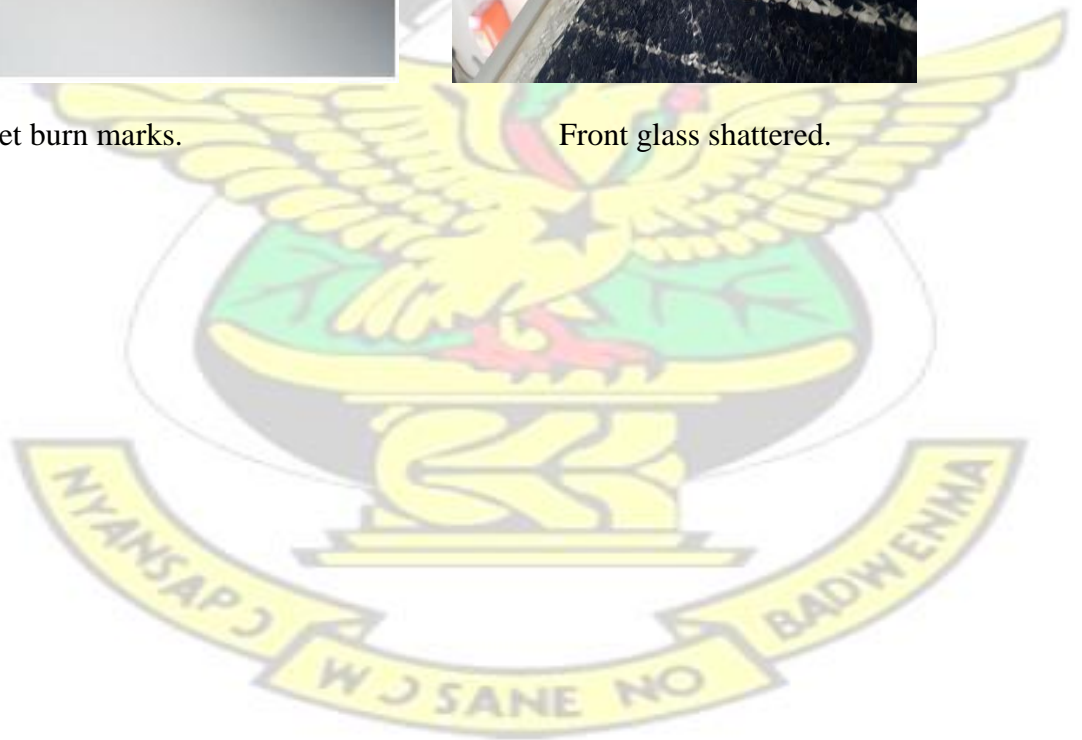
Junction box lid fell off.



Back sheet burn marks.



Front glass shattered.

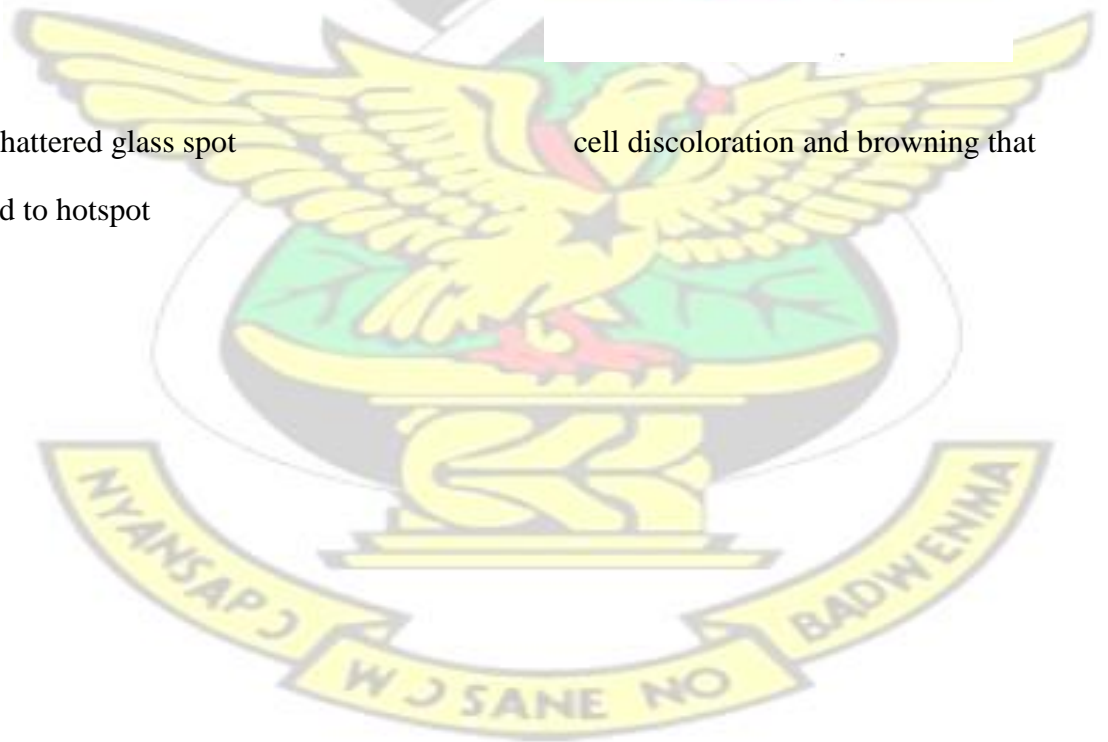


K



Dent/ shattered glass spot
can lead to hotspot

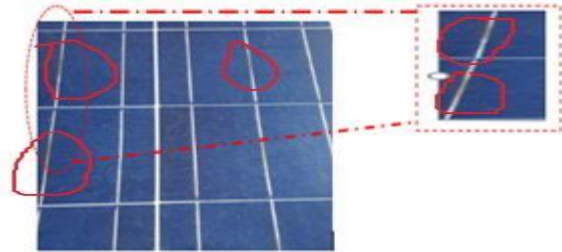
cell discoloration and browning that





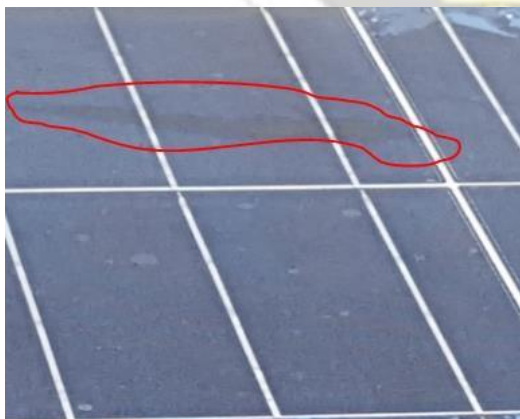
Moisture intuition leading to delamination

Cell browning/ discoloration

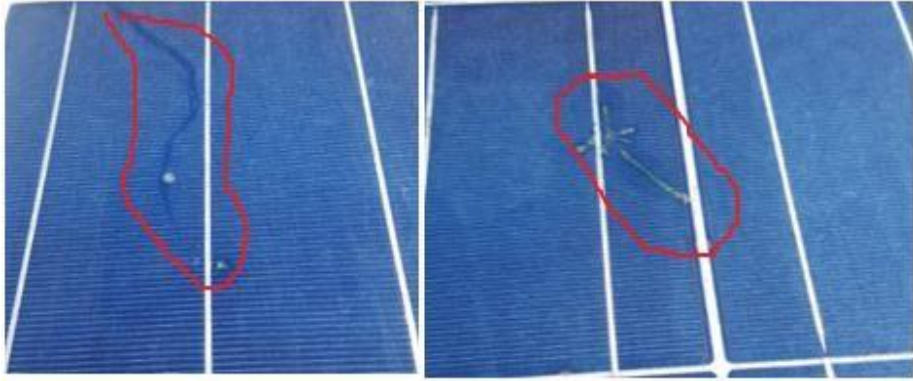


Back sheet delamination leading to cracks

cell interconnect discoloration



Cell burn marks

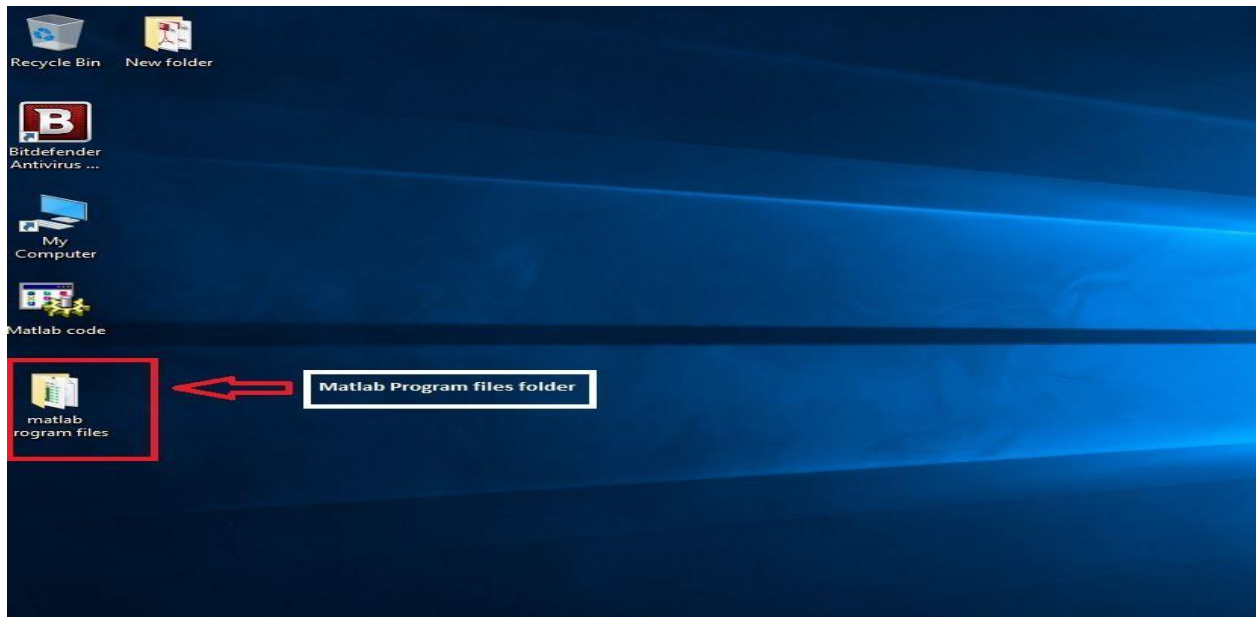


Snail crack propagating on module

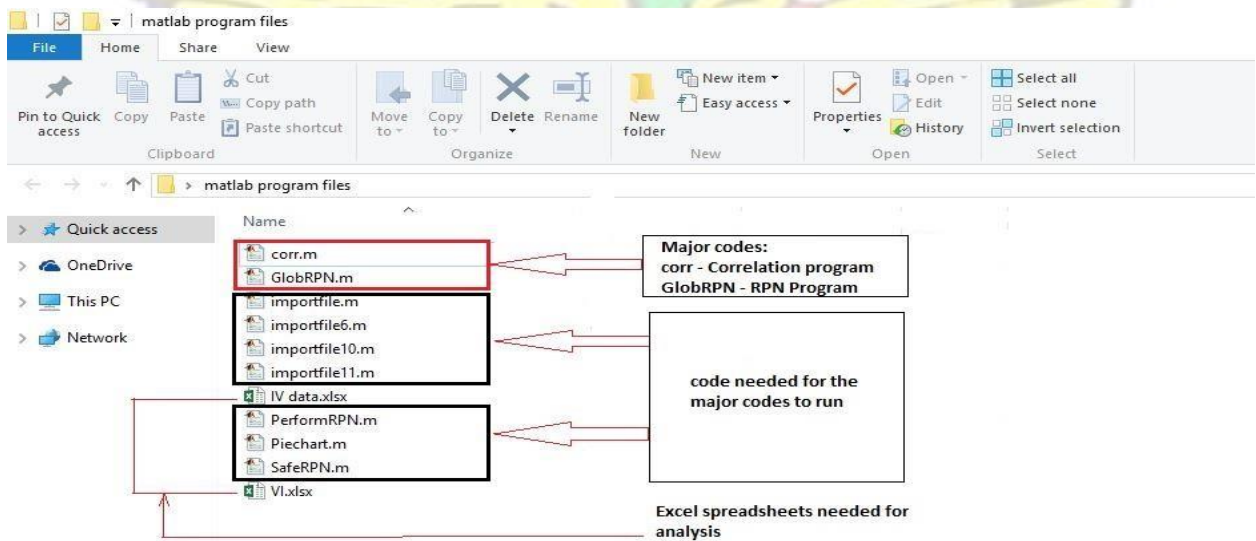


Cell interconnect discoloration

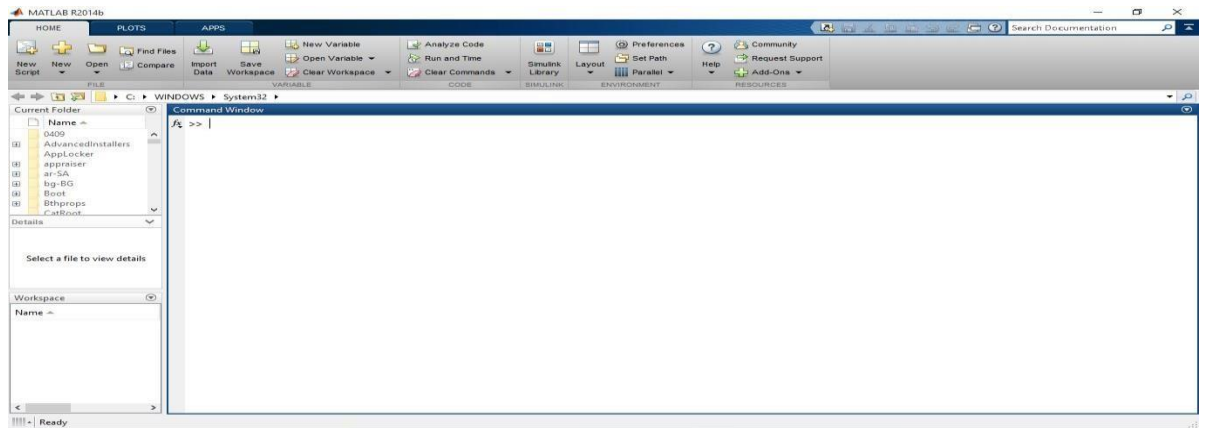




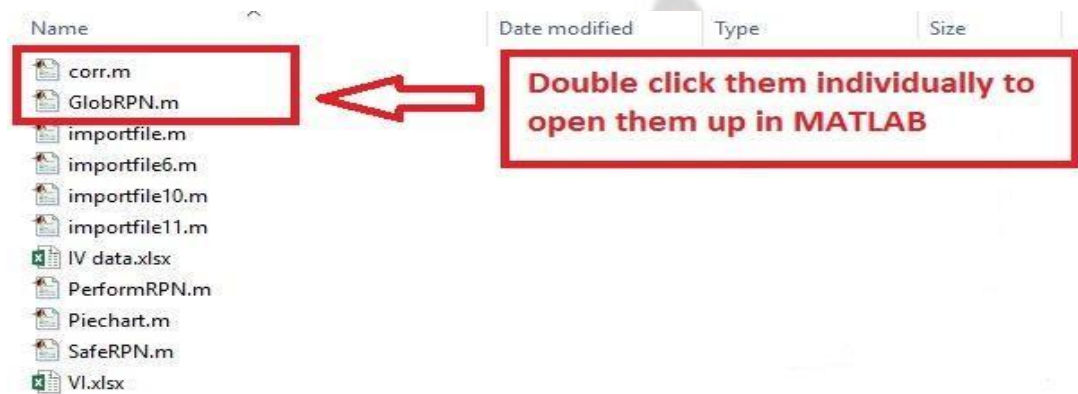
Step 2: Following MatLab code files, as shown in fig below, should be inside the folder created for storing the MatLab programs. Major codes that are needed are corr.m and GlobRPN.m as shown in fig below. Other codes needed for the major codes to run are also highlighted. Excel spreadsheets IV data.xlsx and VI.xlsx are to be changed every time different power plant data is to be analyzed, but the naming of those spreadsheets should be maintained as IV data.xlsx and VI.xlsx. If there is any change in the naming, Program won't work.



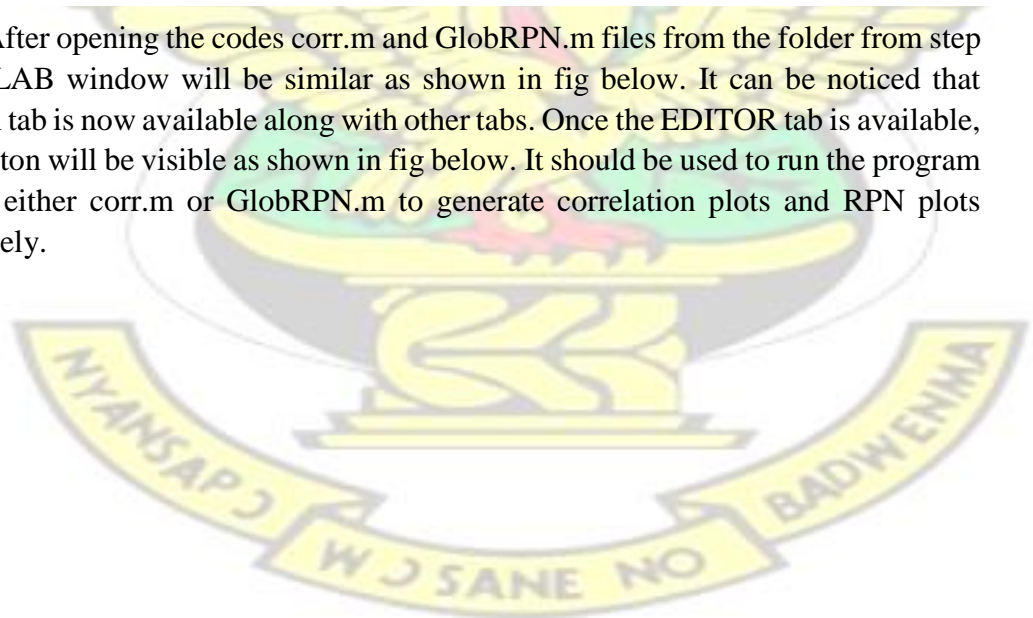
Step 3: MATLAB window will be as shown below, when opened. There will be no editor tab until you open a code as it can be found that there are only HOME, PLOTS and APPS tab available when you open MATLAB initially.

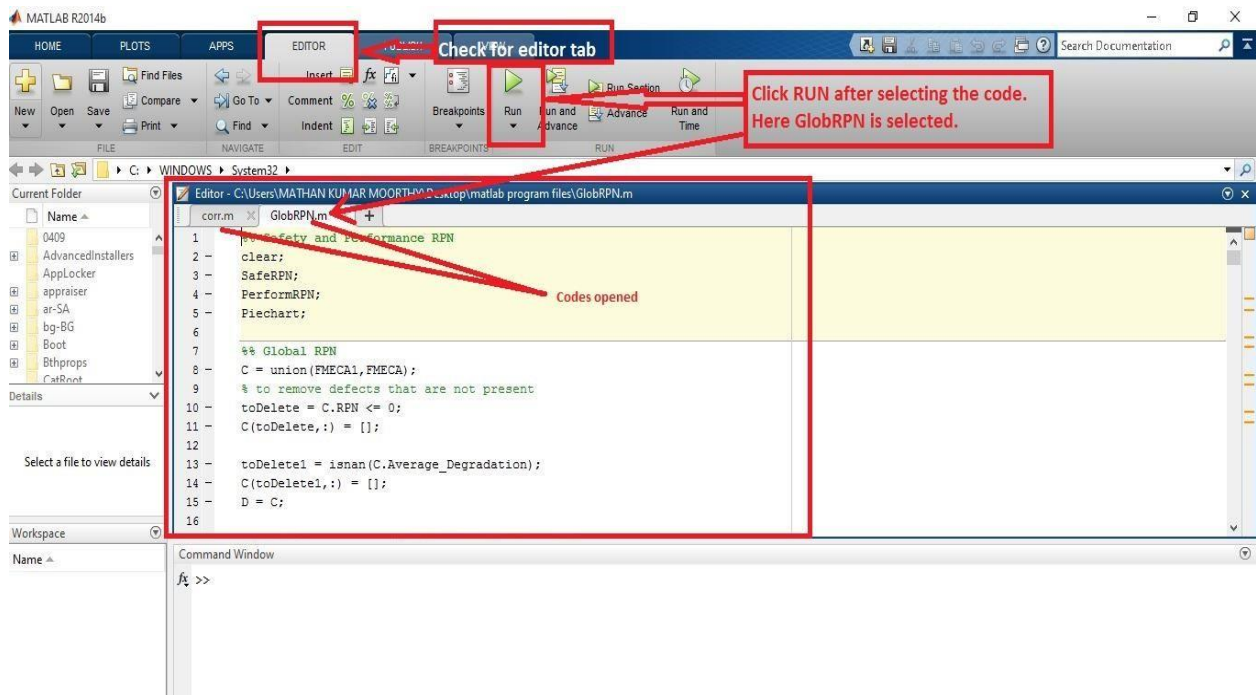


Step 4: Open codes corr.m and GlobRPN.m from the folder from step 1 as shown in fig below.

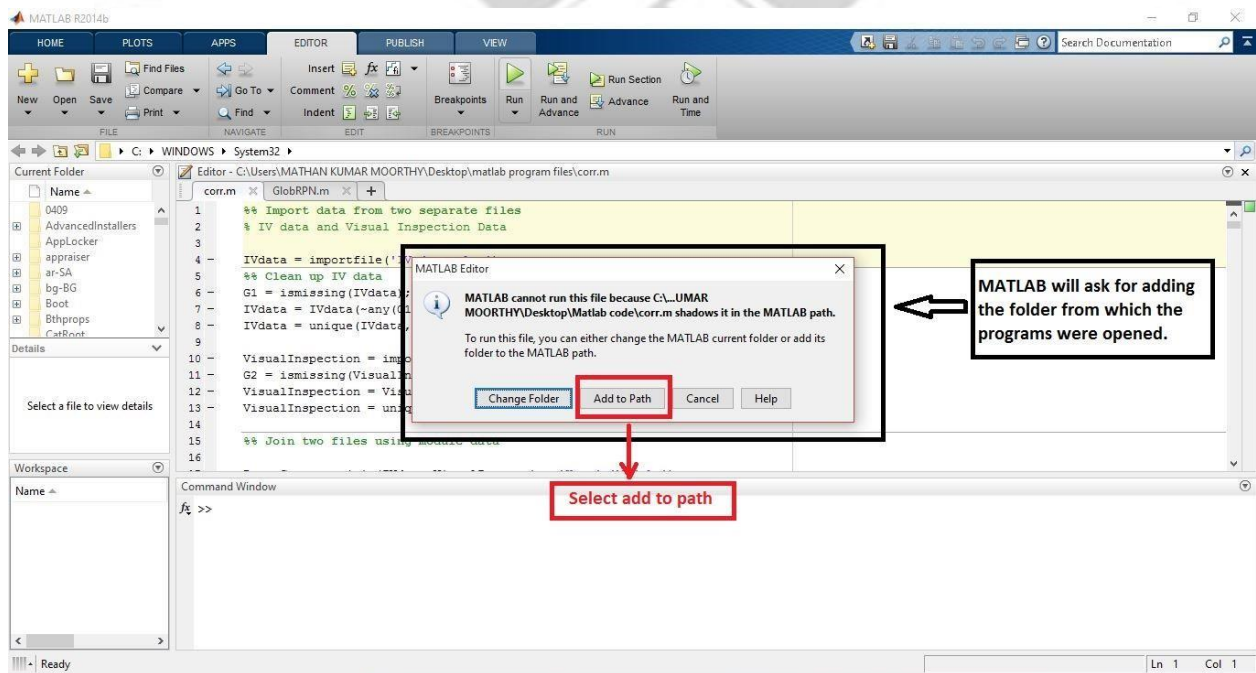


Step 5: After opening the codes corr.m and GlobRPN.m files from the folder from step 1, MATLAB window will be similar as shown in fig below. It can be noticed that EDITOR tab is now available along with other tabs. Once the EDITOR tab is available, RUN button will be visible as shown in fig below. It should be used to run the program required either corr.m or GlobRPN.m to generate correlation plots and RPN plots respectively.

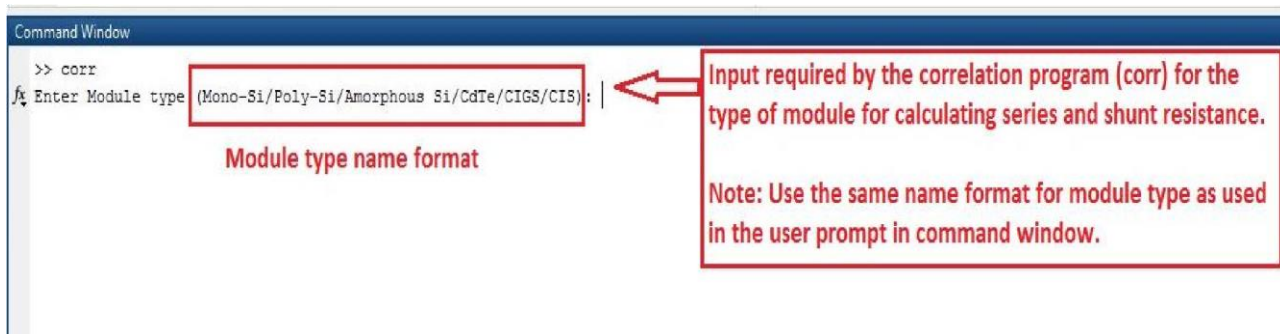




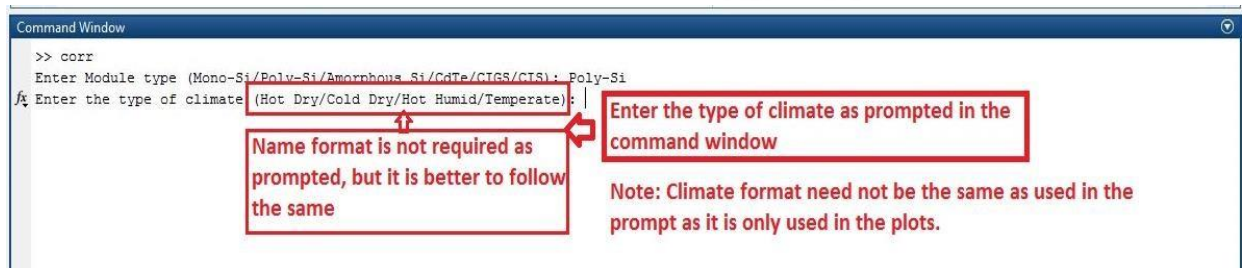
Step 6: When code corr.m is run initially, MATLAB will ask for adding the folder to its path so that it can recognize the code. Click **Add to path** to add the folder to MATLAB path. *Note: Skip this step if path has been already added.*



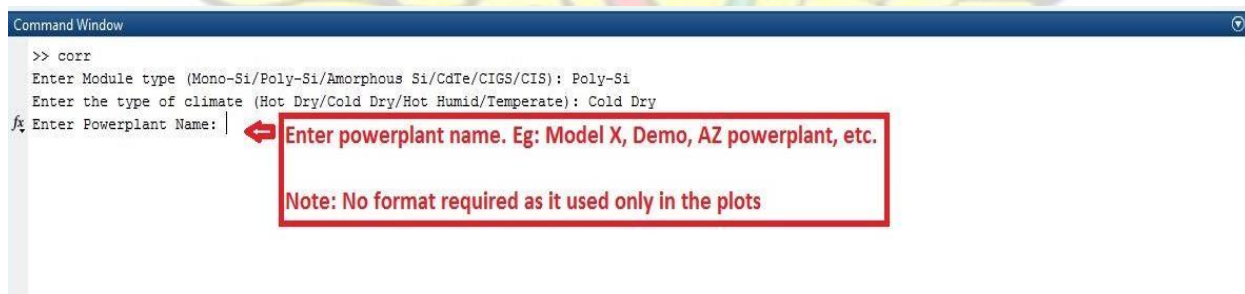
Step 7: When code corr.m is run, user prompt will appear asking to enter type of module in the PV power plant. Eg: Mono-Si, Poly-Si, etc. User should make sure to use the same naming format that the user prompt shows as shown in fig below, as it is required for calculating series and shunt resistance for the PV modules in that particular PV power plant. *Note: Program will exit if different naming formats are used.*



Step 8: After entering the module type, click ENTER in the keyboard. Next, prompt to enter type of climate will appear. User can enter the type of climate as Hot Dry, Cold Dry, etc. *Note: No Naming format is required here.*



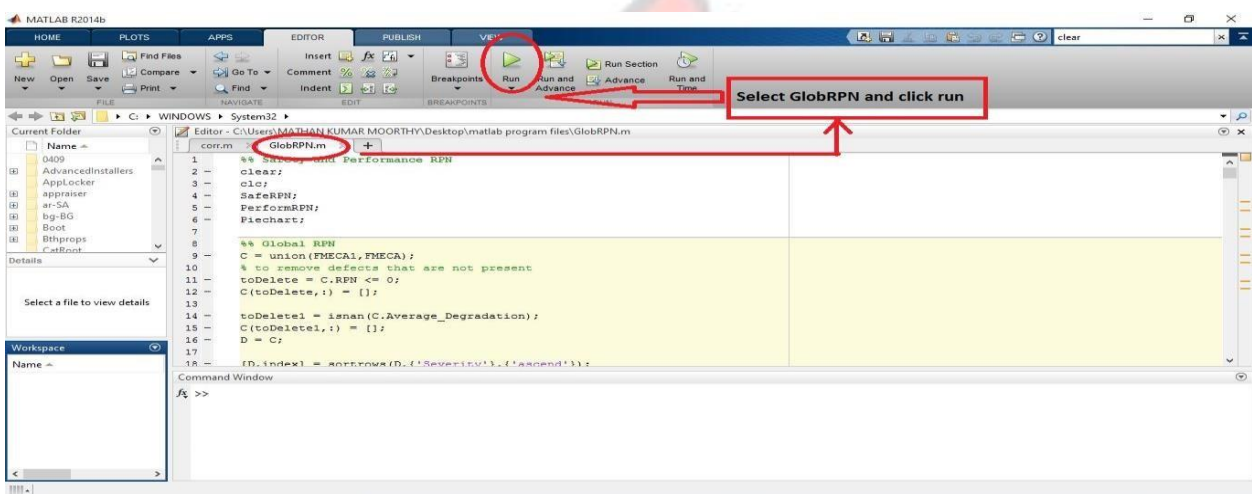
Step 9: After entering the type of climate, click ENTER in keyboard. Next, prompt to enter power plant name will appear as shown in fig below. User can enter the name of power plant in any way needed. Eg: Model XYZ, Demo, Arizona PV Power Plant, etc. *Note: No Naming format is required here.*



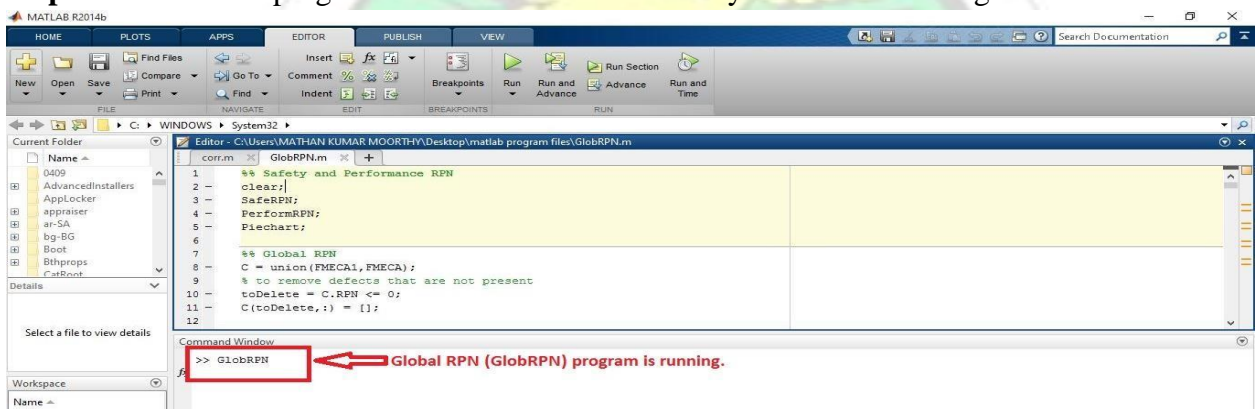
Step 10: After entering power plant name, click ENTER in keyboard. Correlation plots will be generated at the end of the running of corr.m code denoted by >> as shown in fig below.



Step 11: After getting output plots from corr.m, select GlobRPN.m tab and click RUN as shown in fig below. **Note:** It is recommended to clear the workspace before running the program.

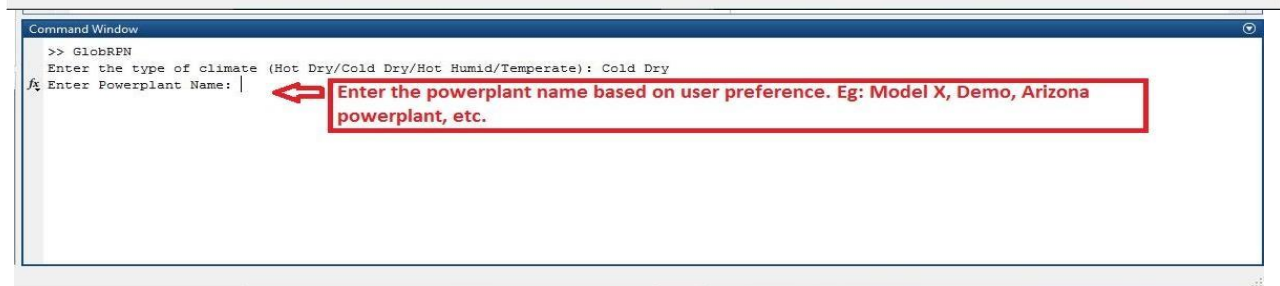
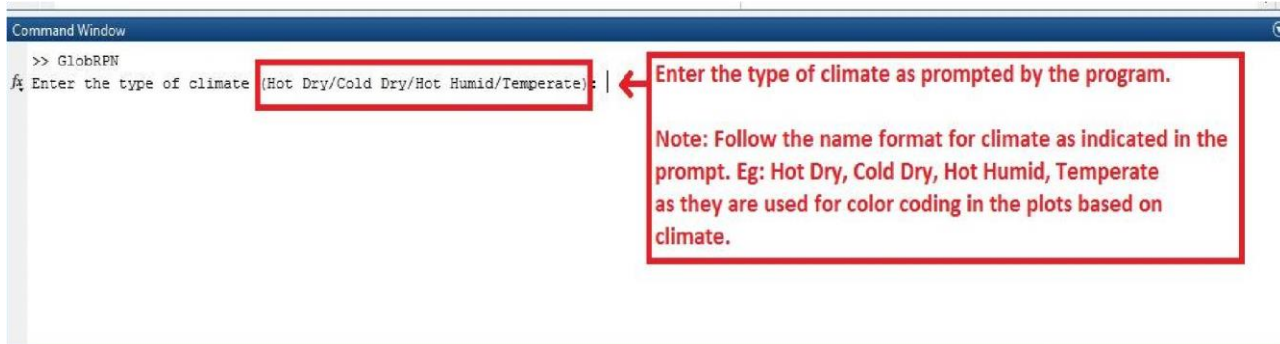


Step 12: Start of the program GlobRPN.m is indicated by >> as shown in fig below.

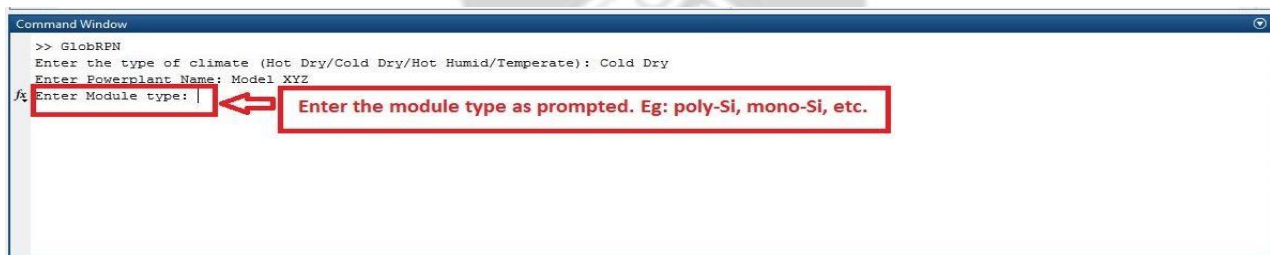


Step 13: Once the GlobRPN.m program is started, user prompt for entering the type of climate will pop up in the command window, as shown in fig below. **Note:** It is to be noted that naming format for the climate should be similar to that shown in the user prompt. Eg: Use Hot Dry to denote hot dry conditions as indicated in the prompt and nothing like hot dry or hotdry or hot-dry, etc., as it will cause the program to exit.

Step 14: After entering the type of climate, click ENTER in the keyboard. Prompt for entering power plant name will appear, as shown in fig below. **Note:** User can enter any name without any restriction on naming format.



Step 15: After entering power plant name, click ENTER in keyboard. Prompt to enter module type will appear. User can enter the type of module. Eg; Mono-Si, mono Si, mono-Si, etc. *Note: User can follow any naming format.*



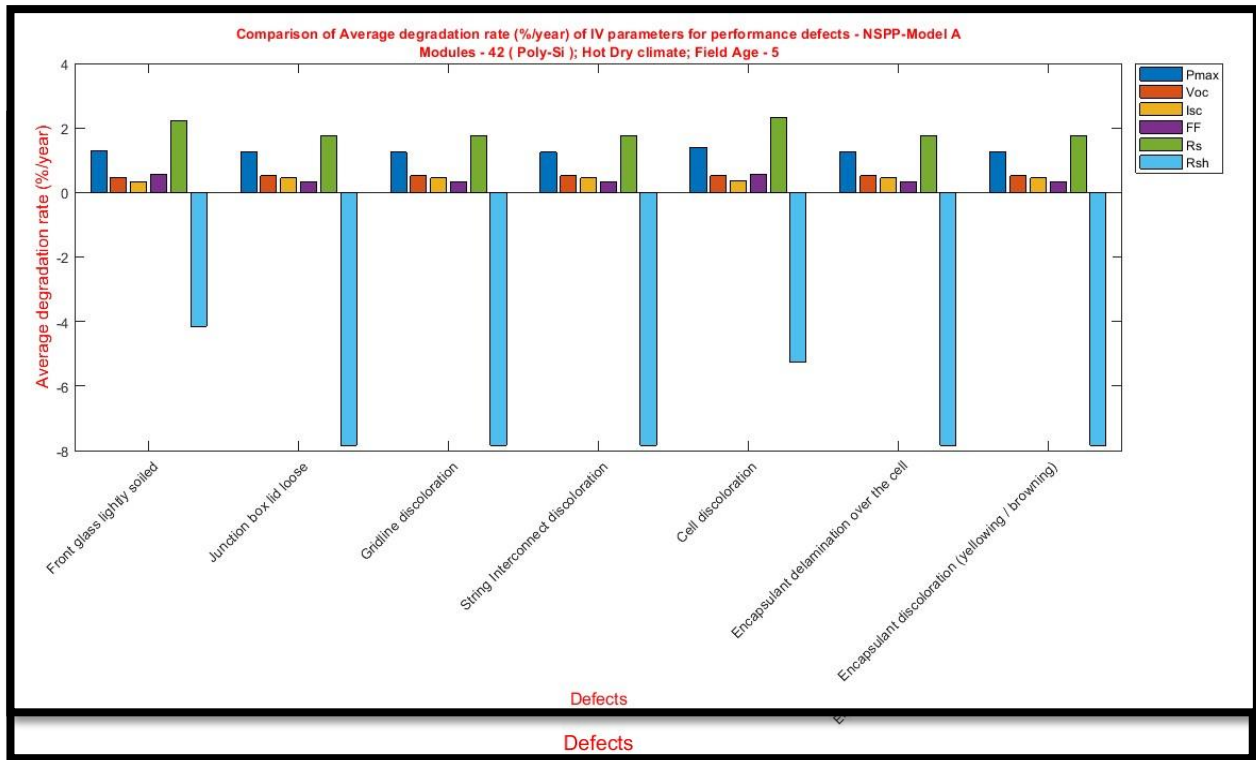
Step 16: After entering module type, click ENTER in keyboard. It will generate plots concerned with RPN and program will end denoted by >> as shown in fig below.



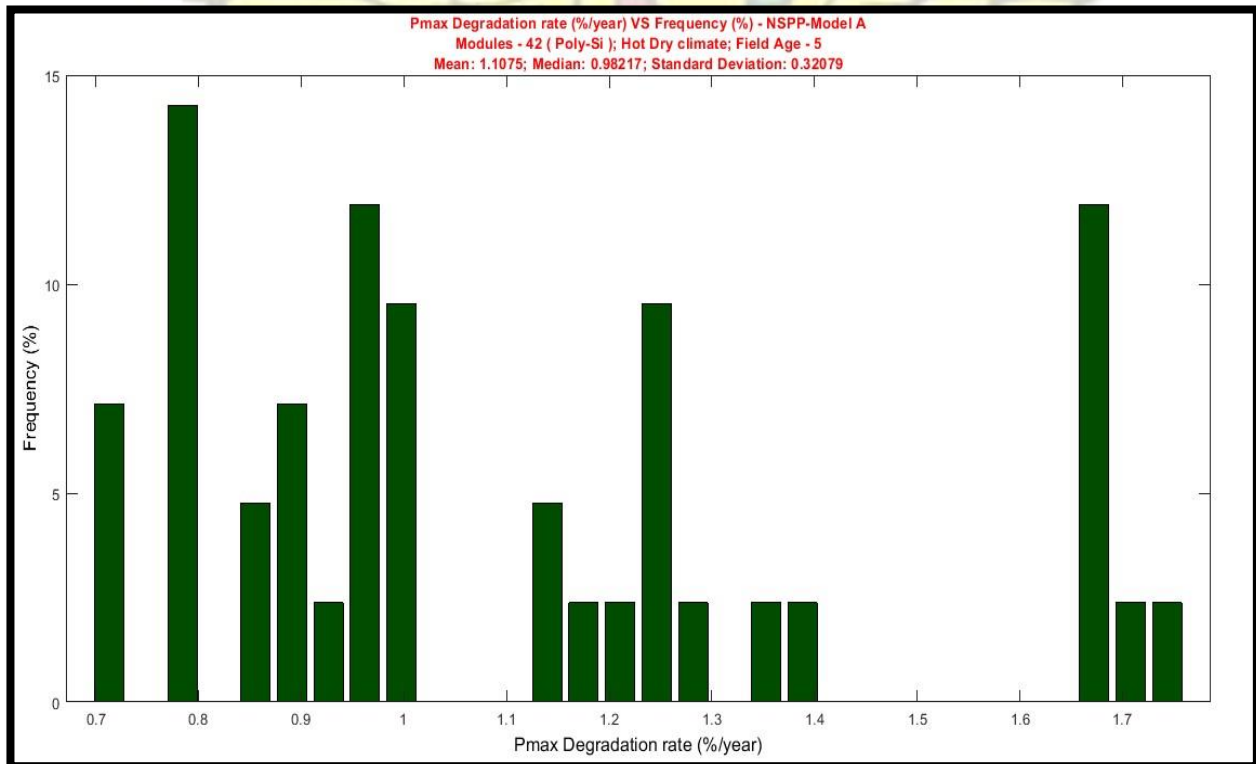
APPENDIX C: MATLAB RESULTS

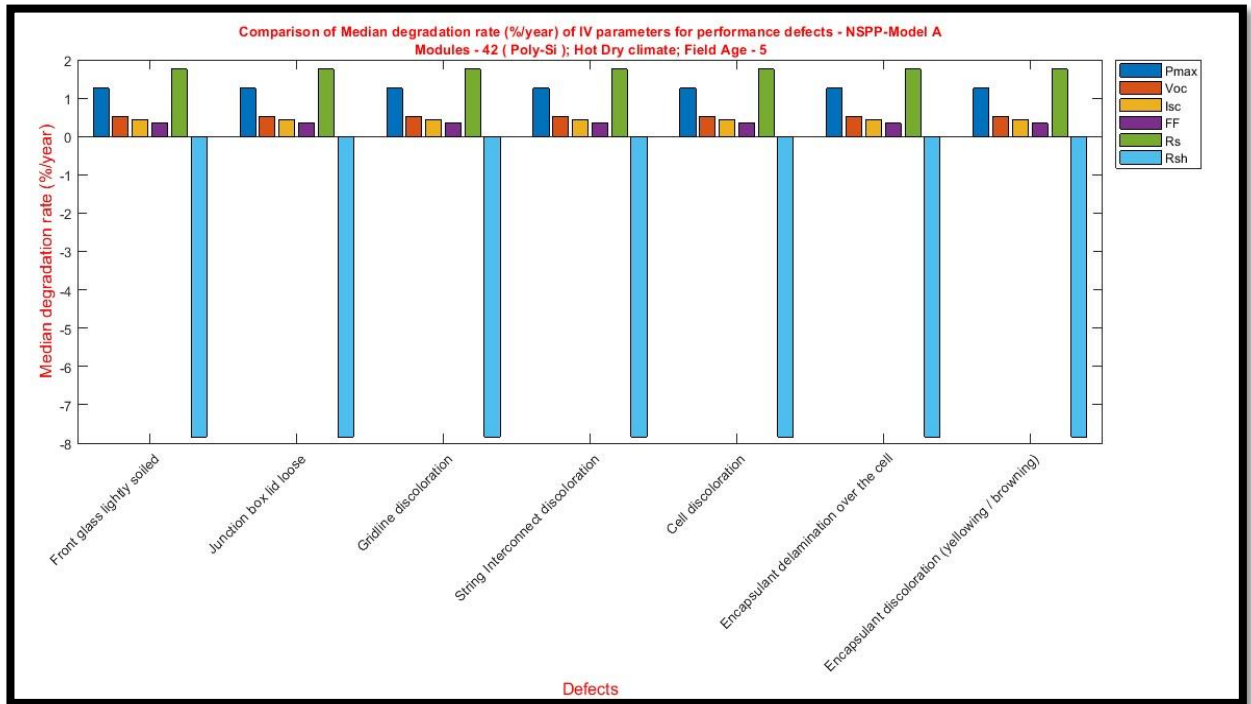
RESULTS OF ANALYSIS FOR MODEL A and MODEL B FMECA-
REMAINING RPN RESULTS FOR MODEL A

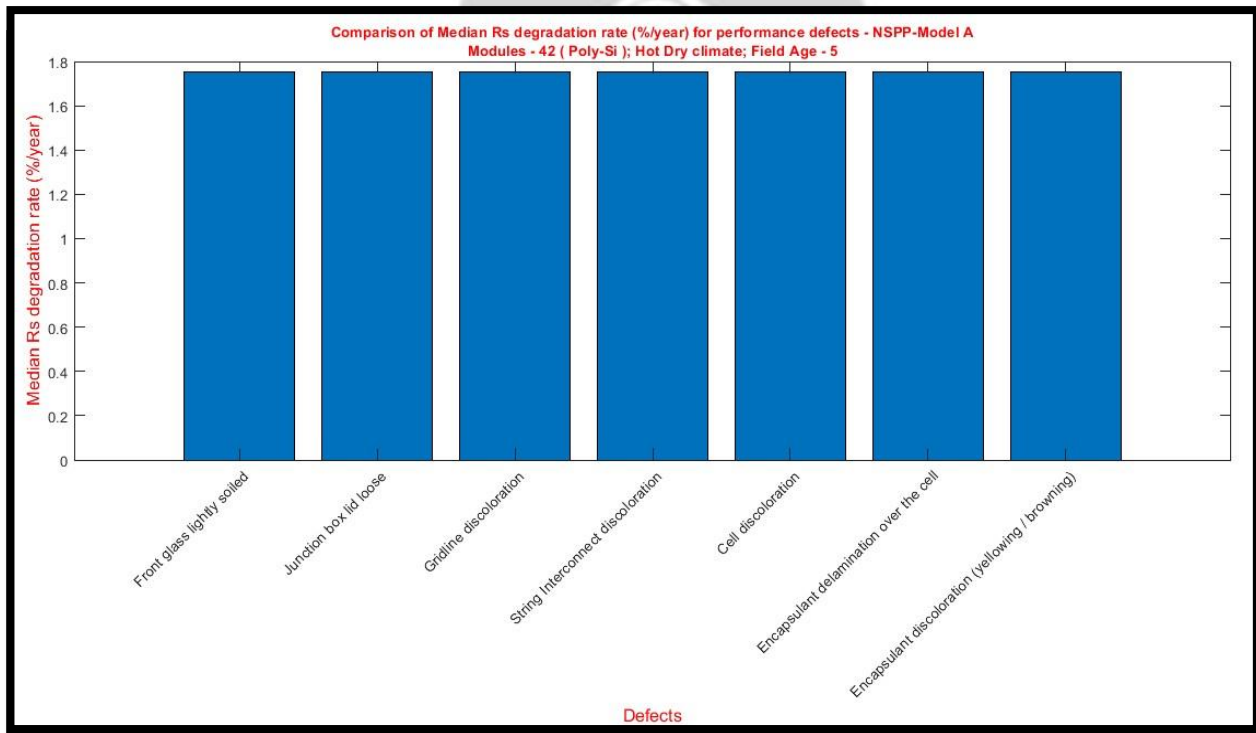
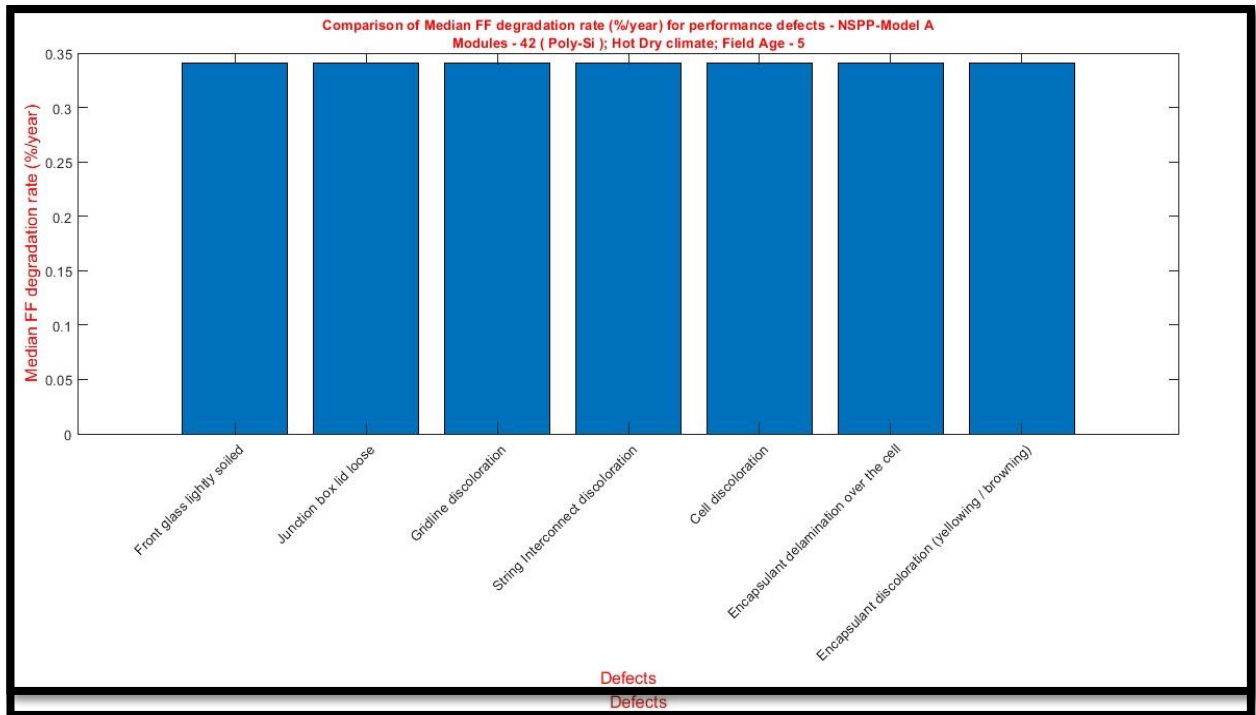


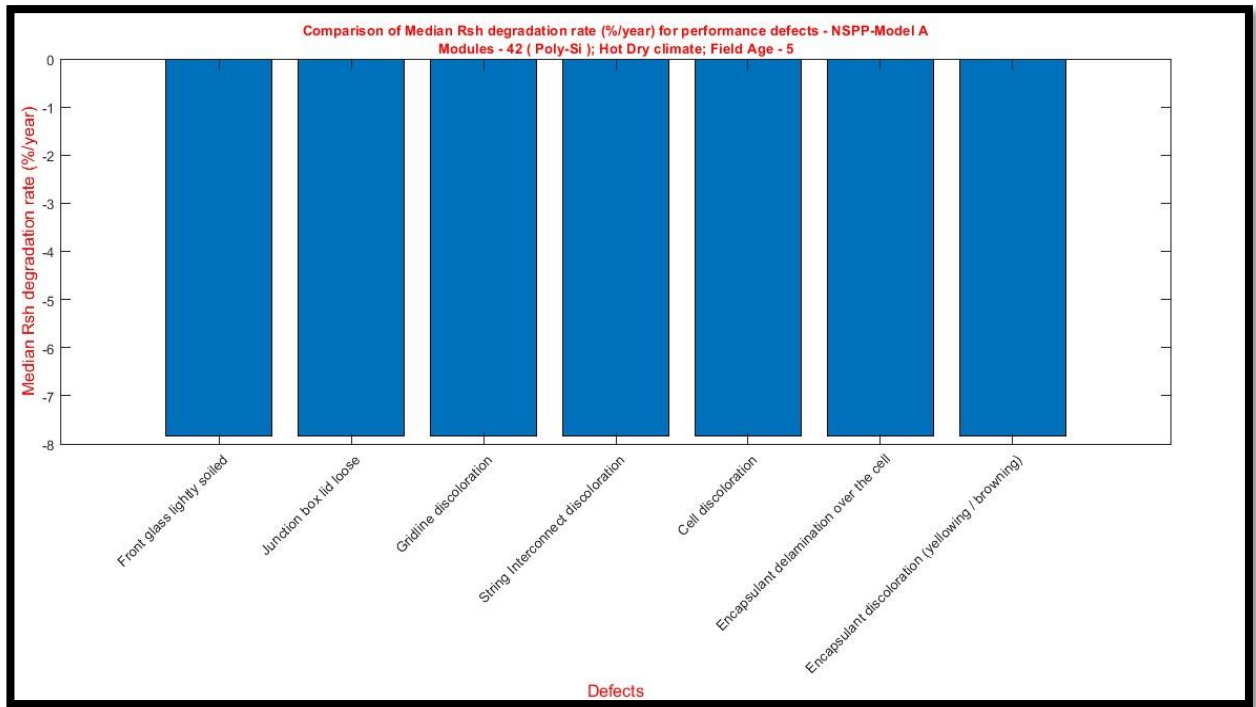


OTHER CORRELATION RESULTS







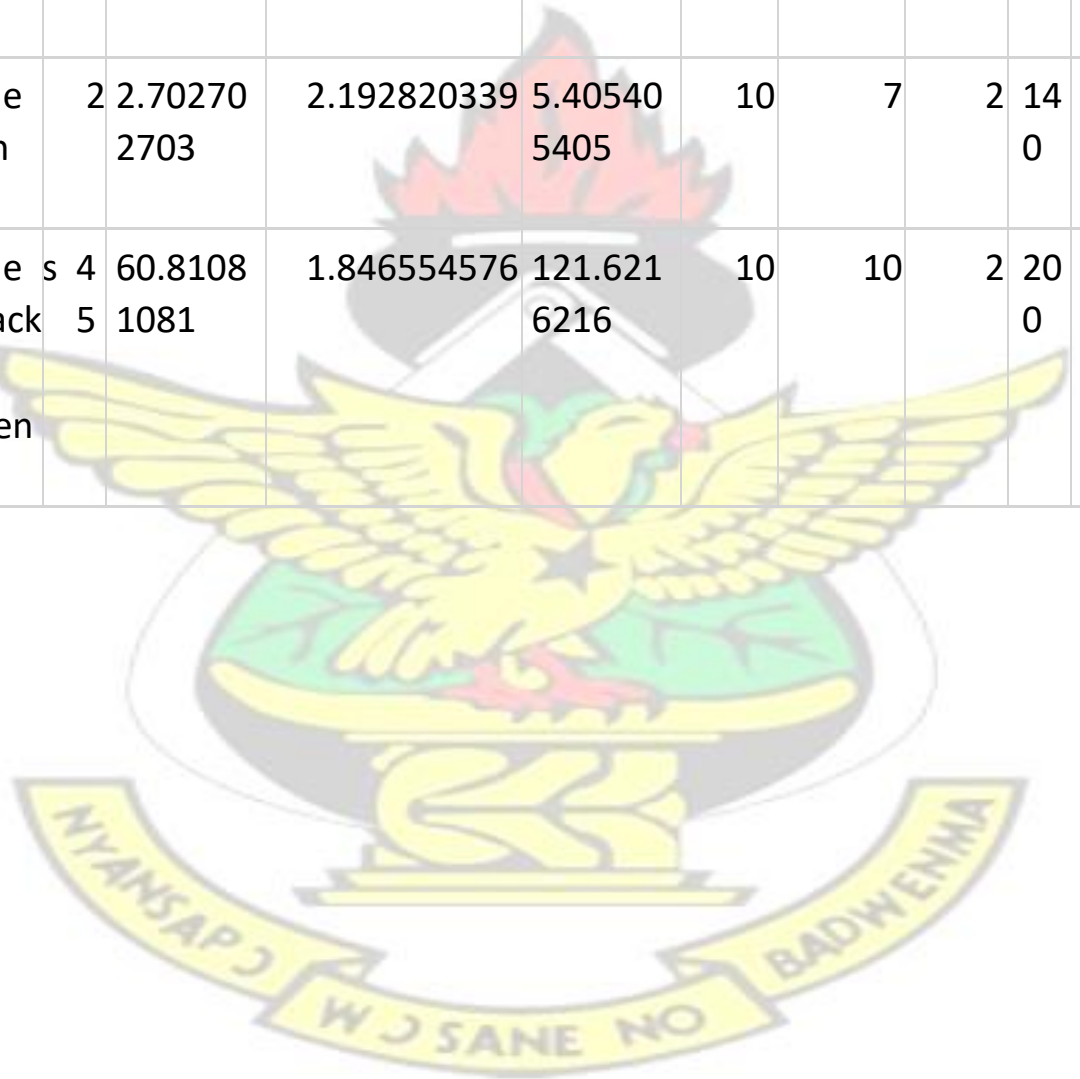


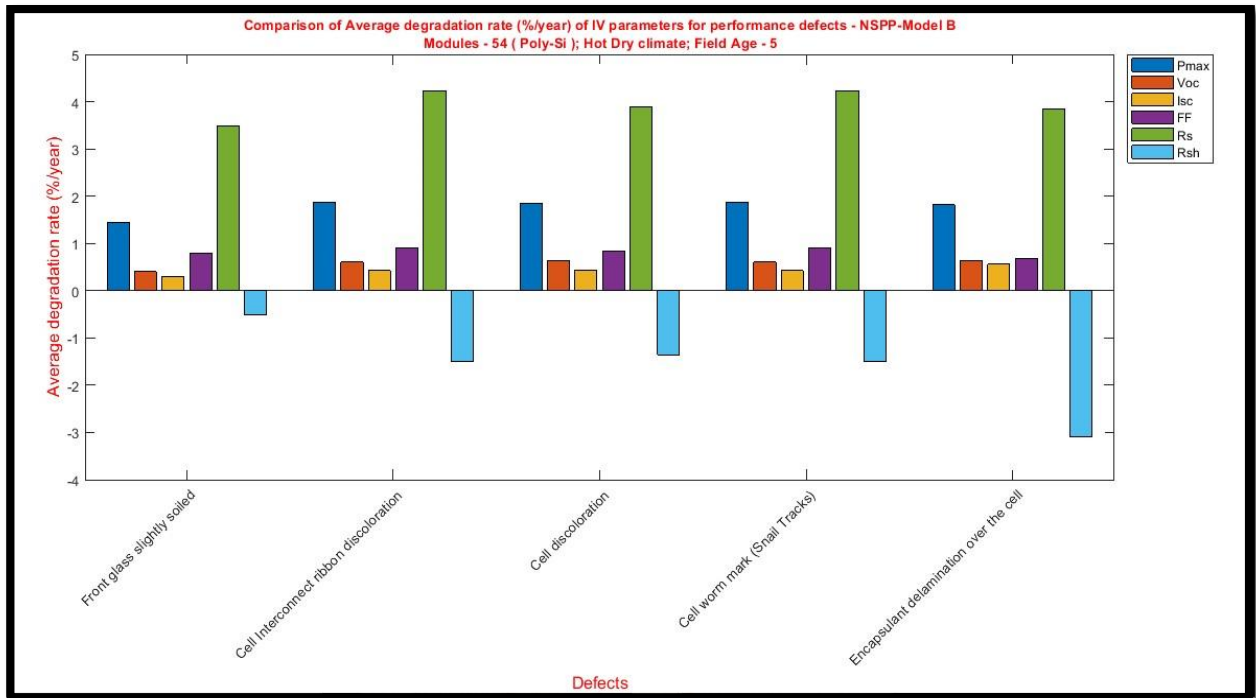
OTHER FMECA-RPN RESULTS FOR MODEL B

Summary for FMECA results from Program

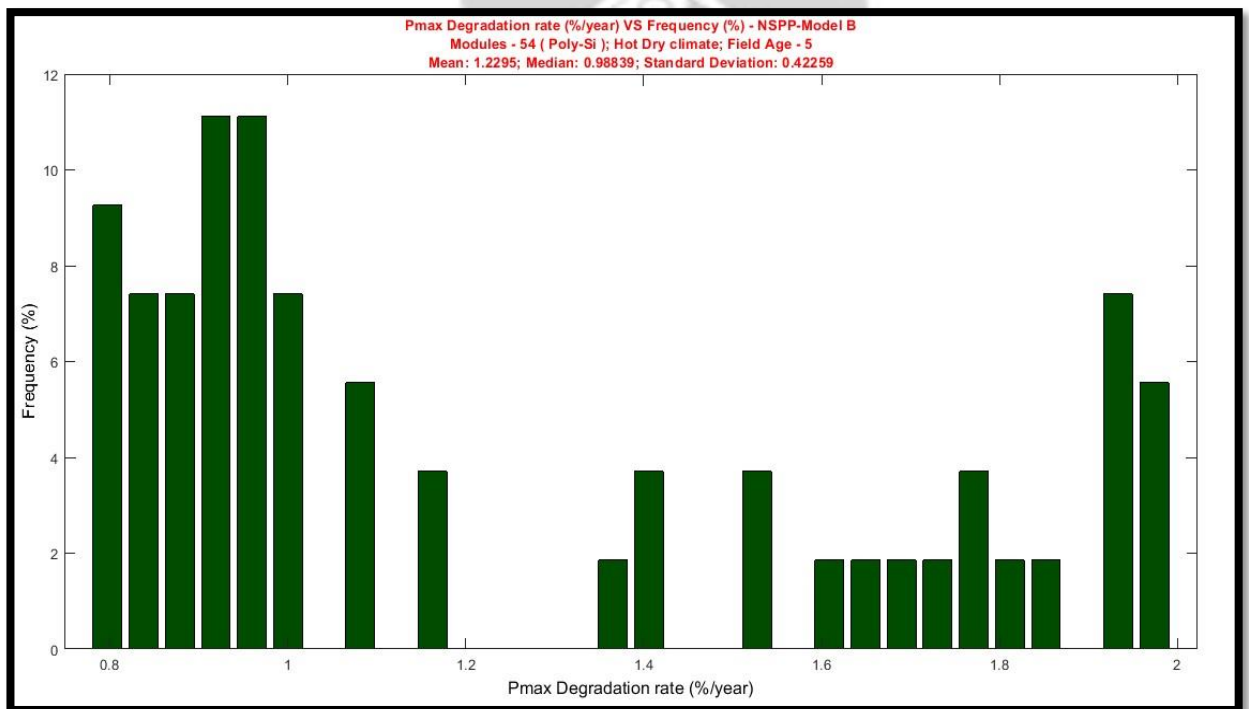
Defects	Total	Percentage	Average_Degradation	CNF/100	Severity	Occurrence	Detection	RPN	RPN_SO
Front glass lightly soiled	34	45.9459	1.838545763	91.89189189	8	10	2	160	80
Cell Interconnect ribbon discoloration	25	33.78378378	2.165477153	67.56756757	9	10	2	180	90
Cell discoloration	10	13.51351351	2.008731525	27.02702703	9	9	2	162	81

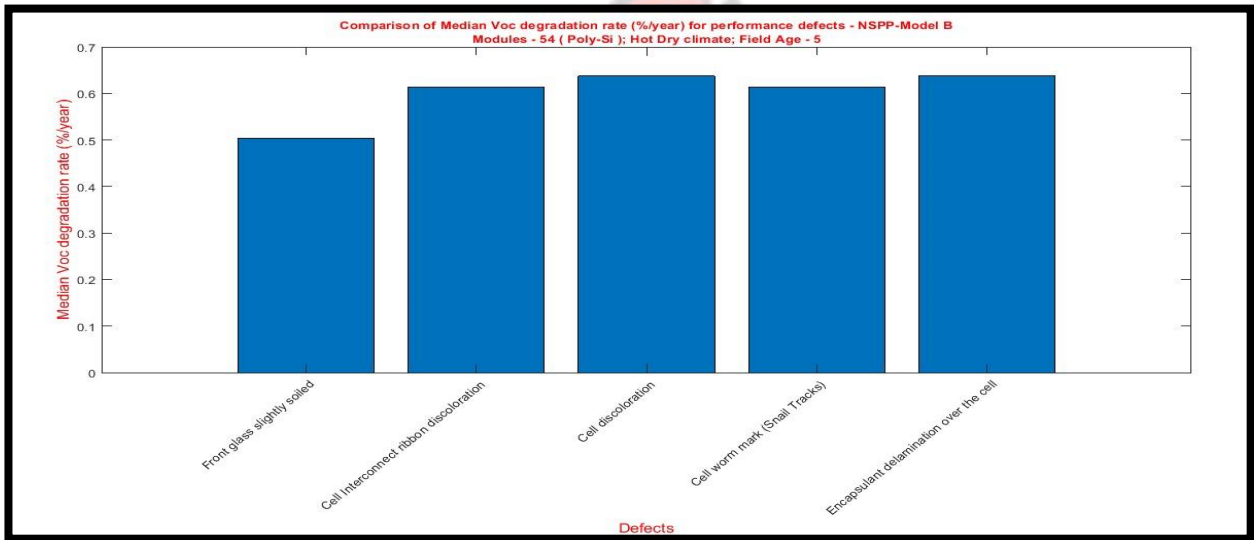
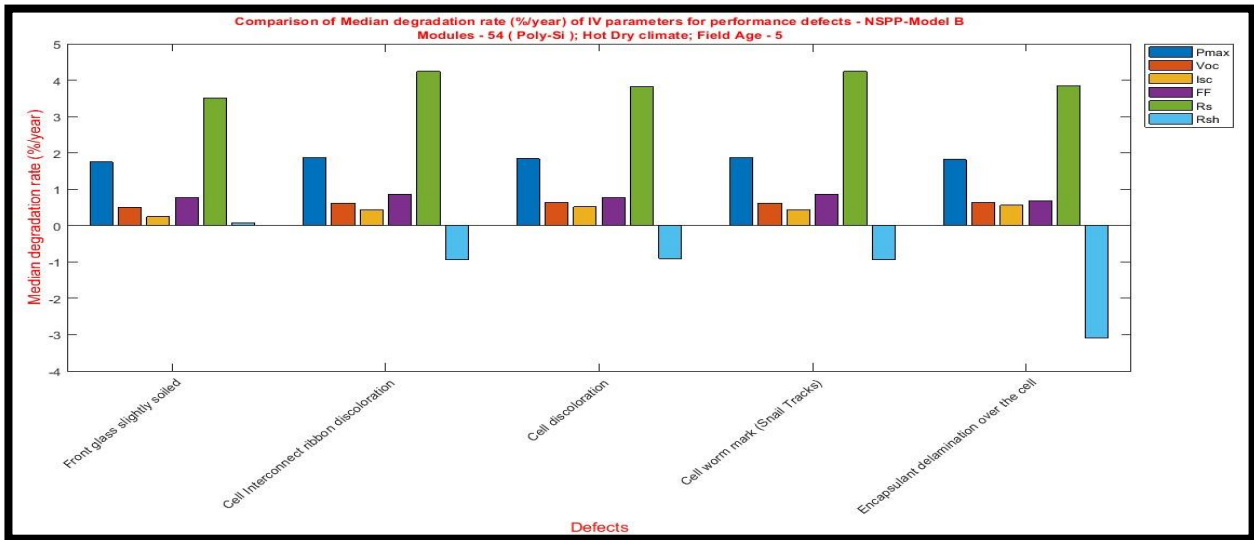
Cell worm mark (Snail Tracks)	19	25.67567568	2.086092061	51.35135135	9	10	2	180	90
Encapsulant delamination overth	7	9.459459459	2.070961743	18.91891892	9	8	2	144	72
Backsheet burn mark	2	2.702702703	2.192820339	5.405405405	10	7	2	140	70
Backsheet crack/cut between cell	45	60.81081081	1.846554576	121.6216216	10	10	2	200	100

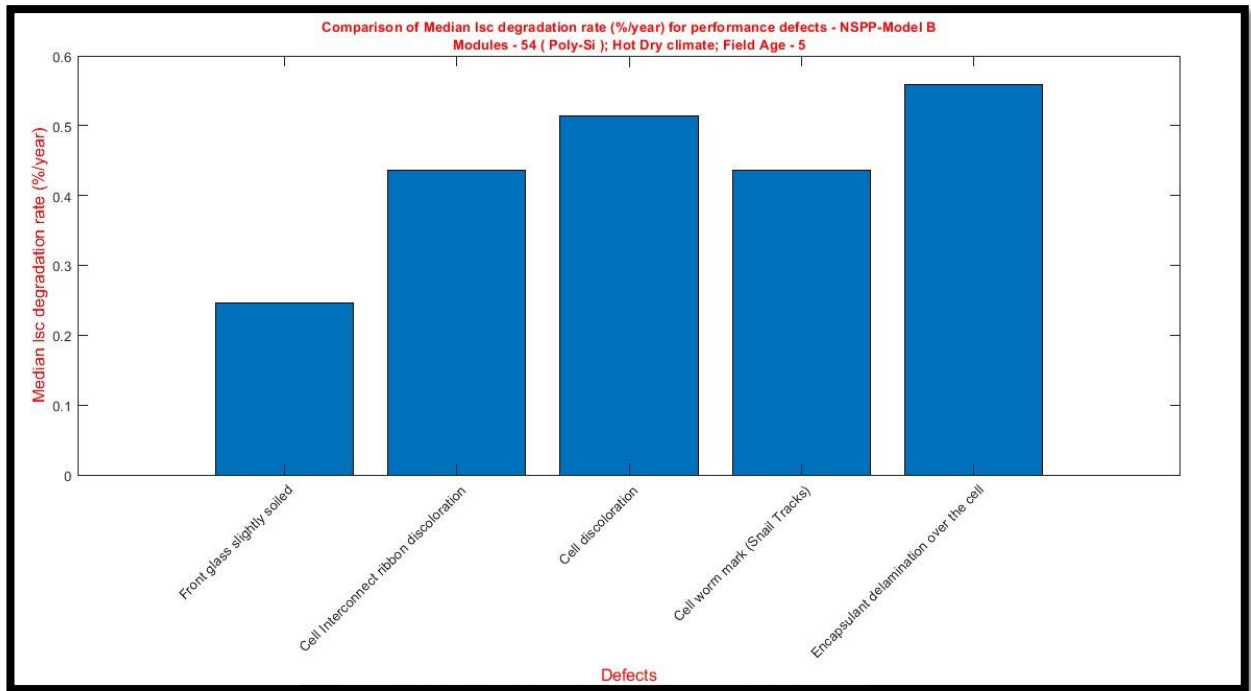


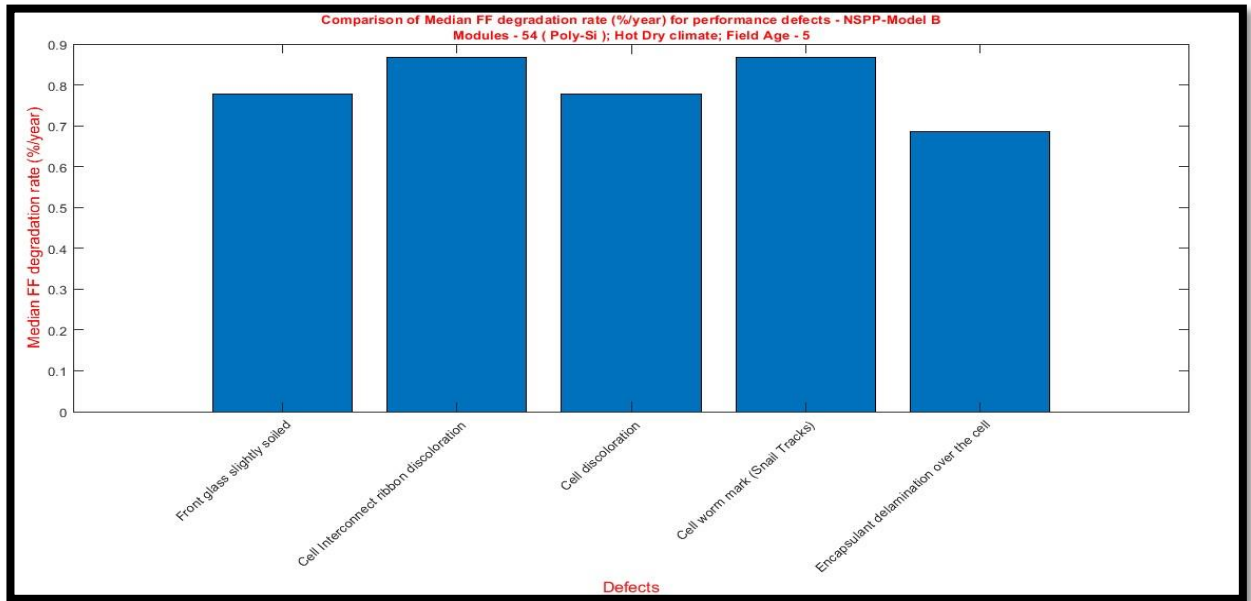


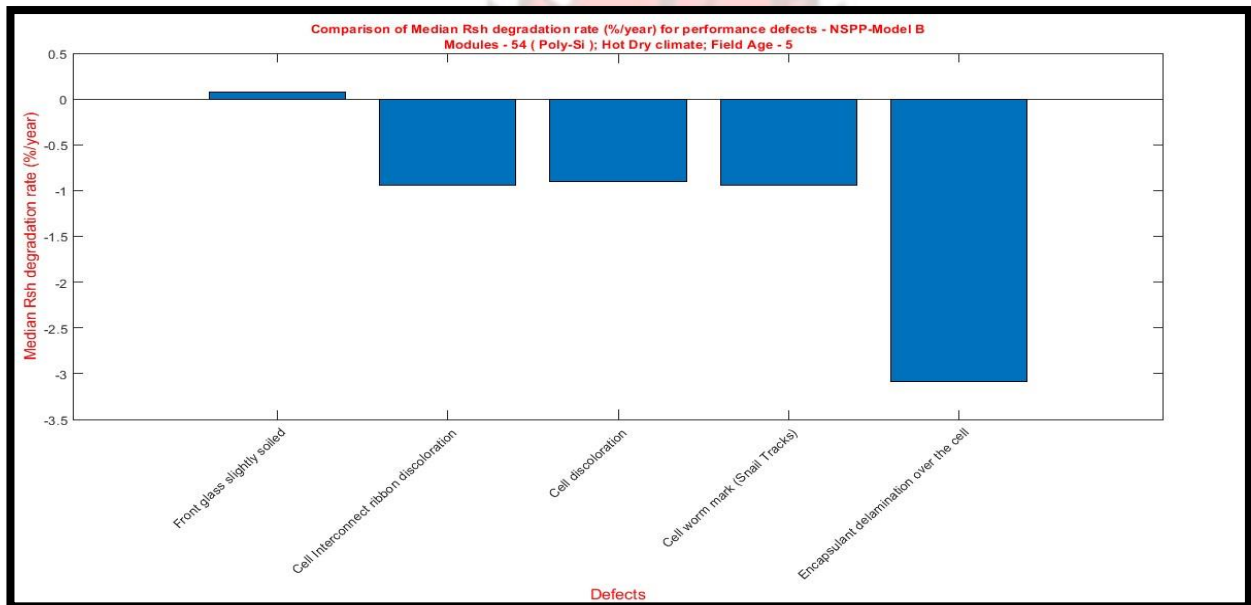
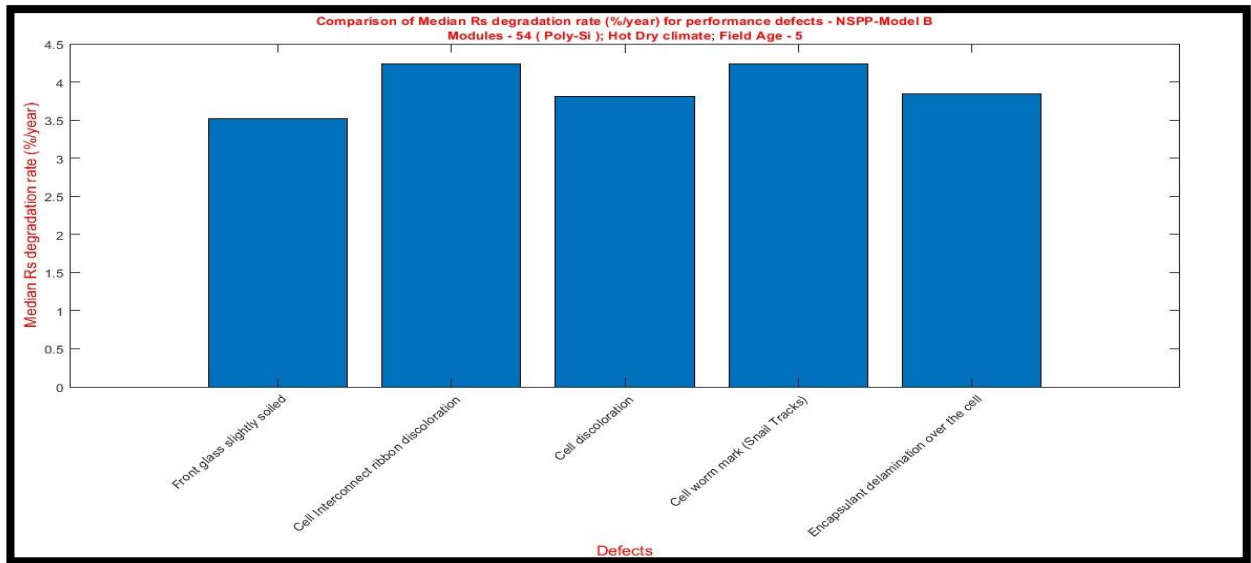
OTHER CORRELATION RESULTS FOR MODEL B



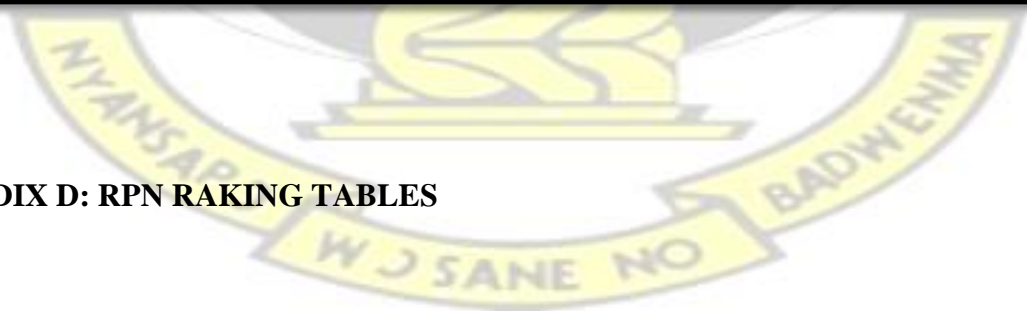








APPENDIX D: RPN RAKING TABLES



Various tables used to rank Detection, Occurrence and Severity values Table for determining Detection (D) & Severity (S) for PV Modules

Ranking	Detection Criteria	Severity Criteria
1	Monitoring System itself will detect the failure mode with warning 100%	No effect, Rd < 0.3%
2	Very high probability (most likely) of detection through visual inspection	Insignificant, Rd approx. to 0.3%
3	50/50 probability (less likely) of detection through visual inspection	Minor Cosmetic defect, Rd < 0.5%
4	Very high probability (most likely) of detection using conventional handheld tool e.g. IR, Megger	Cosmetic defect with Rd < 0.6%
5	50/50 probability (less likely) of detection using conventional handheld tool e.g. IR, Megger	Reduced performance, Rd < 0.8%
6	Very high probability (most likely) of detection using non-conventional handheld tool e.g. diode/line checker	Performance loss approx. to typical warranty limit, Rd approx. to 1%
7	50/50 probability (less likely) of detection using non-conventional handheld tool e.g. diode/line checker	Significant degradation, Rd approx. to 1.5%
8	Very high probability (most likely) of detection using performance measurement equipment e.g. IV tracer	Remote safety concerns, Rd < 1%

9	50/50 probability (less likely) of detection using performance measurement equipment e.g. IV tracer	Remote safety concerns, Rd < 2%
10	Detection impossible in the field	Safety hazard, Catastrophic

(Shrestha et al, 2014).

KNUST

Table for determining Occurrence (O) for PV Modules

Failure Mode Occurrence	Frequency CNF/1000	Ranking O
Remote: Failure is unlikely	<= 0.01 module per thousand per year	1
Low: Relatively few failures	0.1 module per thousand per year	2
	0.5 module per thousand per year	3
Moderate: Occasional failures	1 module per thousand per year	4
	2 module per thousand per year	5
	5 module per thousand per year	6
High: Repeated failures	10 module per thousand per year	7
	20 module per thousand per year	8

Very high: Failure is almost inevitable	50 module per thousand per year	9
	≥ 100 module per thousand per year	10

The cumulative number of module failures per thousand per year (CNF) is computed as follows:

KNUST

$$\text{CNF} = \frac{1000 \times \text{system \% defects}}{\text{system operating time}}$$

Series and Shunt coefficient table for various PV technologies

Type of module	Series coefficient, C_s	Shunt coefficient, C_{sh}
Mono-Si	0.32	4.92
Poly Si	0.34	5.36
Amorphous-Si	0.59	0.92
Cd Te	0.59	0.92
CIGS	0.59	0.92
CIS	0.59	0.92

Modified Severity table for used for the MatLab program

Severity Criteria	modification to the severity table	Severity ranking
No effect, $R_d < 0.3\%$	No modification	1
Insignificant, R_d approx. to 0.3%	No modification	2

Minor Cosmetic defect, $R_d < 0.5\%$	No modification	3
Cosmetic defect with $R_d < 0.6\%$	No modification	4
Reduced performance, $R_d < 0.8\%$	No modification	5
Performance loss approx. to typical warranty limit, R_d approx. to 1%	No modification	6
Significant degradation, R_d approx. to 1.5%	No modification	7
Remote safety concerns, $R_d < 1\%$	$R_d > 1.5$ & $R_d \leq 2$ for performance defects or Bypass diode OC failure	8
Remote safety concerns, $R_d < 2\%$	$R_d > 2$ for performance defects $R_d \leq 2\%$	9
Safety hazard, Catastrophic	$R_d > 2\%$ 18 safety failures	10

(Shrestha et al, 2014).